論文 / 著書情報
Article / Book Information

題目(和文)	
Title(English)	Reversible Crosslinking ? Decrosslinking Systems Based on Reversible Addition ? Elimination between Vicinal Tricarbonyl Compounds and Alcohols
著者(和文)	米川盛生
Author(English)	Morio Yonekawa
出典(和文)	学位:博士(工学), 学位授与機関:東京工業大学, 報告番号:甲第9277号, 授与年月日:2013年9月25日, 学位の種別:課程博士, 審査員:高田 十志和,手塚 育志,石曽根 隆,早川 晃鏡,小西 玄一,遠藤 剛
Citation(English)	Degree:Doctor (Engineering), Conferring organization: Tokyo Institute of Technology, Report number:甲第9277号, Conferred date:2013/9/25, Degree Type:Course doctor, Examiner:,,,,,
学位種別(和文)	博士論文
Type(English)	Doctoral Thesis

Doctoral Dissertation

Reversible Crosslinking – Decrosslinking Systems Based on Reversible Addition – Elimination between Vicinal Tricarbonyl Compounds and Alcohols

Morio Yonekawa

Takata Research Group

Department of Organic and Polymeric Materials

Tokyo Institute of Technology

Contents

Chapter 1

Introduction

1.1 Reversibly Formed and Dissociated Covalent Bonds in Supramolecular and Polymer Chemistry

In polymer chemistry and supramolecular chemistry, a promising strategy for synthesizing complex molecules with sophisticated structure is to utilize covalent bonds which can be formed and dissociated efficiently in a reversible fashion.[1] Chemists have utilized this reversibility for nanostructure fabrication, the development of adaptive materials, and identification of biologically active compounds. In general, reversible reactions can be classified into three types of equilibrium controlled reactions: (a) formation/scission of a new type of bond, (b) direct exchange reaction, and (c) metathesis (Scheme 1.1). The thermodynamic equilibrium of a reversible bond formation–dissociation is generally manipulated in one of two ways: (i) the equilibrium can be driven in one direction by adjusting the reaction conditions, *i.e.*, adding or removing starting material or product, or (ii) the starting materials can be chosen so as to encourage the formation of a particular product, *i.e.*, by incorporating certain steric or electronic recognition features into the precursors which favor the formation of the desired product. This reversible covalent chemistry involves imine bond, disulfide bond, Diels–Alder reaction, radical exchange, olefin metathesis, and so on.

Scheme 1.1 Three types of reversible reactions: (a) formation/scission of a new type of bond (e.g. imine condensation), (b) direct exchange reaction (e.g. imine exchange), and (c) metathesis type reaction (e.g. imine metathesis)

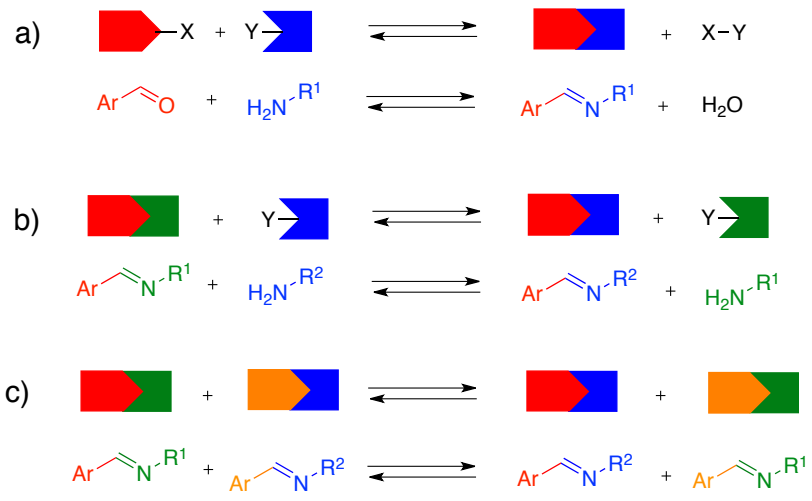

Thermodynamic covalent bond chemistry has a long history in polymer science from ring–chain equilibria (including ring-opening polymerizations) and reactive polymer blends (e.g. transesterification of reactions in polyester blends).[2] In equilibrium polymerizations, monomers, oligomers, and polymers can be interchanged through the formation and scission of covalent bonds in response to external stimuli. Thermodynamic behaviors caused by changes in temperature and concentration were examined during polymerizations of vinyl monomers[3], cyclic ether[4], cyclic acetal[5], cyclic esters[6], and cyclic amides[7].

The olefin metathesis reaction is an interchange of carbon atoms between two double bonds, which suggests that this process has the potential to be a reversible one. In 1977, Dolgoplosk *et al.* reported a ring-opening metathesis polymerization of cyclooctene **1**, by employing WCl_6/*i*Bu_2AlCl in benzene at room temperature (Scheme 1.2).[8] During the polymerization, there is an initial sharp increase in the viscosity of the mixture and then, in the course of time, it decreases slowly. This behavior is explained by the initial formation of high molecular weight polymer **2**, followed

thereafter by the formation of a mixture of cyclic species and shorter polymers. More recently, Grubbs and co-workers reported acyclic diene metathesis (ADMET) polymerization of allylic ether terminated oligoethers,[9] utilizing high tolerant benzylidene ruthenium complex as a catalyst.[10]

Scheme 1.2 ROMP of cyclooctene **1** catalyzed by WCl_6/iBu_2AlCl

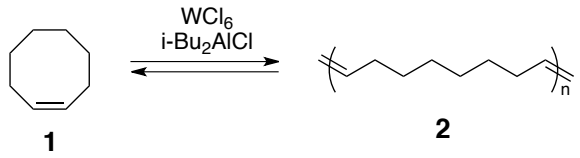

1 **2**

Brunelle and co-workers have developed a high-yielding synthesis of a variety of macrocylic carbonates by using a pseudo high dilution technique, and used them as synthetic intermediates for polycarbonates (Scheme 1.3).[11] This kinetically controlled procedure involves treating the monomeric bischloroformate **3** with an aqueous NaOH solution (in the presence of an amine catalyst) in a reaction which results in both hydrolysis and condensation to give the macrocyclic products **4** (m = 2–20) in high yields. Polymerization of these macrocycles can be induced using a variety of catalysts and conditions. For example, the polymerization of the bisphenol A macrocyclic derivatives **4** (R = $C(Me)_2$) with $[Ti(O\text{-}iPr)_2(acac)_2]$ resulted in the formation of commercially important bisphenol A polycarbonate **5** (M_w = 248,000, PDI = 2.5).[12]

Scheme 1.3 Kinetic formation of the macrocyclic carbonates **4** and their subsequent thermodynamic polymerization to yield the polycarbonates **5**

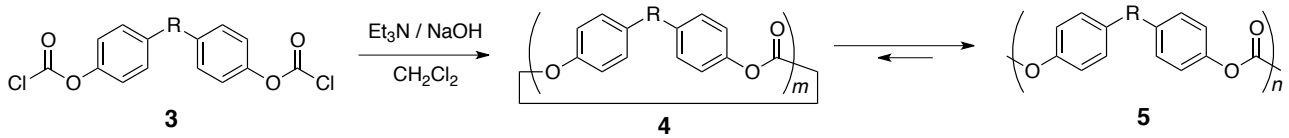

3 **4** **5**

Endo *et al.* reported that cationic polymerization of spiro-orthoester **6** proceeds at low

temperature to give poly(cyclic orthoester) **7** (Scheme 1.4).[13] Since this reaction is a typical equilibrium polymerization, the obtained polymer **7** could be readily converted into the original monomer **6** by treatment with acid catalyst at room temperature. A similar thermodynamic equilibrium was observed between bicyclic-orthoester **8** and its polymer **9**.[14]

Scheme 1.4 Equilibrium polymerizations of spiro-orthoesters and bicyclic-orthoester

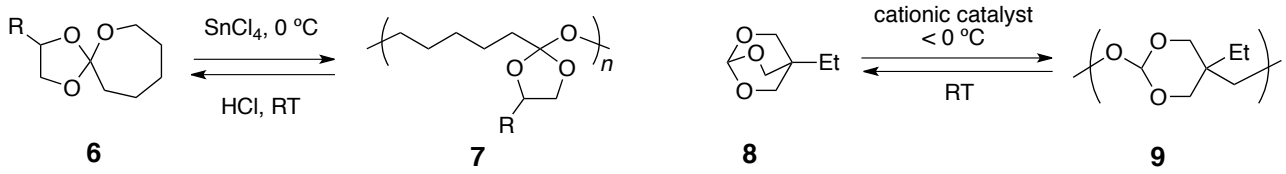

6 **7** **8** **9**

In recent polymer chemistry, reversible covalent bonds have been successfully used for "controlled" radical polymerization reactions[15] such as (a) nitroxide-mediated radical polymerization (NMP)[16], (b) atom transfer radical polymerization (ATRP)[17], and (c) reversible addition-fragmentation chain transfer radical polymerization (RAFT)[18]. In these precision polymerizations, reversible covalent bonds in polymer chain ends of dormant species **10** go into rapid equilibrium and play an essential role to keep the instantaneous concentrations of growing active species **11** low (Scheme 1.5).

Scheme 1.5 Equilibria between propagation radicals **11** and covalent domant species **10** in (a) NMP of polystyrene using 2,2,6,6-tetramethylpiperidine 1-oxyl (TEMPO) **12**, (b) ATRP of PMMA, and (c) RAFT polymerization of styrene

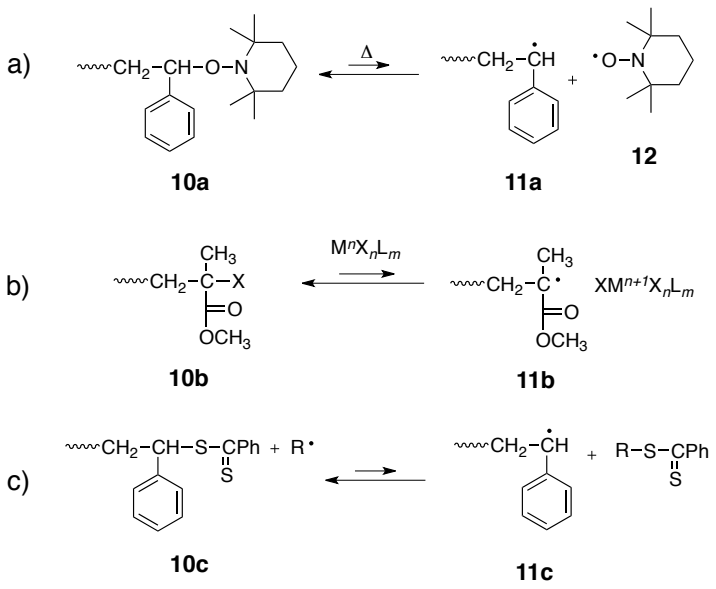

Formation of imine bond is a reversible reaction, which operates under thermodynamic control (Scheme 1.1). Therefore it has been employed widely in the construction of supramolecules.[19] Quan and Cram synthesized a large container-like molecule, octaimine hemicarcerand **14**, from a tetrafromyl cavitand and *m*-phenylenediamine **13**.[20] The ability to open and close the hemicarcerand **14**, by sequential imine exchange and then imine formation, was exploited for the controlled release of ferrocene (Fc) from the corresponding Fc-containing hemicarceplex **15** (Scheme 1.6).[21] The half-life for the release of Fc from **15** in $CDCl_3$ was shown to be >4000 h. However, the addition of *m*-phenylenediamine **13** (in addition to the acid) accelerated the release of Fc and resulted in a half-life of 180 h. When *m*-phenylenediamine **13** is present, imine exchange may be operating, thereby opening a "door" in the hemicarceplex shell through which the Fc can escape.

Scheme 1.6. Acid-catalyzed reversible encapsulation of ferrocene in a hemicarcerand **14**

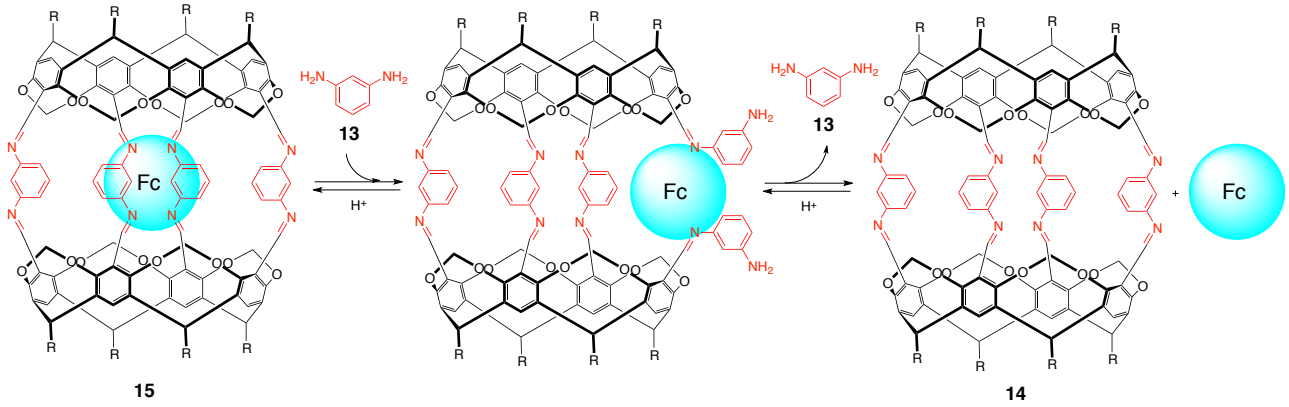

Zhao and Moore have designed a sophisticated reversible covalent polymer system based on imine metathesis (Scheme 1.7).[22] Curved tetrameric *m*-phenylene ethynylene oligomers **16** and **17** bearing bis-imino end groups were synthesized and used as monomers for imine metathesis polymerization in acetonitrile or chloroform in the presence of an acid catalyst. In polar acetonitrile, high-molecular weight polymer **18** was generated because of formation of helical assembly stabilized by intrahelix solvophobic interactions. In contrast, a lower degree of polymerization was observed in non-polar chloroform.

Scheme 1.7 Imine metathesis polymerization of bis-imino *m*-pheylene ethynylene oligomers **16** and **17**

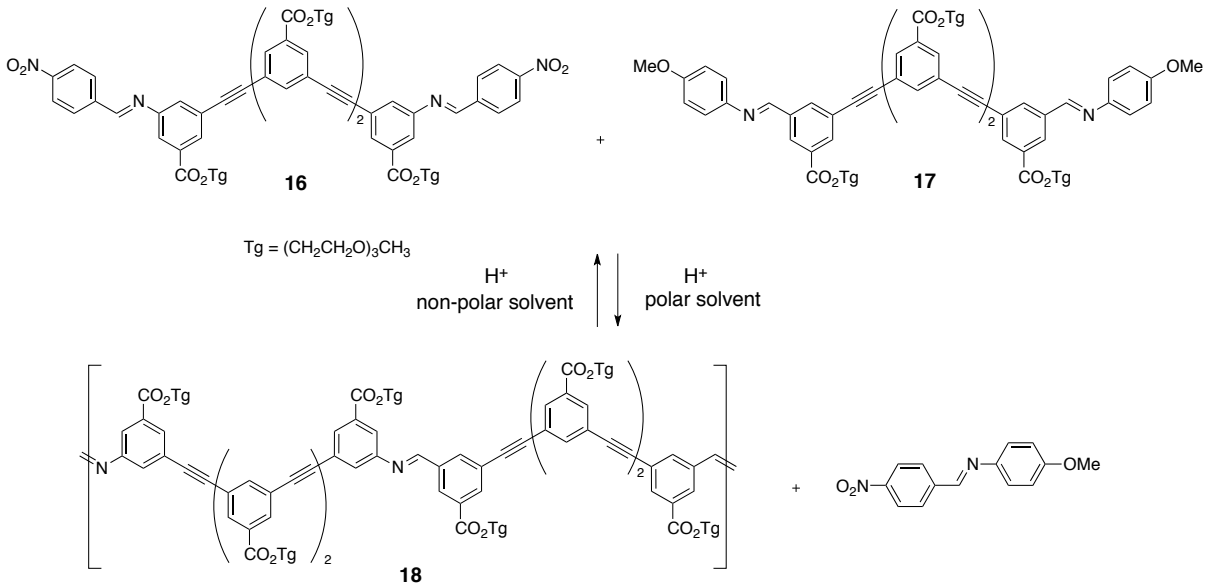

Reversible covalent bonds have been used recently to develop a novel class of polymers having dynamic properties, the so-called "dynamers", such as a changeable and tunable constitution even after polymerization.[23] Lehn and co-workers have developed a number of main-chain dynamic covalent polymers based on the (acyl)hydrazone bond: an acid-sensitive bond formed between an aldehyde and a hydrazide.[24] These structurally dynamic polymers **19** show the ability to exchange components after polymerization by simply mixing different monomers **20** or polymers and submitting them to acidic conditions. Under such conditions these polymers exchange and shuffle components to produce distinct moieties **21** not present in the starting materials (Scheme 1.8).

Scheme 1.8 Monomer exchange reactions of polyacylhydrazones

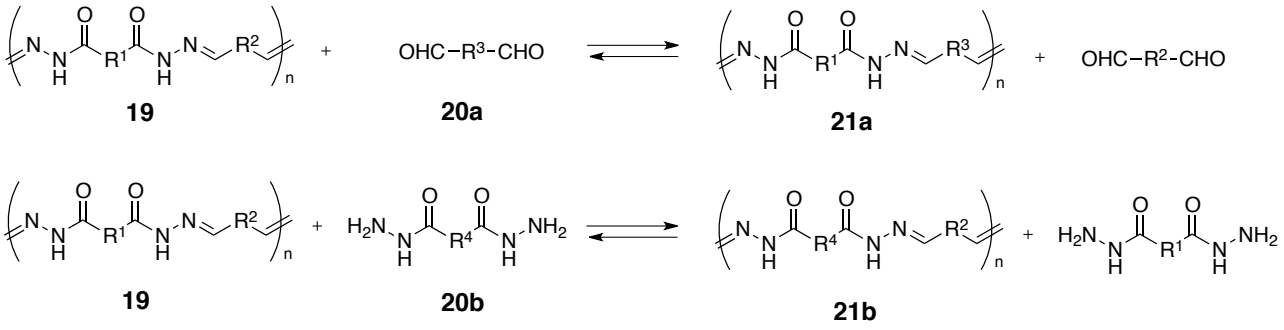

Stoddart and co-workers reported the thermodynamically controlled synthesis of a dialkylammonium based [2]rotaxane in which a crown ether like macrocycle is clipped around a dumbbell-shaped component (Scheme 1.9).[25] When 2,6-pyridinedicarboxaldehyde **22** is treated with diamine **23**, an equilibrium mixture, which appears to be comprised of many different cyclic and acyclic oligomeric species, is obtained after 24 h. However, addition of a dumbbell-shaped ammonium component **25** to this equilibrium mixture has a dramatic effect. After only 4 mins, a new equilibrium state is reached, in which the main component is the [2]rotaxane **26**. This result suggests that the dibenzylammonium ion **25** templates the formation of the crown ether like macrocycle **24** around itself, thus generating the interlocked molecule **26**.[26]

Scheme 1.9 The reaction of macrocycle **24** with **25** leading to the equilibrium being shifted to form almost exclusively the [2]rotaxane **26**

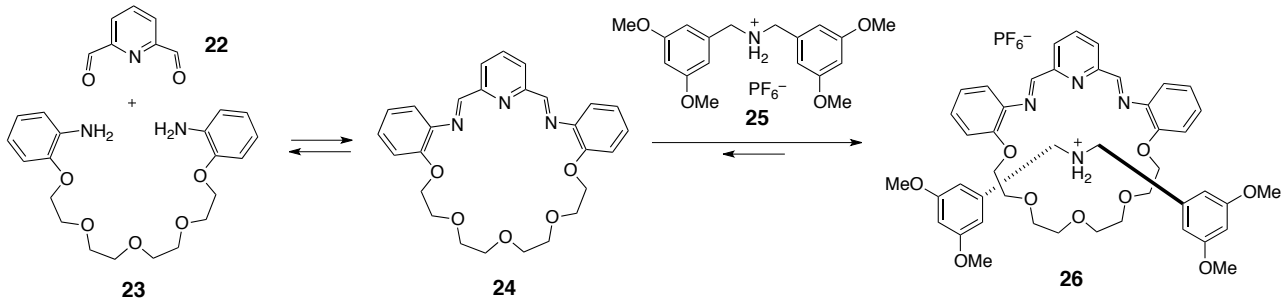

The same group also achieved synthesis of the stable Borromean-ring structure, three interlocked rings in an inseparable union, by employing tridentate 2,6-bisiminopyridyl and bidentate 2,2'-bipyridyl moieties as the endo and exo ligands, respectively (Scheme 1.10).[27] Bis-amine terminated 2,2'-bipyridyl **27** and 2,6-diformylpyridine **28** were reacted in boiling methanol in the presence of zinc acetate affording the hexanuclear Borromean ring compound **29** in 80% yield. Its interlocked nature was confirmed unambiguously by X-ray crystallography.

Scheme 1.10 (Top) Schematic assembly of a Borromean link (Bottom) Reversible reaction of 2,6-diformylpyridine **28** with a diamine containing a dipyridyl binding site **27**, in the presence of zinc acetoacetate affords a molecular Borromean link **29**

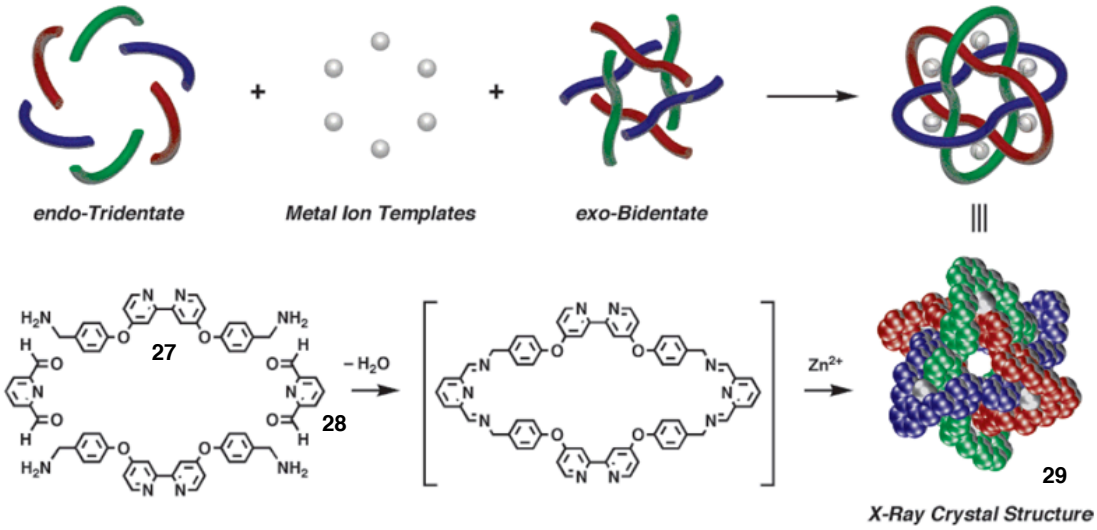

Thiol groups and disulfide linkages undergo a spontaneous reaction, in which the thiol group displaces one sulfur atom of the disulfide bond (Scheme 1.11), that is, a small amount of thiol can act as a catalyst for reversible disulfide exchange reaction.[28]

Scheme 1.11 Reversible cleavage of disulfide linkage

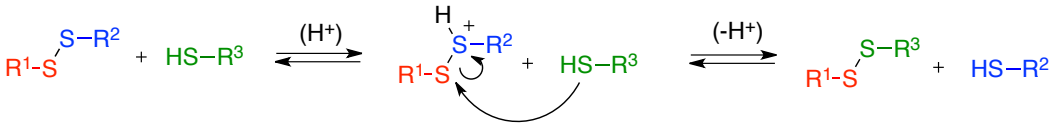

The first report of this potentially reversible bond being employed to construct an interlocked molecule under thermodynamic control appeared in early 2000 by Takata *et al*.[29] When a bifunctional secondary ammonium salt bearing disulfide linkage and bulky end-caps **30** was mixed with dibenzo-24-crown-8 (DB24C8) and a catalytic amount of benzenethiol, crown ether entered into disulfide linkage to afford [2] and [3] rotaxanes, **33** and **34**, respectively (Scheme 1.12). This mechanism of the formation of these rotaxanes is so called "unlock–lock" process; The initial S–S bond cleavage by the catalysis of thiol results in the formation of half rotaxane or pseudorotaxane, both of which can thread in the wheel and undergo end-capping as "unlock" process to give [2]rotaxane **33**. Similar process gives [3]rotaxane **34**.

Scheme 1.12 Formation of rotaxanes based on reversible thiol–disulfide exchange

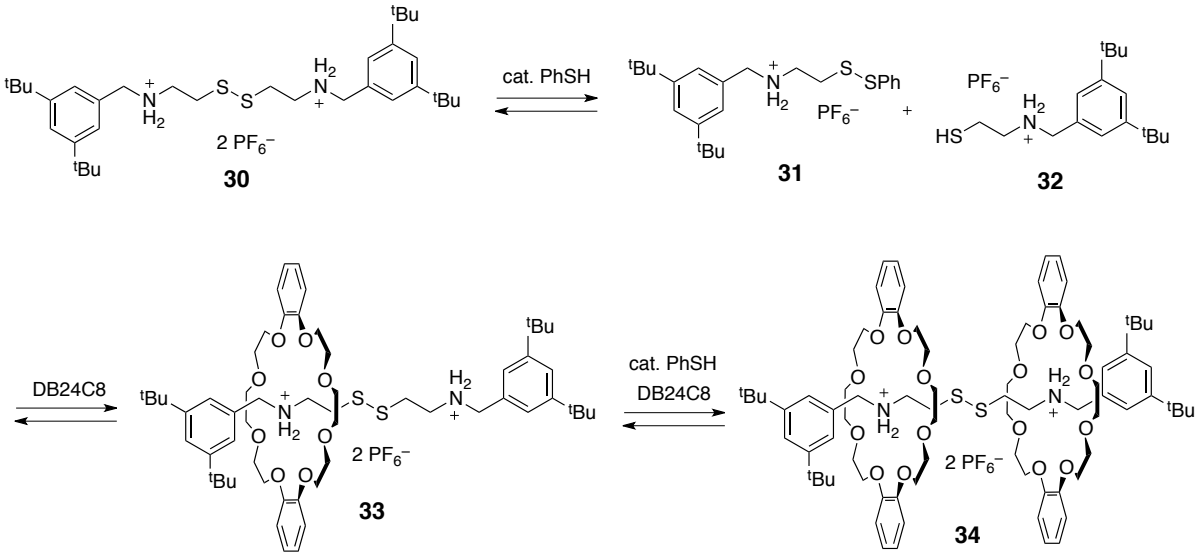

Combinatorial chemistry under thermodynamic control is called dynamic combinatorial chemistry; that is, in a dynamic combinatorial library (DCL), all costituents are in equilibrium.[30] Dynamic combinatorial chemistry relies on the selection of the thermodynamically most stable product from an equilibrating mixture. When a template is added to the mixture and binds to a specific library member, this species is stabilized and the equilibrium will shift, resulting in an increase in the concentration of the selected library member ("amplification"). Templates can be used to select species that can act as hosts or receptors (Scheme 1.13), as well as for the discovery of new guests or ligands. Otto *et al.* prepared dithiol building blocks **35**–**37** and analyzed how DCLs made from these building blocks responded to the addition of a variety of ammonium guests **38**–**40** (Scheme 1.14).[31] Guest **38** induced the amplification of heterotrimer host **41** with a high affinity. Remarkably, exposure of the same library to guests **39** and **40** induced the amplification of new receptors **42** and **43**, respectively.

Scheme 1.13 A small dynamic combinatorial library and its free energy landscape, showing the effect of adding template that strongly and selectively binds to one of the equilibrating species

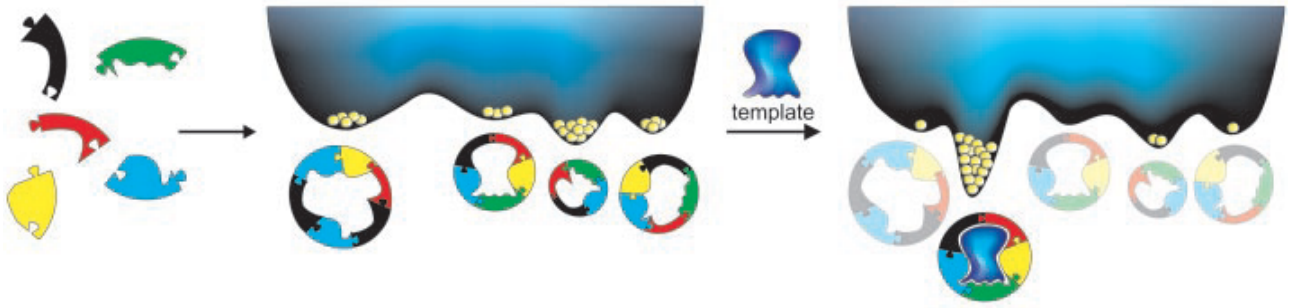

Scheme 1.14 Macrocyclic receptors **41–43** produced from DCL of dithiol building blocks **35–37**

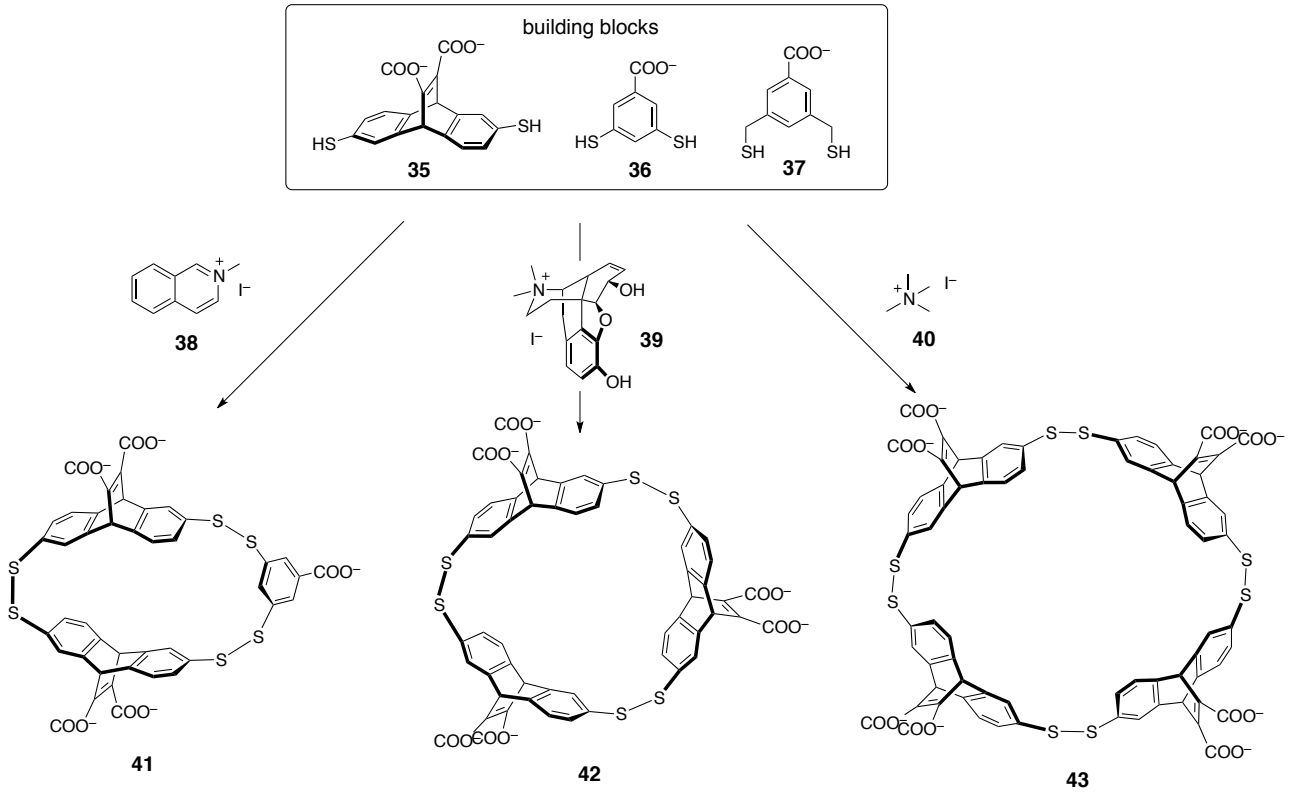

1.2 Reversible Crosslinking and Decrosslinking Systems

Covalently crosslinked networks or thermosets are extensively used as structural materials in a vast array of applications ranging from coatings to composites to biomaterials. Incorporation of dissociable covalent bonds into such network polymers allows decrosslinking of three dimensionally networked polymers into the corresponding linear ones, which can be crosslinked again on demand. These systems have been extensively investigated from the viewpoint of chemical recycling[32] as well as self-healing materials[33].

Endo *et al.* have investigated a polymer networks that can be interconverted with a linear polymers on the basis of aforementioned ring–chain equilibria of spiro-orthoester and bicyclic-orthoester (Scheme 1.4). They designed copolymers having spiro- and bicyclic-orthoester moieties as pendant groups (**44** and **46**, respectively), which were reversibly changed between the networks (**45** and **47**, respectively) and linear structures in the presence of cationic catalysts (Scheme 1.15). Crosslinking was enhanced with an increase in the concentration of the polymer, whereas recovery of the starting linear polymer through decrosslinking increased with decreasing concentration of the crosslinked polymer.[34,35] Similar reversible ring opening–closing systems associated with six-membered cyclic carbonate[36] and five-membered cyclic dithiocarbonate[37] have been reported.

Scheme 1.15 Reversible network formation and dissociation of spiro- and bicyclic-orthoesters

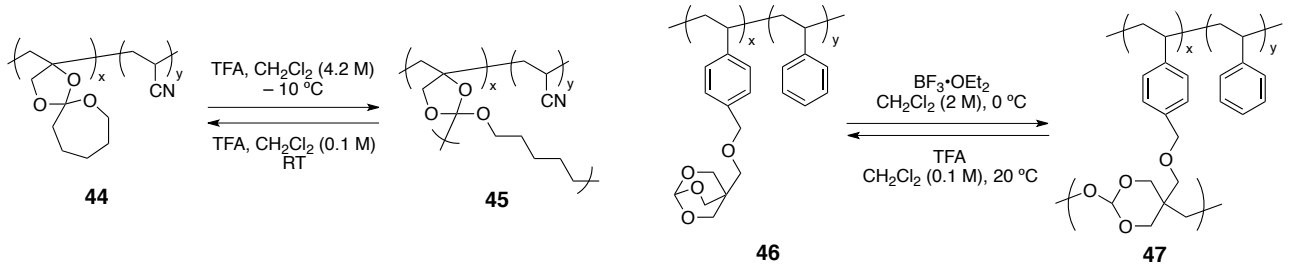

Takata and co-workers applied the interlocked system utilizing the reversible disulfide linkage into recyclable crosslinked polymers (Scheme 1.16).[38] Polyurethane having crown ether **48** was prepared and the crosslinking reaction was carried out by mixing with the bis-ammonium salt **49** in the presence of benzenethiol or **50** in chloroform. The resulting networked polymer **51** could be degraded into thiol **50** and poly(crown ether) **48** by the addition of an equimolar amount of benzenethiol as a reducing agent for the disulfide linkages in DMF that prevents the hydrogen bonds between the *sec*-ammonium salt and the DB24C8 moieties.

Scheme 1.16 Polyrotaxane network synthesized on the basis of disulfide exchange

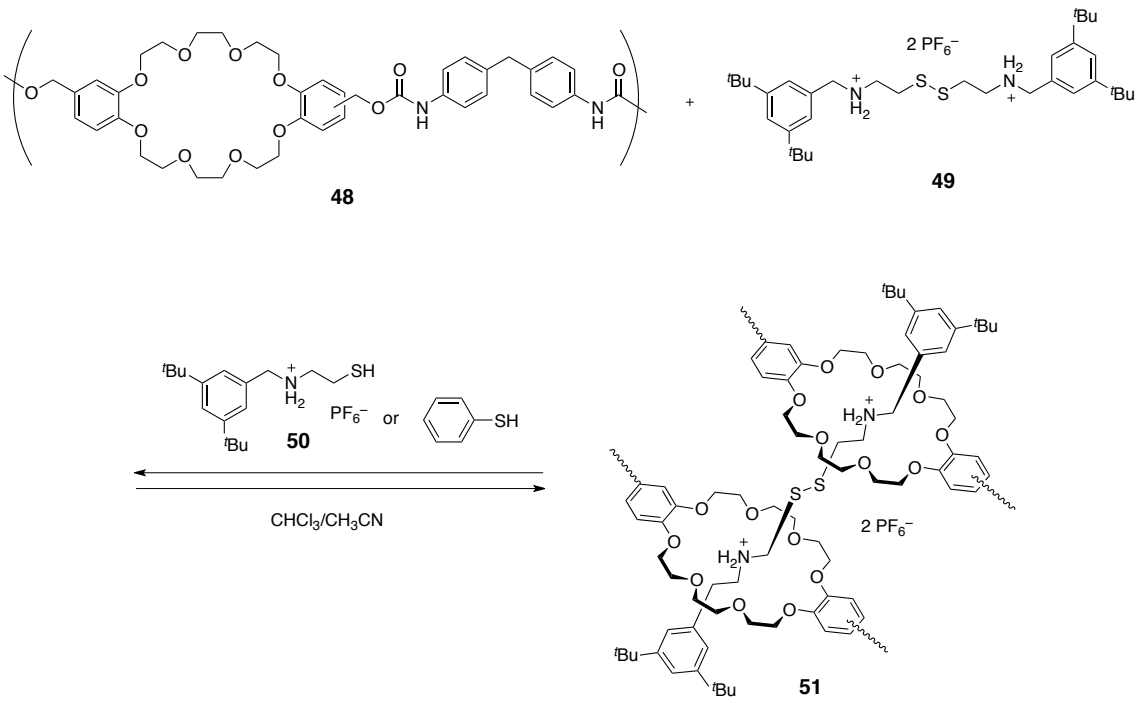

Matyjaszewski *et al.* prepared self-healing polymeric materials with branched architectures and S–S functionalities at the periphery of branches by ATRP. Self-healing behaviors of its polymer films based on thiol–disulfide exchange reactions were investigated in detail using atomic force microscopy (AFM).[39]

TEMPO-containing alkoxyamine derivatives are widely used as unimolecular initiators for

living radical polymerization (Scheme 1.5a). Based on this radically exchangeable alkoxyamine bonds, Otsuka and Takahara have reported a series of thermodynamic polymer crosslinking systems (Scheme 1.17).[40] They prepared two kinds of random copolymers (**52** and **53**) having the potential to generate nitroxide radical and styryl radical, respectively. Upon heating the mixture of **52** and **53** in anisole, the thermodynamic exchange reaction was conducted between the nitroxide radical on the side chain of **52** and styryl radical on the side chain of **53**. Thus the solution became a gel at high concentrations. The dissociation reaction of the networked polymer **54** was achieved by heating the mixture of **54** and an excess of nonfuctionalized alkoxyamine derivative **55**. After heating, copolymers **52** and **53** were reformed. Recently, they have made a polymer gel that can be healed without the need for an external stimulus at room temperature, capitalizing on the reversible formation of diarylbibenzofuranone (DABBF) crosslinkers from the dimerization of stable arylbenzofuranone (ABF) radicals.[41]

Scheme 1.17 Thermodynamic polymer crosslinking system based on radically exchangeable covalent bonds

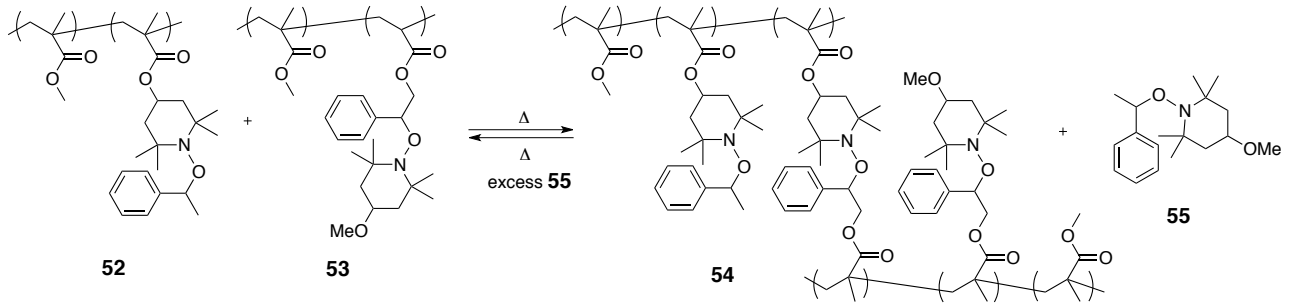

Diels–Alder (DA) reactions are among the most fascinating organic reactions, in terms of both their synthetic potential and reaction mechanism. Consequently, they are recently re-evaluated as a click chemistry[42] and a thermoreversible covalent chemistry[43]. Furan and maleimide have been the predominant functional groups to create thermoreversible DA networks due to the convenient temperature range in which this reaction shifts from products to reactants.[44] Wudl and colleagues

made use of this reaction to develop a material with mechanical properties that compare with commercial epoxy resins, but with the capacity to re-heal under mild conditions (Scheme 1.18).[45] This re-healable resin comprised a trifunctional maleimide **56** and tetrafunctional furan **57**, polymerized at 75 ºC to give a transparent solid **58**. The material was then subjected to fracture-mending studies; after the structural fracture of a monolith, it was treated at 120 ºC under nitrogen for 2 h, after which it had recovered a significant portion of the material's mechanical properties (approximately 41% of the original fracture load).

Scheme 1.18 Re-healable resin based on Diels–Alder reaction

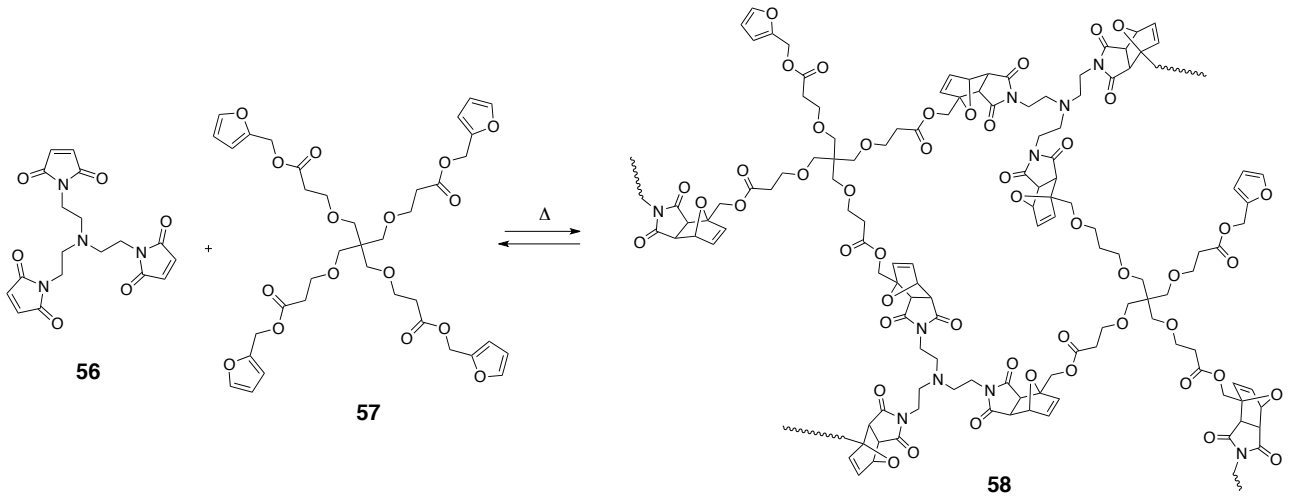

Recently, Lehn and co-workers explored the DA reactions of anthracene–tricynoacrylate[46] and fulvene–tricynoacrylate[47]. They extended these novel linkages in a network and observed self-healing properties.[48]

1.3 Vicinal Tricarboyl Compounds

Vicinal tricarbonyl compounds, such as 1,2,3-indanetrione (dehydrated ninhydrin), dehydroascorbic acid, alloxan, and diphenylpropanetrione (DPPT), have by definition the three contiguous carbonyl groups, and are characterized by a highly activated central carbonyl group.[49,50] Ninhydrin **60** is the hydrate of 1,2,3-indanetrione **59** and used to detect ammonia or primary and secondary amines.[51] When reacting with these free amines, it produces a deep purple color known as Ruhemann's purple **61** (Scheme 1.19a). Also, most of the amino acids are hydrolyzed and react with ninhydrin. Therefore, ninhydrin is most commonly used to detect fingerprints. Dehydroascorbic acid **63** is an oxidized form of ascorbic acid **62** (Vitamin C). It is reduced back to ascorbate by glutathione and other thiols in cells. In aqueous solution, dehydroascorbic acid **63** exists as monohydrate **64** or dihydrate **65**; the cyclic hemiketal structure **64** is the predominant one (Scheme 1.19b). Alloxan **66** is prepared by oxidation of uric acid by nitric acid or oxidation of barbituric acid by CrO_3. Alloxan is a strong oxidizing agent and one-electron reduction of alloxan hydrate **67** results in alloxan radical **68**, which dimerizes to product alloxantin **69**, known as one of the reductones which play an important role in oxidation–reduction systems (Scheme 1.19c).[52]

Scheme 1.19 Representative vicinal tricarbonyl compounds: indanetrione **59**, dehydroascorbic acid **63**, and alloxan **66**

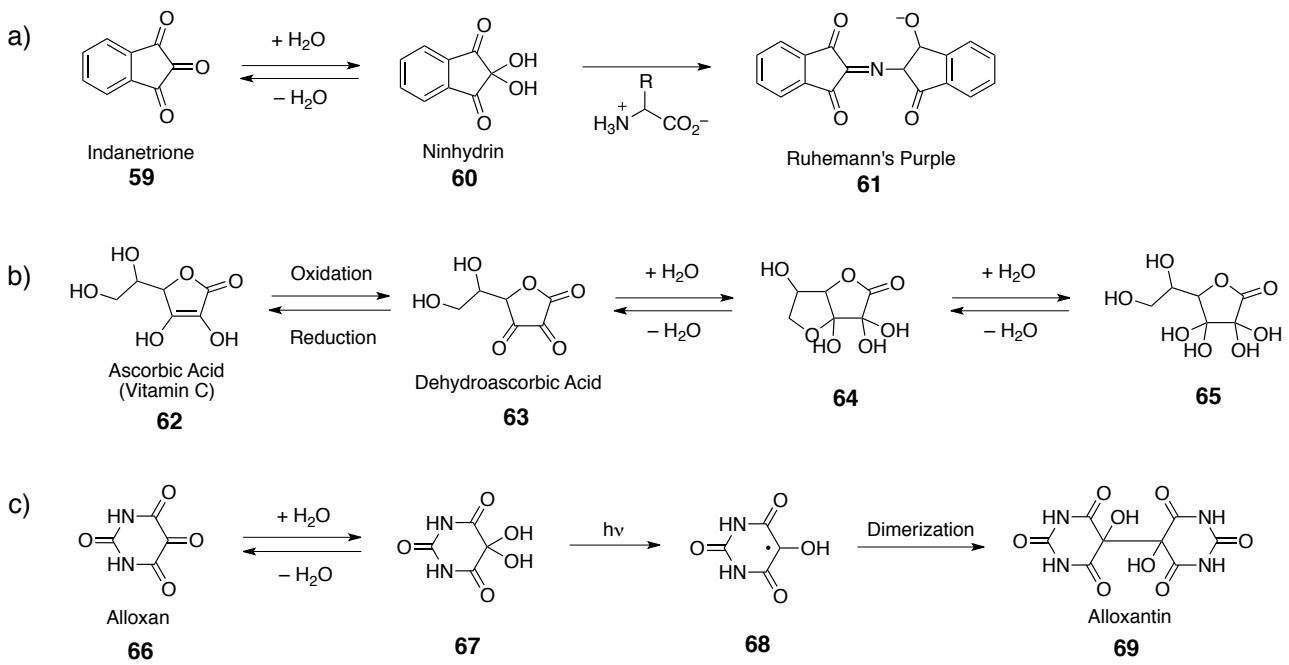

Endo and Okawara synthesized a polymer bearing alloxan structure **71** via oxidation of copolymer of allyl barbituric acid and vinyl acetate **70** with CrO_3 (Scheme 1.20).[53] Photoreduction of hydrate of alloxan polymer **72** resulted in a polymer containing alloxan radical **73**, which did not dimerize and was stable in air because of the steric hindrance of the polymer matrix chain.

Scheme 1.20 Synthesis of a polymer bearing alloxan and its photoreduction

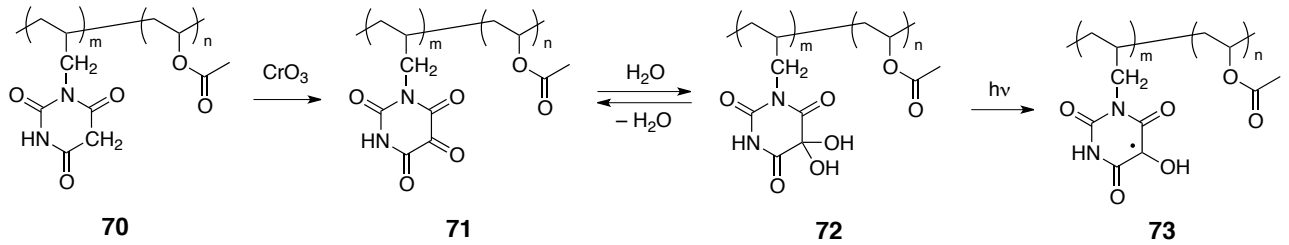

The most characteristic feature of vicinal tricarbonyl compound **74** is its highly electrophilic nature of the central carbonyl group. It is activated by the adjacent two carbonyls and significantly

reactive toward various nucleophiles, such as water, alcohols, amines, and thiols to produce the corresponding *gem*-diol **75**, hemiketal **76**, hemiaminal **77**, and hemithioketal **78**, respectively (Scheme 1.21). Reactions proceed at much lower temperatures, often without the catalysis required for simpler carbonyl compounds. Generally, these addition reactions are reversible. For example, hydrates **75** can be dehydrated to give pure free vicinal tricarbonyls **74** by heating under vacuum,[54] sublimation,[55] distillation,[56] crystallization,[57] azeotropic removal of water,[58] and utilization of dehydrating agents such as molecular sieves or P_2O_5.[59] Moreover, of particular interest is that the reversible addition and elimination process is accompanied by disappearance and appearance of the distinctive color due to the collapse and recovery of the contiguous three carbonyl groups, respectively, hence being detectable by the naked eye.

Scheme 1.21 Reversible addition of water, alcohols, thiols, and amines to vicinal tricarbonyl compounds

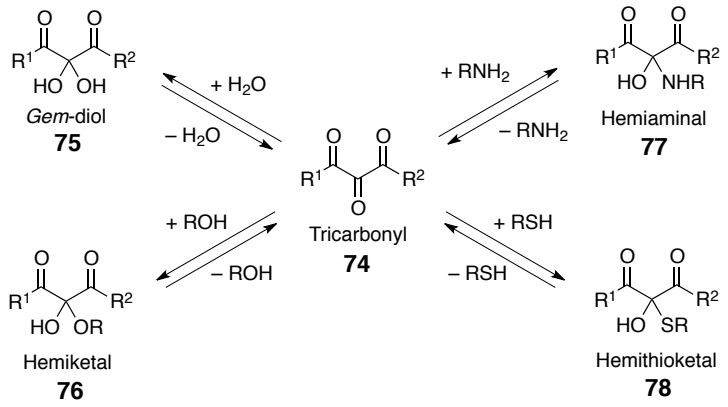

Recently, Endo *et al.* reported design and synthesis of a polystyrene bearing acyclic vicinal tricarbonyl structures in the side chains **79** and detailed investigation of its reversible addition–elimination behavior of water and alcohols to the vicinal tricarbonyl polymer (Scheme 1.22).[60,61] The vicinal tricarbonyl pendants of **79** readily reacted with water or alcohols to quantitatively yield the corresponding *gem*-diol polymer **80** or hemiketal polymer **81**, respectively. On the other hand, heating **80** or **81** under vacuum afforded the original polymers with the vicinal tricarbonyl pendants

80 without deteriorating the polymer structure.

Scheme 1.22 Reversible addition of water or alcohols to a polystyrene bearing vicinal tricarbonyl structure **79**

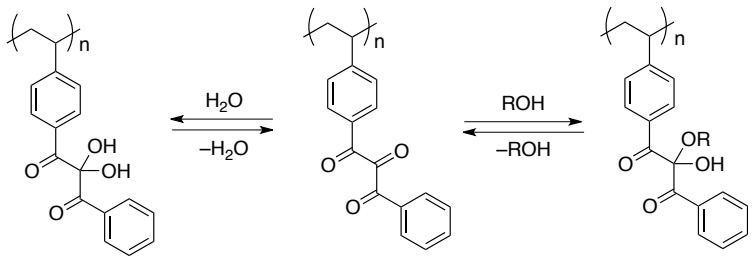

80 **79** **81**

1.4 Brief Overview of the Present Thesis

As mentioned at the beginning of Section 1-2, the incorporation of reversible covalent bonds within networked polymers is lying at the center of the design and synthesis of new polymer materials possessing chemically recyclable or self-healable properties. Although a variety of reversible covalent bonds have been strenuously investigated for such purposes, most of them require strong external stimuli such as heating, light, and catalyst to trigger their bond formation–dissociation process. Therefore, it is still an important and challenging task to explore new reversible covalent bonds that can form and dissociate under mild conditions and to incorporate them within three-dimensionally networked polymer materials. Against this background, the author took notice of the potential usefulness of the reversible addition–elimination reactions of alcohols with vicinal tricarbonyl groups, which proceed in both directions under mild conditions without catalyst. In addition, the reaction progress is detectable by the naked eye. Consequently, one can expect that incorporating the vicinal tricarbonyl–alcohol linkage within networked polymers will lead to polymer materials that can be reversibly crosslinked and decrosslinked under mild conditions without strong external stimuli.

On the basis of the above information, the author has studied to construct reversibly crosslinked and decrosslinked systems under mild conditions without catalyst utilizing vicinal tricarbonyl functionalities. These studies are described in the following four chapters.

Chapter 2 reports the reversible crosslinking and decrosslinking system of a polystyrene bearing monohydrate structure of vicinal tricarbonyl groups with an α,ω-diol, utilizing the direct water–alcohol exchange reactions on the vicinal tricarbonyl moieties.

Chapter 3 focuses on the synthesis and characterization of an acyclic bifunctional vicinal

tricarbonyl compound (bistriketone), its hydrate, and its ethanol-adduct.

Chapter 4 reports the construction of the reversibly crosslinked and decrosslinked systems of commercially available alcoholic polymers, namely, poly(2-hydroxyethyl methacrylate) (PHEMA) and poly(vinyl alcohol) (PVA), using the bifunctional vicinal tricarbonyl compound.

Chapter 5 summarizes the achievements of each chapter and describes perspectives on polymer materials with vicinal tricarbonyl–alcohol linkages.

1.5 References

1) S. J. Rowan, S. T. Cantrill, G. R. L. Cousins, J. K. M. Sanders, J. F. Stoddart, *Angew. Chem. Int. Ed.* **2002**, *41*, 898–952.

2) For selected reviews on reversible covalent polymers, see: (a) T. Maeda, H. Otsuka, A. Takahara, *Prog. Polym. Sci.* **2009**, *34*, 581–604. (b) A. G. Tennyson, B. Norris, C. W. Bielawski, *Macromolecules* **2010**, *43*, 6923–6935. (c) R. J. Wojtecki, M. A. Meador, S. J. Rowan, *Nat. Mater.* **2011**, *10*, 14–27. (d) A. W. Jackson, D. A. Fulton, *Polym. Chem.* **2013**, *4*, 31–45.

3) T. Ishizone, K. Ohmura, Y. Okazawa, A. Hirao, S. Nakahama, *Macromolecules* **1998**, *31*, 2797–2803.

4) (a) K. J. Ivin, J. Leonard, *Polymer* **1965**, *6*, 621–624. (b) M. P. Dreyfuss, P. Dreyfuss, *J. Polym. Sci., Part A-1* **1966**, *4*, 2179–2200.

5) J. M. Andrews, J. A. Semlyen, *Polymer* **1972**, *13*, 142–144.

6) A. Duga, S. Penczek, *Macromolecules* **1990**, *23*, 1636–1639.

7) (a) A. V. Tobolsky, A. Eienberg, *J. Am. Chem. Soc.* **1959**, *81*, 2302–2305. (b) O. Fukumoto, *J. Polym. Sci.* **1956**, *22*, 263–270.

8) B. A. Dolgoplosk, K. L. Makovetsky, Y. V. Korshak, I. A. Oreskin, E. I. Tinyakova, V. A. Yakovlev, *Recl. Trav. Chim. Pays-Bas* **1977**, *96*, M35–M46.

9) M. J. Marsella, H. D. Maynard, R. H. Grubbs, *Angew. Chem. Int. Ed. Engl.* **1997**, *36*, 1101–1103.

10) (a) P. Schwab, M. B. France, J. W. Zillar, R. H. Grubbs, *Angew. Chem. Int. Ed. Engl.* **1995**, *34*, 2039–2041. (b) P. Schwab, R. H. Grubbs, J. W. Ziller, *J. Am. Chem. Soc.* **1996**, *118*, 100–110.

11) (a) D. J. Brunelle, E. P. Boden, T. G. Shannon, J. Am. Chem. Soc. 1990, 112, 2399–2402. (b) D. J. Brunelle, E. P. Boden, *Makromol. Chem. Macromol. Symp.* **1992**, *54/55*, 397–412.

12) J. C. Carpenter, *Makromol. Chem. Macromol. Symp.* **1992**, *42/43*, 397–412.

13) (a) S. Chikaoka, T. Takata, T. Endo, *J. Polym. Sci., Part A: Polym. Chem.* **1990**, *28*, 3101–3106. (b) S. Chikaoka, T. Takata, T. Endo, *Macromolecules* **1991**, *24*, 331–332. (c) S. Chikaoka, T. Takata, T. Endo, *Macromolecules* **1991**, *24*, 6557–6566.

14) Y. Yokoyama, A. B. Padias, E. A. Bratoeff, H. K. Hall, Jr. *Macromolecules* **1982**, *15*, 11–17.

15) W. A. Braunecker, K. Matyjasweski, *Prog. Polym. Sci.* **2007**, *32*, 93–146.

16) C. J. Hawker, A. W. Boston, *Chem. Rev.* **2001**, *101*, 3661–3688.

17) M. Kamigaito, T. Ando, M. Sawamoto, *Chem. Rev.* **2001**, *101*, 3689–3745.

18) A. B. Lowe, C. L. McCormick, *Prog. Polym. Sci.* **2007**, *32*, 283–351.

19) (a) M. E. Belowich, J. F. Stoddart, *Chem. Soc. Rev.* **2012**, *41*, 2003–2024. (b) Y. Xin, J. Yuan, *Polym. Chem.* **2012**, *3*, 3045.

20) M. L. C. Quan, D. J. Cram, *J. Am. Chem. Soc.* **1991**, *113*, 2754–2755.

21) S. Ro, S. J. Rowan, A. R. Pease, D. J. Cram, J. F. Stoddart, *Org. Lett.* **2000**, *2*, 2411–2414.

22) (a) D. Zhao, J. S. Moore, *J. Am. Chem. Soc*. **2002**, *124*, 9996–9997. (b) D. Zhao, J. S. Moore,

Macromolecules **2003**, *36*, 2712–2720.

23) J.-M. Lehn, *Prog. Polym. Sci.* **2005**, *30*, 814–831.

24) (a) W. G. Skene, J.-M. Lehn, *Proc. Natl. Acad. Sci. USA* **2004**, *101*, 8270–8275. (b) N. Giuseppone, J.-M. Lehn, *J. Am. Chem. Soc.* **2004**, *126*, 11448–11449. (c) J. F. Folmer-Andersen, J.-M. Lehn, *J. Am. Chem. Soc.* **2011**, *133*, 10966–10973.

25) P. T. Glink, A. I. Oliva, J. F. Stoddart, A. J. P. White, D. J. Williams, *Angew. Chem. Int. Ed.* **2001**, *40*, 1870–1875.

26) (a) S. J. Cantrill, S. J. Rpwan, J. F. Stoddart, *Org. Lett.* **1999**, *1*, 1363–1366.

(b) S. J. Rowan, J. F. Stoddart, *Org. Lett*. **1999**, *1*, 1913–1916.

27) (a) K. S. Chichak, S. J. Cantrill, A. R. Pease, S.-H. Chiu, G. W. V. Cave, J. L. Atwood, J. F. Stoddart, *Science* **2004**, *304*, 1308–1312. (b) J. S. Siegel, *Science* **2004**, *304*, 1256–1258. (c) S. J. Cantrill, K. S. Chichak, A. J. Peters, J. F. Stoddart, *Acc. Chem. Res.* **2005**, *38*, 1–9.

28) W. J. Lees, G. M. Whitesides, *J. Org. Chem.* **1993**, *58*, 642–647.

29) (a) Y. Furusho, T. Hasegawa, A. Tsuboi, N. Kihara, T. Takata, *Chem. Lett.* **2000**, *29*, 18–19. (b) Y. Furusho, T. Oku, T. Hasegawa, A. Tsuboi, N. Kihara, T. Takata, *Chem. Eur. J.* **2003**, *9*, 2895–2903.

30) (a) I. Huc, J.-M. Lehn, *Proc. Natl. Acad. Sci. USA* **1997**, *94*, 2106–2111. (b) J.-M. Lehn, *Chem. Eur. J.* **1999**, *5*, 2455–2463. (c) P. T. Corbett, J. Leclaire, L. Vial, K. R. West, J.-L. Wietor, J. K. M. Sanders, S. Otto, *Chem. Rev.* **2006**, *106*, 3652–3711.

31) (a) S. Otto, R. L. E. Furlan, J. K. M. Sanders, *Science* **2002**, *297*, 590–593. (b) P. T. Corbett, L. H. Tong, J. K. M. Sanders, S. Otto, *J. Am. Chem. Soc.* **2005**, *127*, 8902–8903.

32) For selected reviews on polymer recycling, see: (a) F. Sanda, T. Endo, *Polym. Recycl.* **1998**, *3*, 159–163. (b) T. Endo, D. Nagai, *Macromol. Symp.* **2003**, *201*, 203. (c) T. Takata, *Polym. J.* **2006**, *38*, 1–20. (d) H. Nishida, *Polym. J.* **2011**, *43*, 435–447.

33) For selected reviews on self-healing materials, see: (a) M. D. Hagar, P. Greil, C. Leyens, S. van der Zwaag, U. S. Schubert, *Adv. Mater.* **2010**, *22*, 5424–5430. (b) C. J. Kloxin, T. F. Scott, B. J. Adzima, C. N. Bowman, *Macromolecules* **2010**, *43*, 2643–2653. (c) N. K. Guimard, K. K. Oehlenschlaeger, J. Zhou, S. Hilf, F. G. Schumidt, C. Barner-Kowollik, *Macromol. Chem. Phys.* **2012**, *213*, 131–143.

34) (a) T. Endo, T. Suzuki, F. Sanda, T. Takata, *Macromolecules* **1996**, *29*, 3315–3316. (b) T. Endo, T. Suzuki, F. Sanda, T. Takata, *Macromolecules* **1996**, *29*, 4819. (c) T. Endo, T. Suzuki, F. Sanda, T. Takata, *Bull. Chem. Soc. Jpn.* **1997**, *70*, 1205–1210. (d) K. Yoshida, F. Sanda, T. Endo, *J. Polym. Sci., Part A: Polym. Chem.* **1999**, *37*, 2551–2558.

35) M. Hitomi, F. Sanda, T. Endo, *Macromol. Chem. Phys.* **1999**, *200*, 1268–1273.

36) J. Matsuo, K. Aoki, F. Sanda, T. Endo, *Macromolecules* **1998**, *31*, 4432–4438.

37) T. Nakamura, B. Ochiai, T. Endo, *Macromolecules* **2005**, *38*, 4065–4066.

38) (a) T. Oku, Y. Furusho, T. Takata, *J. Polym. Sci. Part A: Polym. Chem.* **2003**, *41*, 119–123. (b) T. Oku, Y. Furusho, T. Takata, *Angew. Chem. Int. Ed.* **2004**, *43*, 966–969. (c) T. Bilig, T. Oku, Y. Furusho, Y. Koyama, S. Asai, T. Takata, *Macromolecules* **2008**, *41*, 8496–8503. (d) Y. Koyama, T. Yoshii, Y. Kohsaka, T. Takata, *Pure Appl. Chem.* **2013**, *85*, 835–842.

39) (a) J. Kamada, K. Koynov, C. Corten, A. Juhari, J. A. Yoon, M. W. Urban, A. C. Balazs, K. Matyjaszewski, *Macromolecules* **2010**, *43*, 4133–4139. (b) J. A. Yoon, J. Kamada, K. Koynov, J. Mohin, R. Nicolaÿ, Y. Zhang, A. C. Balazs, T. Kowalewski, K. Matyjaszewski, *Macromolecules* **2012**, *45*, 142-149.

40) (a) H. Otsuka, K. Aotani, Y. Higaki, A. Takahara, *Chem. Commun.* **2002**, 2838–2839. (b) Y. Higaki, H. Otsuka, A. Takahara, *Macromolecules* **2004**, *37*, 1696–1701. (c) G. Yamaguchi, Y. Higaki, H. Otsuka, A. Takahara, *Macromolecules* **2005**, *38*, 6316–6320. (d) Y. Higaki, H. Otsuka, A. Takahara, *Macromolecules* **2006**, *39*, 2121–2125. (e) H. Otsuka, K. Aotani, Y. Higaki, Y. Amamoto, A. Takahara, *Macromolecules* **2007**, 40, 1429–1434. (f) Y. Amamoto, Y. Higaki, Y. Matsuda, H. Otsuka, A. Takahara, *Chem. Lett.* **2007**, *36*, 774–775. (g) Y. Amamoto, Y. Higaki, Y. Matsuda, H. Otsuka, A. Takahara, *J. Am. Chem. Soc*. **2007**, *129*, 13298–13304. (h) Y. Amamoto, M. Kikuchi, H. Masunaga, S. Sasaki, H. Otsuka, A. Takahara, *Macromolecules* **2009**, *42*, 8733–8738. (i) Y. Amamoto, M. Kikuchi, H. Masunaga, S. Sasaki, H. Otsuka, A. Takatahara, *Macromolecules* **2010**, *43*, 1785–1791. (j) J. Su, Y. Amamoto, M. Nishihara, A. Takahara, H. Otsuka, *Polym. Chem.* **2011**, *2*, 2021–2026.

41) (a) K. Imato, M. Nishizawa, T. Kanehara, Y. Amamoto, A. Takahara, H. Otsuka, *Angew. Chem. Int. Ed.* **2012**, *51*, 1138–1142. (b) M. Nishihara, K. Imato, A. Irie, T. Kanehara, A. Kano, A. Maruyama, A. Takahara, H. Otsuka, *Chem. Lett.* **2013**, *42*, 377–379.

42) (a) H. C. Kolb, M. G. Finn, K. B. Sharpless, *Angew. Chem. Ind. Ed.* **2001**, *40*, 2004-2021. (b) C. R. Becer, R. Hoogenboom, U. S. Schubert, *Angew. Chem. Int. Ed.* **2009**, *48*, 4900–4908.

43) Y.-L. Liu, T.-W. Chuo, *Polym. Chem.* **2013**, *4*, 2194–2205.

44) (a) C. Goussé, A. Gandini, P. Hodge, *Macromolecules* **1998**, *31*, 314–321. (b) Y. Imai, H. Itoh, K. Naka, Y. Chujo, *Macromolecules* **2000**, *33*, 4343–4346. (c) R. Gheneim, C. Perez-Berumen, A. Gandini, *Macromolecules* **2002**, *35*, 7246–7253. (d) X. Chen, F. Wudl, A. K. Mal, H. Shen, S. R. Nutt, *Macromolecules* **2003**, *36*, 1802–1807. (e) Y. Zhang, A. A. Broekhuis, F. Piccioni, *Macromolecules* **2009**, *42*, 1906–1912. (f) K. Ishida, V. Weibel, N. Yoshie, *Polymer* **2011**, *52*, 2877–2882. (g) N. Yoshie, S. Saito, N. Oya, *Polymer* **2011**, *52*, 6074–6079. (h) K. C. Koehler, K. S. Anseth, C. N. Bowman, *Biomacromolecules* **2013**, *14*, 538–547.

45) X. Chen, M. A. Dam, K. Ono, A. Mal, H. Shen, S. R. Nutt, K. Sheran, F. Wudl, *Science* **2002**, *295*, 1698–1702.

46) P. Reutenauer, P. J. Boul, J.-M. Lehn, *Eur. J. Org. Chem.* **2009**, *11*, 1691–1697.

47) P. J. Bowl, P. Reutenauer, J.-M. Lehn, *Org. Lett.* **2005**, *7*, 15–18.

48) P. Reutenauer, E. Buhler, P. J. Boul, S. J. Candau, J.-M. Lehn, *Chem. Eur. J.* **2009**, *15*, 1893–1900.

49) (a) M. B. Rubin, R. Gleiter, *Chem. Rev.* **2000**, *100*, 1121–1164. (b) M. B. Rubin, *Chem. Rev.* **1975**, *75*, 177–202.

50) H. H. Wasserman, J. Parr, *J. Acc. Chem. Res.* **2004**, *37*, 687–701.

51) For selected reviews on ninhydrin and related compounds, see: (a) A. Schönberg, E. Singer, *Tetrahedron* **1978**, *34*, 1285–1300. (b) M. M. Joullié, T. R. Tompson, N. H. Nemeroff, *Tetrahedron* **1991**, *47*, 8791–8830.

52) (a) T. Endo, M. Okawara, *Bull. Chem. Soc. Jpn.* **1979**, *52*, 3473–3474. (b) T. Endo, M.

Okawara, *J. Polym. Sci.: Polym. Chem. Ed.* **1979**, *17*, 3667–3674. (c) T. Endo, M. Okawara, *J. Org. Chem.* **1980**, *45*, 2663–2666.

53) T. Endo, E. Fujiwara, M. Okawara, *J. Polym. Sci. Polym. Chem. Ed.* **1981**, *19*, 1091–1099.

54) (a) M. Hirama, Y. Fukuzawa, S. Ito, *Tetrahedron Lett.* **1978**, *19*, 1299–1302. (b) R. Moubasher, A. M. Othman, *J. Am. Chem. Soc.* **1950**, *72*, 2667–2669. (c) A. R. Lepley, J. P. Thelman, *Tetrahedron* **1966**, *22*, 101–110.

55) (a) J. C. Netto-Ferreira, M. T. Silva, F. P. Puget, *J. Photochem. Photobiol. A: Chem.* **1998**, *119*, 165–170. (b) M. T. Silva, R. Braz-Filho, J. C. Netto-Ferreira, *J. Braz. Chem. Soc.* **2000**, *11*, 479–485.

56) (a) M. R. Mahran, W. M. Abdou, M. M. Sidky, H. Wamhoff, *Synthesis* **1987**, *5*, 506–508. (b) D. B. Sharp, H. A. Hoffman, *J. Am. Chem. Soc.* **1950**, *72*, 4311–4313.

57) J. D. Roberts, D. R. Smith, C. C. Lee, *J. Am. Chem. Soc.* **1951**, *73*, 618–625.

58) G. B. Gill, M. S. H. Idris, K. S. Kirollos, *J. Chem. Soc., Perkin Trans. 1* **1992**, 2355–2365.

59) A. Schönberg, E. Singer, *Chem. Ber.* **1970**, *103*, 3871–3884.

60) (a) T. Dei, K. Morino, A. Sudo, T. Endo, *J. Polym. Sci., Part A: Polym. Chem.* **2011**, *49*, 2245–2251. (b) T. Dei, K. Morino, A. Sudo, T. Endo, *J. Polym. Sci., Part A: Polym. Chem.* **2012**, *50*, 2619–2625.

61) K. Morino, A. Sudo, T. Endo, *Macromolecules* **2012**, *45*, 4494–4499.

Chapter 2

Reversible Crosslinking and Decrosslinking System of Polystyrenes Bearing the Monohydrate Structure of Vicinal Tricarbonyl Group through Water–Alcohol Exchange

2.1 Introduction

Vicinal tricarbonyl compounds, such as alloxan, 1,2,3-indanetrione, dehydroascorbic acid, and diphenylpropanetrione (DPPT, **1**), have by definition the three contiguous carbonyl groups, and are characterized by a highly electrophilic central carbonyl group, which is activated by the adjacent two carbonyls and significantly reactive toward various nucleophiles, such as water and alcohols (Scheme 2.1).[1,2] Hence, vicinal tricarbonyl compounds are usually obtained as their hydrated forms (2,2-*gem*-diol, DPPT-H_2O, **2**) as a result of hydration with moisture in air or solvents used during the isolation processes (Scheme 2.1a). These hydrates can be dehydrated to give pure free vicinal tricarbonyls (**1**) by heating under vacuum,[3–5] sublimation,[5,6] distillation,[7–10] crystallization,[9] azeotropic removal of water,[10] and utilization of dehydrating agents such as molecular sieves 4A or P_2O_5.[6,10,11] This reversible hydration–dehydration nature of vicinal tricarbonyls enables us to utilize them as recyclable dehydrating agents.[12] Of particular interest is that the reversible hydration process is accompanied by disappearance and appearance of the distinctive yellow color due to the collapse and recovery of the contiguous three carbonyl groups, respectively, hence being detectable by the naked eye.[1,2] The vicinal tricarbonyl compounds exhibit a similar behavior toward alcohols (Scheme 2.1b); the addition of alcohols readily proceeds at ambient temperature to form the corresponding alcohol adducts (hemiketal, DPPT-ROH, **3**) without any catalyst, being accompanied

by disappearance of their distinctive color arising from the vicinal tricarbonyl structures. Conversely, the vicinal tricarbonyl compounds are obtained by heating under vacuum to remove the alcohols.

Scheme 2.1 Reversible Addition of Water and Alcohols to Vicinal Tricarbonyl Groups

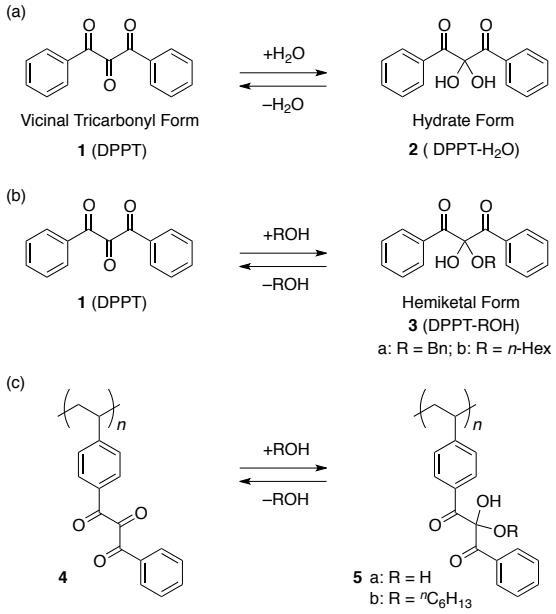

Motivated by the characteristic features of vicinal tricarbonyl compounds, Endo *et al.* recently reported design and synthesis of a polystyrene derivative bearing acyclic vicinal tricarbonyl structures in the side chains (**4**) and detailed investigation of its reversible addition–elimination behavior of water and alcohols to the vicinal tricarbonyl polymer (Scheme 2.1c).[13-16] The vicinal tricarbonyl pendants of **4** readily reacted with water or alcohols to quantitatively yield the corresponding water or alcohol adduct polymer **5**. On the other hand, heating **5** under vacuum afforded the original polymers with the vicinal tricarbonyl pendants **4** without deteriorating the polymer structure.

Polymer materials that can be reversibly crosslinked and decrosslinked through covalent bonds have recently attracted much attention from the standpoint of chemical recycling as well as

self-healing materials.[17-19] Taking advantage of the reversible nature of the alcohol addition to vicinal tricarbonyl groups, Endo *et al.* developed a new reversible crosslinking system from the vicinal tricarbonyl polymers **4** and an α,ω-diol as the crosslinking reagent. However, the vicinal tricarbonyl polymer system has some drawback toward materials application; the decrosslinking step utilizing the elimination of alcohols requires heating at around 100 °C under reduced pressure. In addition, the polymers bearing vicinal tricarbonyl pendants are susceptible to moisture and need to be preserved under dry conditions. Therefore, new processes or systems that can be reversibly crosslinked and decrosslinked under mild conditions are desired to be developed.

Over the course of the study to develop new polymer materials based on the vicinal tricarbonyl structures, the author noted that the two reversible reactions, the reversible addition of water and that of alcohol, indicated that the apparently direct exchange of water and alcohols on the vicinal tricarbonyls *in situ* is possible by way of vicinal tricarbonyl intermediates (Figure 2.1a). On the basis of this equilibrium, the author envisaged that use of the *gem*-diol polymers would lead to a new system that can be reversibly crosslinked and decrosslinked system under mild conditions through the direct water–alcohol exchange reaction (Figure 2.1b). However, no detailed study for such direct water–alcohol exchange reactions had been reported to date. Therefore, the author started from the systematic study of the water–alcohol exchange reactions using a unit model compound, and then the author went into the *gem*-diol polymers. Herein, the author describes the reversible crosslinking and decrosslinking system of polystyrene bearing the *gem*-diol structure of vicinal tricarbonyl group using an α,ω-alcohol exploiting the direct water–alcohol exchange reaction along with the detailed investigation using a unit model compound.

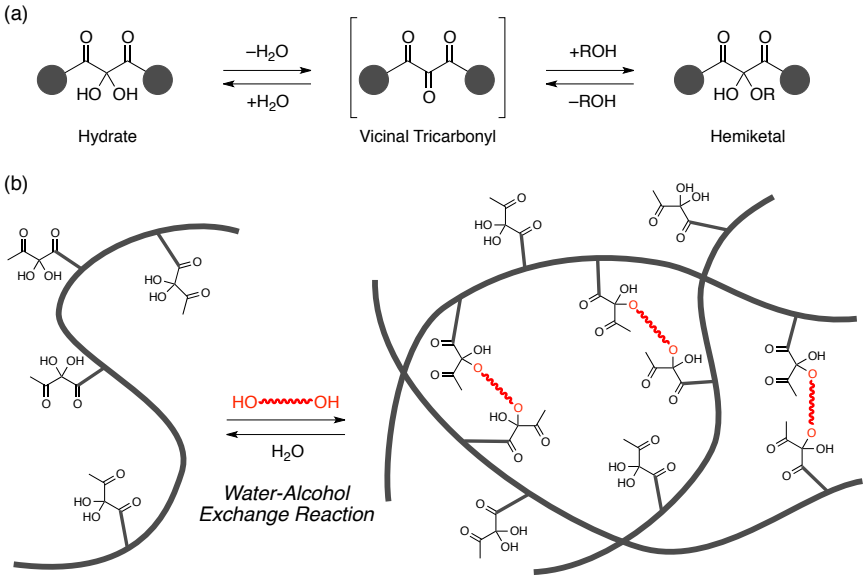

Figure 2.1 Schematic illustrations of (a) water–alcohol exchange reaction on vicinal tricarbonyl groups and (b) reversible crosslinking and decrosslinking of polymers bearing vicinal tricarbonyl pendants using α,ω-diols through water–alcohol exchange reaction.

2.2 Experimental Section

2.2.1 Materials

Chloroform, chloroform-*d* ($CDCl_3$) and dimethyl solfoxide-d_6 (DMSO-d_6) were distilled over molecular sieves 4A (MS 4A). Acetone and acetone-d_6 were distilled over $CaCl_2$. Benzyl alcohol and 1-hexanol were distilled over CaH_2. 1,4-Dioxane was distilled over sodium benzophenone ketyl. D_2O (Merck KGaA, Germany), *n*-Hexane (Wako Pure Chemical Industries, Japan) and 1,6-hexanediol (Wako) were purchased and used without further purification. Diphenylpropanetrione monohydrate (**2**, DPPT-H_2O), diphenylpropanetrione-benzyl alcohol adduct (**3a**, DPPT-BnOH) and polymer bearing monohydrate structure of vicinal tricarbonyl moieties **5a** were synthesized according to the literature.[13] The number-average molecular weight of **5a** was estimated to be 1.5 x 10^4 with a polydispersity index (PDI) of 10.3 by size exclusion chromatography (SEC) based on PSt standards. Polymer **5a** with number-average molecular

weight of 3.8 x 10^3 with a PDI of 2.9 was prepared from the polymer synthesized by radical polymerization of 4-vinyldibenzoylmethane with 20 mol% of 2,2'-azobis(isobutyronitrile) (AIBN) at 80 ºC for 18 h.

2.2.2 General Measurements

^{1}H NMR spectra were measured on a JEOL JNM-ECS 400 spectrometer at a resonance frequency of 400 MHz with tetramethylsilane (TMS) as an internal standard. NMR chemical shifts were reported in delta unit (δ). IR spectra were recorded on a Thermo Scientific Nicolet iS10 spectrometer. UV–vis spectra were measured with a JASCO V-570 spectrophotometer in a 1-cm quartz cell. Number-average and weight-average molecular weights (M_n, M_w) and polydispersity indices (M_w/M_n) of the polymers were estimated by size exclusion chromatography (SEC) using tetrahydrofuran (THF) as the eluent at a flow rate of 0.6 mL/min at 40 ºC, performed on a Tosoh chromatograph model HLC-8320 system equipped with Tosoh TSKgel SuperHM-H styrogel columns (6.0 mm ϕ x 15 cm, 3 and 5 μm bead sizes), UV–vis detector (254 nm). The molecular weight calibration curve was obtained with polystyrene standards. Thermogravimetric analysis (TGA) was performed on a Seiko Instrument Inc. TG-DTA 6200 with an aluminum pan under a 150 mL/min N_2 flow at a heating rate of 10 ºC/min. The single crystal X-ray data for the benzyl alcohol adduct (**3a**) was collected on a Bruker Smart Apex CCD-based X-ray diffractometer with Mo-Kα radiation (λ = 0.71073 Å).[20]

2.2.3 Model Reactions

Water–Alcohol Exchange Reaction of DPPT-H_2O 2 with Alcohols. A typical experimental procedure was as follows. **2** (64.1 mg, 0.250 mmol) was dissolved in 0.50 mL of $CDCl_3$ under an

argon atmosphere. To the solution was added BnOH (26.2 μL, 0.250 mmol), and the solution was transferred to an NMR tube. The reaction progress was monitored by ^{1}H NMR.

Water–Alcohol Exchange Reaction of DPPT-BnOH 3a with Water. DPPT-BnOH (7.81 mg, 0.025 mmol) was dissolved in 0.50 mL of a mixture of D_2O and acetone-d_6 (1/9, v/v) under an argon atmosphere, and the solution was transferred to an NMR tube. The reaction progress was monitored by ^{1}H NMR.

Water–Alcohol Exchange Reaction of Polystyrene Derivative 5a with Alcohols. A typical experimental procedure was as follows. Polymer **5a** (282 mg, 1.00 mmol) was dissolved in chloroform (5.0 mL). To the solution was added 1-hexanol (374 μL, 3.00 mmol), and the reaction mixture was stirred at ambient temperature under argon atmosphere for 3 days. The resulting mixture was precipitated with *n*-hexane and filtered to obtain polymer **6** (298 mg, 94%) as a pale yellow solid. ^{1}H NMR (400 MHz, acetone-d_6, 298 K): δ 8.17–5.20 (br, aromatic-*H*, –O*H*), 3.70–3.30 (br, –OC*H*$_2$–), 2.40–0.50 (br, aliphatic-*H*) ppm. IR (ATR) 3415 (O–H), 2929 (C–H), 1721 (central C=O), 1682 (side C=O) cm^{-1}.

Recovery of Polymer 5a from Polymer 6 through Water–Alcohol Exchange Reaction with Water. Polymer **6** (151 mg, 0.469 mmol) was dissolved in 10 mL of a mixture of water and acetone (1/9, v/v), and the resultant solution was stirred at ambient temperature for 3 days. The resulting mixture was precipitated with a large amount of water and filtered to obtain polymer **5a** (127 mg, 96%) as a pale yellow solid. ^{1}H NMR (400 MHz, acetone-d_6, 298 K): see Figure 2.9.

2.2.4 Crosslinking and Decrosslinking

Crosslinking of Polystyrene Derivative 5a through the Water–Alcohol Exchange Reaction with 1,6-Hexanediol. To a solution of polymer **5a** (282 mg, 1.00 mmol) in acetone (0.50 mL) was added 1,6-hexanediol (11.8 mg, 0.100 mmol), and the reaction mixture was stirred at ambient temperature under argon atmosphere for 5 days. The resultant highly viscous mixture was filtered and washed with acetone (5.0 mL). The insoluble part was dried *in vacuo* at room temperature to afford the networked polymer **7** (292 mg, 99%) as a yellow solid. IR (ATR) 3392 (OH), 2932 (C–H), 1721 (central C=O), 1674 (side C=O) cm^{-1}.

Recovery of Polymer 5a by Decrosslinking of Networked Polymer 7 through the Water–Alcohol Exchange Reaction with Water. A pea-sized piece of networked polymer **7** (168 mg) was immersed in 10 mL of water–acetone (1/9, v/v) and the mixture was gently stirred at room temperature. The polymer swelled gradually and then completely dissolved within 2 days. The resultant solution was stirred for one more day, and then mixture was reprecipitated with a large amount of water and filtered to obtain polymer **5a** (149 mg, 0.527 mmol, 91%) as a pale yellow solid. ^{1}H NMR (400 MHz, acetone-d_6, 298 K): see Figure 2.13.

2.3 Results and Discussion

2.3.1 Reversible Water–Alcohol Exchange Reaction of Monohydrate of DPPT

The author chose the monohydrate of diphenylpropanetrione **2** (DPPT-H_2O) as a unit model compound for polystyrene bearing monohydrate structure of vicinal tricarbonyl group and investigated its water–alcohol exchange reaction in detail. Before investigating the model reaction, the author prepared the benzyl-alcohol adduct of diphenypropanetrione **3a** (DPPT-BnOH) according to the previous report.[15] Single crystals of **3a** suitable for X-ray analysis were grown from a solution in benzyl alcohol. The X-ray analysis revealed that the benzyl alcohol was added to the central carbonyl group, and the central carbon atom adopted the tetrahedral configuration (Figure 2.2).[20] The author monitored the water–alcohol exchange reaction of **2** with benzyl alcohol in $CDCl_3$ by ^1H NMR. Figure 2.3 shows the time dependence of partial ^1H NMR spectra in the aromatic region of an equimolar mixture of **2** and benzyl alcohol ($[\mathbf{2}]_0 = [BnOH]_0 = 0.5$ M) after mixing at ambient temperature, indicating that three species, *i.e.*, **2**, and diphenylpropanetrione (DPPT, **1**), and BnOH adduct (DPPT-BnOH, **3a**) were involved in the equilibrium. The existence of **1** was also evidenced by the naked-eye observation that the reaction mixture took on the distinctive yellow color due to the contiguous three carbonyl groups.[1,13-15] The *ortho*-proton signals of the benzene rings of **1**, **2**, and **3a** appeared as three clearly separated ones at around 8 ppm, with which the author estimated the content ratios of the three species. The contents of the three species were plotted against the reaction time as shown in Figure 2.4A. At an early stage of the reaction (10 min, Figure 2.3a), the major part of the mixture was **2**, and a small amount of **1** with a trace amount of **3a** were detected after 1h (Figure 2.3b). The content of **1** reached maximum a few hours later, and the content of **3a** gradually increased with time, while **1** and **2** decreased monotonously (Figure 2.3c). The mixture reached equilibrium within 48 h, at which the content ratios of **1**, **2**, and **3a** were 18%,

33%, and 49%, respectively (Figure 2.3d). The initial concentration of the starting materials and the reaction temperature markedly affected the reaction rate as well as the position of the equilibrium of the water–alcohol exchange reaction. When the initial concentrations of **2** and BnOH were set to 0.1 M, the reaction became significantly slow and 4 days were required for reaching equilibrium at ambient temperature, where the content ratios of **1**, **2**, and **3a** were 38%, 34%, and 28%, respectively (Figure 2.4B). In contrast, the rate of the exchange reaction became much higher at 50 ºC than that at ambient temperature and the equilibrium state was achieved within half a day. The position of the equilibrium state was also shifted to a certain extent toward the free tricarbonyl **1**; the contents of **1**, **2**, and **3a** at equilibrium were 49%, 15%, and 36%, respectively at 50 °C (Figure 2.4C).

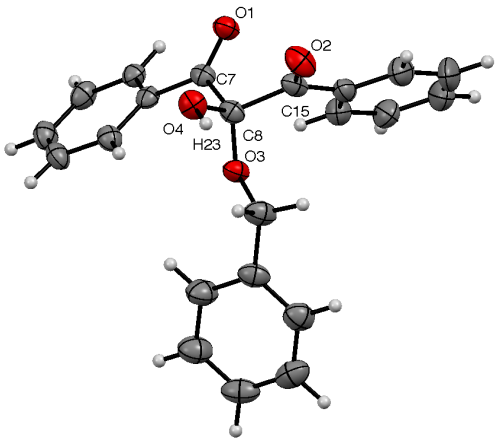

Figure 2.2 ORTEP structure of **3a** with thermal ellipsoids at 50% probability. Selected data: bond lengths; O1-C7 1.214 Å, O2-C15 1.208 Å, O3-C8 1.407 Å, O4-C8 1.394 Å, angles; O3-C8-O4 113.36º, C7-C8-C15 110.12º, dihedral angles; O1-C7-C8-O3 -133.36º, O2-C15-C8-O3 -129.29º.

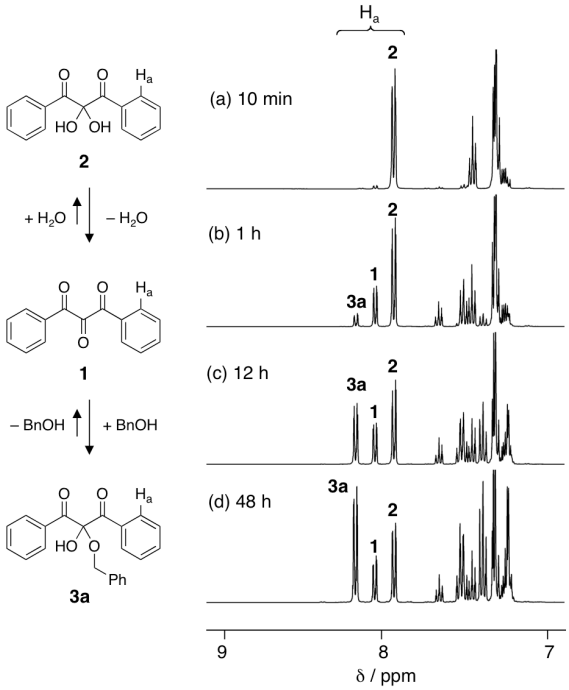

Figure 2.3 ^{1}H NMR spectra of the reaction mixture of DPPT-H_2O **2** with equimolar benzyl alcohol in $CDCl_3$ at ambient temperature after (a) 10 min, (b) 1 h, (c) 12 h, and (d) 48 h (400 MHz, 298 K). $[\mathbf{2}]_0 = [BnOH]_0 = 0.5$ M.

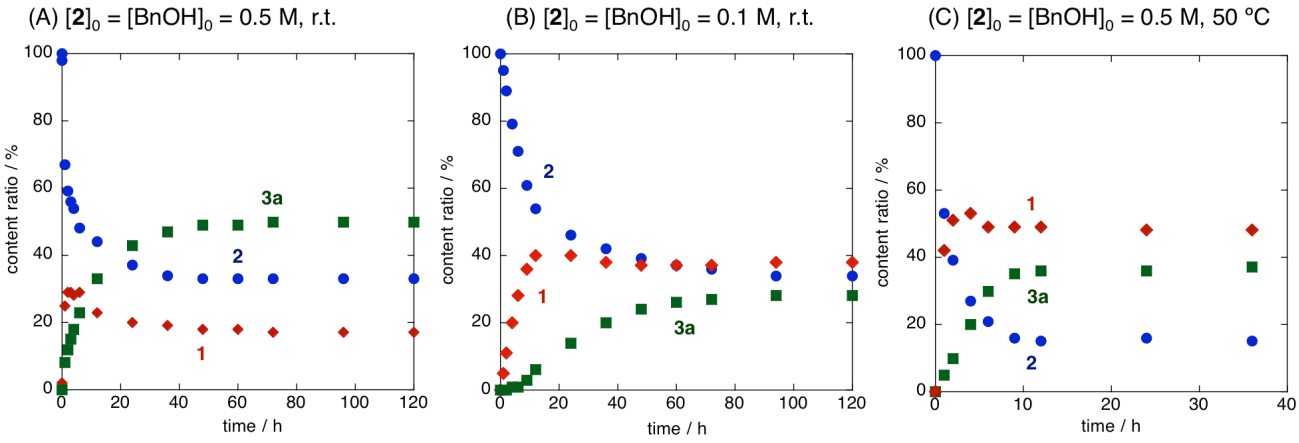

Figure 2.4 Changes in the content ratio of **1**, **2**, and **3a** upon mixing DPPT-H_2O **2** and BnOH in $CDCl_3$: (A) $[\mathbf{2}]_0 = [BnOH]_0 = 0.5$ M, r.t., (B) $[\mathbf{2}]_0 = [BnOH]_0 = 0.1$ M, r.t., and (C) $[\mathbf{2}]_0 = [BnOH]_0 = 0.5$ M, 50 ºC.

Next, the author investigated the effect of solvent on the water–alcohol exchange reaction (Figure 2.5). The author chose 1-hexanol instead of benzyl alcohol, because the BnOH adduct showed poor solubility and insufficient peak separation of the ^{1}H NMR spectra in acetone and DMSO. In $CDCl_3$, the exchange reaction with 1-hexanol exhibited a similar behavior to that with benzyl alcohol and the mixture reached equilibrium within 48 h, at which the content ratios of **1**, **2**, and **3b** were estimated to be 11%, 21%, and 68% by using the integrals of the ^{1}H NMR spectrum. The content of the 1-hexanol adduct **3b** at equilibrium was much higher than that of **3a** in $CDCl_3$ probably because of the less steric hindrance of the hydroxyl group in 1-hexanol than that of benzyl alcohol. In contrast, the exchange reaction rate slowed very much in DMSO-d_6 and it took *ca*. 120 h until equilibrium was attained. The content of **3b** was as low as 23% at equilibrium, which was much lower than that in $CDCl_3$. This is consistent with our previously reported result that the addition of alcohol to **1** is slowed in polar solvents,[15] thus indicating that the rate-determining step for the water–alcohol exchange reaction is most likely to be the addition of the alcohol. The reaction rate was even lowered in acetone-d_6 than in DMSO-d_6, and it required more than 240 h to achieve equilibrium, although the content of **3b** was higher than that in DMSO-d_6 at the final equilibrium state.

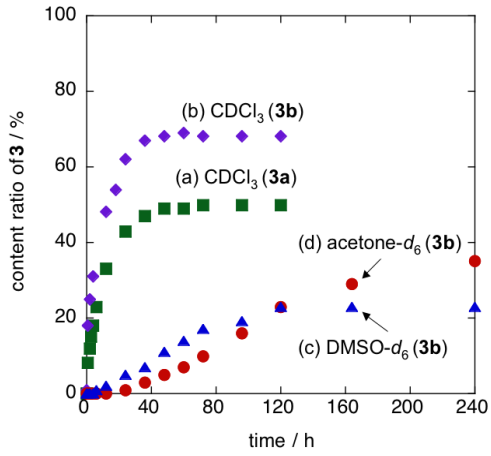

Figure 2.5 Changes in the content ratios of **3a** and **3b** upon mixing with BnOH in $CDCl_3$ (a), and with 1-hexanol in $CDCl_3$ (b), in DMSO-d_6 (c), and in acetone-d_6 (d) at ambient temperature. $[\mathbf{2}]_0 = [\text{1-hexanol}]_0 = 0.5$ M.

The author demonstrated the back reaction directly from **3a** to **2** exploiting the water–alcohol exchange reaction in a similar way to that for the hydration of **1** according to our previous report.[13] The isolated **3a** was dissolved in a mixture of D_2O and acetone-d_6 (1/9, v/v) at ambient temperature, and the exchange reaction was monitored by ^{1}H NMR (Scheme 2.2). After 3 days, an almost quantitative water–alcohol exchange was achieved with generation of **2'** (DPPT-D_2O) in 97% yield confirmed by ^{1}H NMR (Figure 2.6A). Similarly to the forward reaction, the backward reaction was accelerated by heating at 50 ºC, so that **2'** was generated in 97% yield (^{1}H NMR) within 24 h (Figure 2.6B).

Scheme 2.2 Water–Alcohol Exchange Reaction of DPPT-BnOH **3a** with D_2O

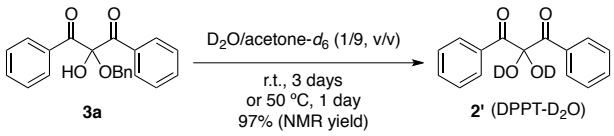

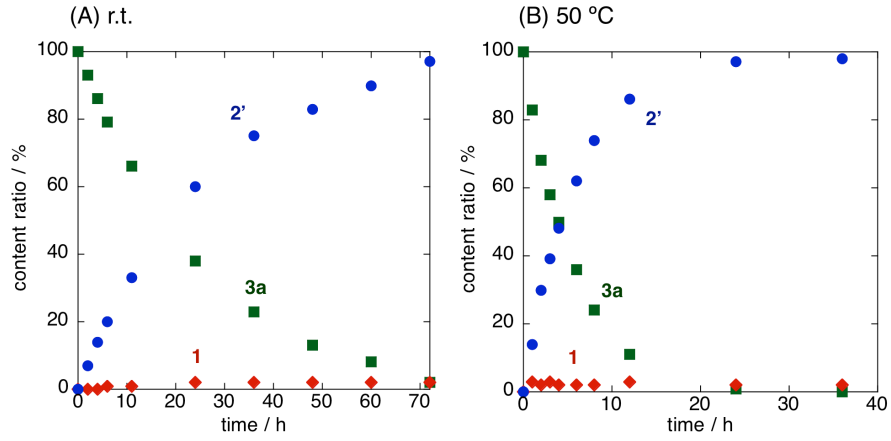

Figure 2.6 Change in the content ratio of DPPT **1**, DPPT-D_2O **2'** and DPPT-BnOH **3a** upon mixing **3a** in D_2O/acetone-d_6 (1/9, v/v) at (A) ambient temperature and (B) at 50 °C. $[\mathbf{3a}]_0$ = 0.05 M.

2.3.2 Reversible Water–Alcohol Exchange Reaction of Monohydrate of Polystyrene Derivative with 1-Hexanol

Based on the results of the model reactions, the author investigated the reversible water–alcohol exchange reaction of the polystyrene bearing monohydrate structure of vicinal tricarbonyl group **5a** with 1-hexanol (Table 2.1). The polymer with *gem*-diol structure **5a** (M_n = 1.5 × 10^4, PDI = 10.3) was prepared according to our previous report.[13] 1-Hexanol was added to a solution of **5a** in $CHCl_3$ ($[\mathbf{5a}]_0$ = 0.2 M) and the reaction mixture was stirred at ambient temperature and took on a yellow color, which suggested the existence of vicinal tricarbonyl units. After 3 days, the resulting mixture was precipitated with *n*-hexane to obtain 1-hexanol adduct of the polymer **6** in 91–96% yield. The IR spectrum showed a weak but distinctive absorption peak at 1721 cm^{-1} assignable to the three contiguous carbonyl groups, indicating that **6** contained vicinal tricarbonyl unit along with *gem*-diol and hemiketal units (Figure 2.7). A weak but distinctive absorption peak at 455 nm observed in the UV/vis spectrum also the existence of the vicinal tricarbonyl unit in the polymer **6** (Figure 2.8).[1,13-15] The hemiketal structure in **6** was confirmed by the appearance of a broad signal

between 3.3 and 3.7 ppm in the ^{1}H NMR spectra that corresponds to that of alkoxymethylene protons of the hemiketal side chain (Figure 2.9). The contents of *gem*-diol, tricarbonyl, and hemiketal structures were estimated by using the integrals of the ^{1}H NMR spectra. When equimolar 1-hexanol was used, the contents of the three units were 39%, 27%, and 34% for *gem*-diol, vicinal tricarbonyl, and hemiketal units, respectively. The content of the hemiketal unit (34%) halved when compared to that of the equilibrium solution of an equimolar mixture of **2** and 1-hexanol in $CDCl_3$ (68%, *vide infra*). This could be attributed to the lowered total concentration as well as the steric hindrance of the polymer backbones. The content of hemiketal unit in **6** increased with an increase in the feed ratio of 1-hexanol, and it reached 62% when 10 equivalent of 1-hexanol was used. The thermogravimetric analysis (TGA) profile of **6** was consistent with the ^{1}H NMR results (Figure 2.10). Only a negligible weight loss was observed up to 220 °C for the tricarbonyl polymer **4** (dehydrated form of **5a**) upon being heated from 30 °C at a rate of 10 °C/min under nitrogen flow. In contrast, the *gem*-diol polymer **5a** showed a weight loss of 6 wt% up to 200 °C, which was in good agreement with the weight of water that can be released potentially from **5a**. The TGA profile of **6** (obtained with 3 eq of 1-hexanol) had two-step weight loss at around 100 °C and 200 °C, which probably correspond to the releases of water and 1-hexanol, respectively. The weight loss up to 250 °C coincides with the combined weight of water and 1-hexanol incorporated in **6** that was estimated by the ^{1}H NMR analysis.

Table 2.1 Water–Alcohol Exchange Reaction of **5a** with 1-Hexanol and Compositions of Resulting Polymers

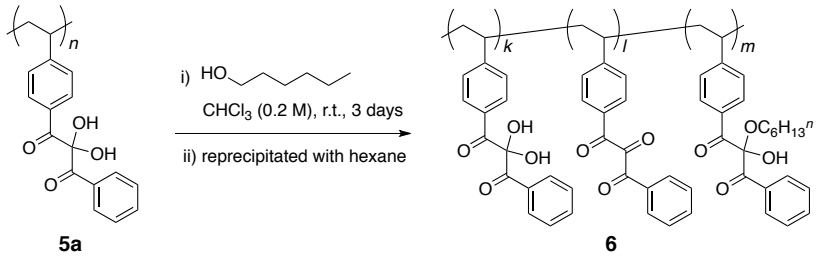

entry	hexanol	content ratio[b] / %			yield[c] / %
		gem-diol	tricarbonyl	hemiketal	
1	1	39	27	34	91
2	3	38	16	46	94
3	10	24	14	62	96

[a] Versus *gem*-diol moieties of **5a**. [b] Determined by integral ratios on ^{1}H NMR spectra. [c] Isolated yield.

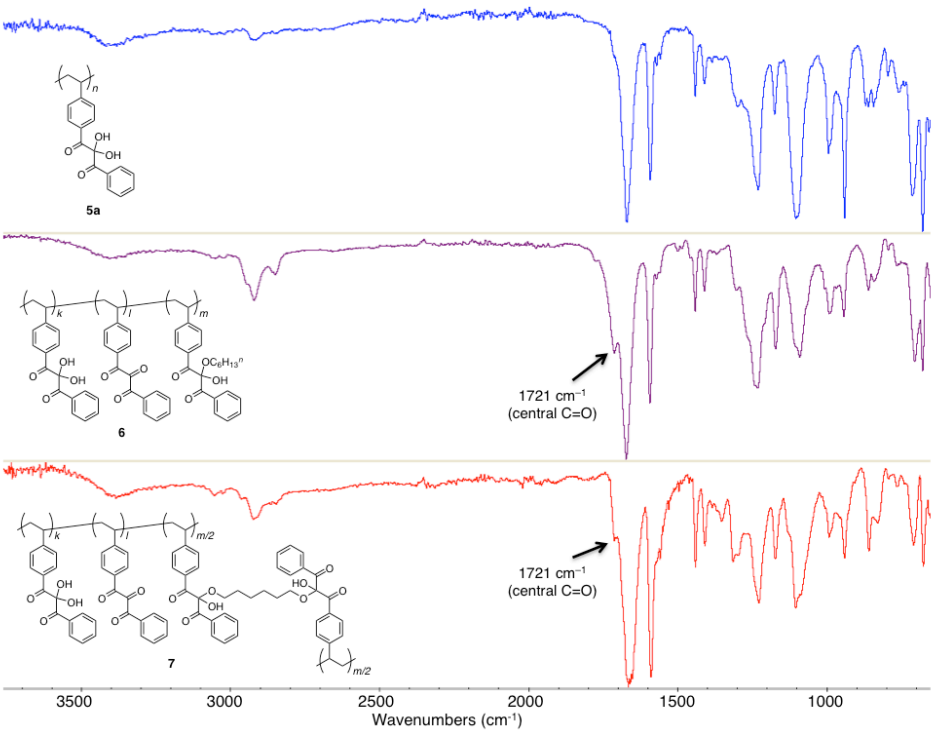

Figure 2.7 IR spectra of **5a**, **6** and **7** (ATR).

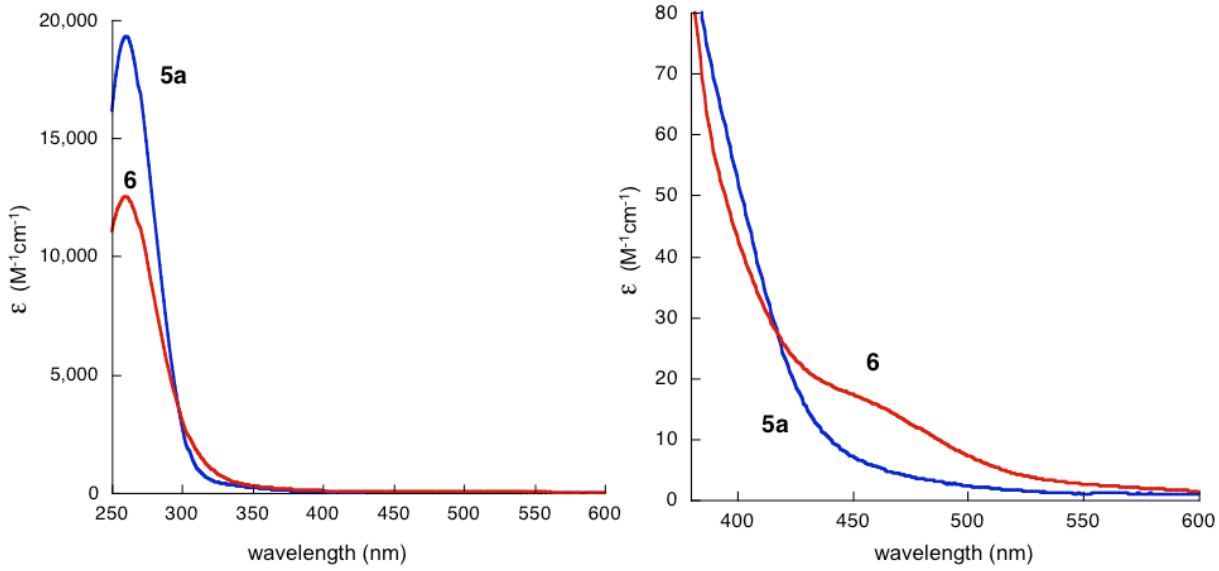

Figure 2.8 UV–vis spectra of **5a** in 1,4-dioxane/water (97/3, v/v, left: 1.0 x 10^{-4} M, right: 5.0 x 10^{-3} M) and **6** in 1,4-dioxane (left: 1.0 x 10^{-4} M, right: 5.0 x 10^{-3} M).

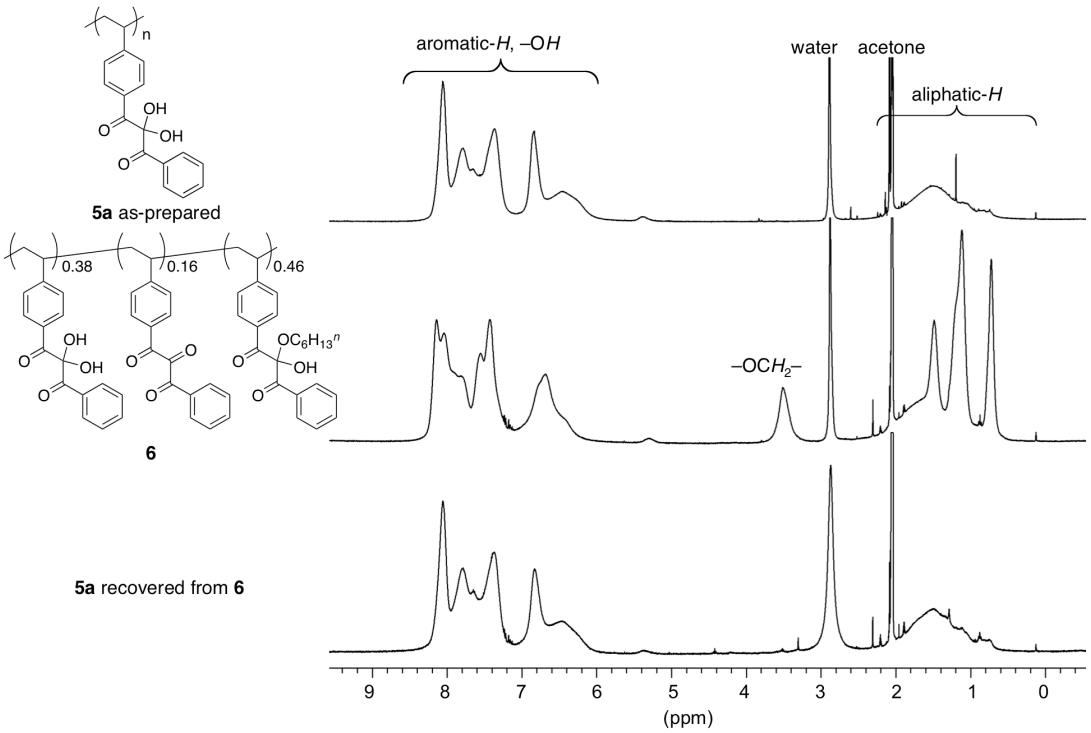

Figure 2.9 ^{1}H NMR spectra of the **5a** as-prepared (top), **6** and the **5a** recovered from the hemiketal polymer **6** (acetone-d_6, 400 MHz, 298K).

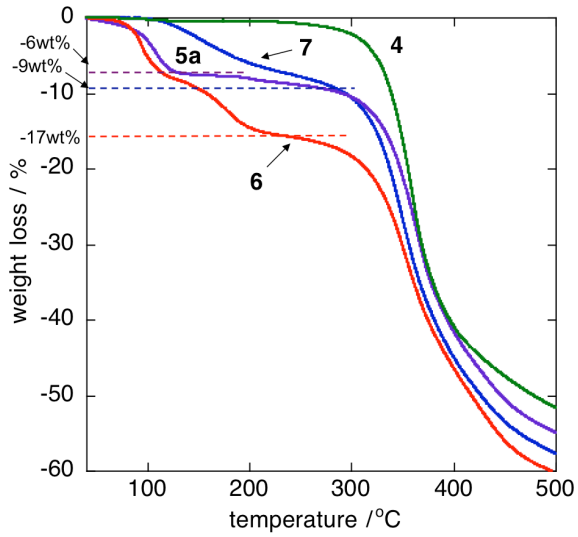

Figure 2.10 TG profiles of **4, 5a, 6** and **7** (heating rate 10 ºC / min, under N_2 flow).

The author also examined the recovery of the *gem*-diol polymer **5a** directly from the hemiketal polymer **6** in the same manner as that for the unit model system (Scheme 2.3). Being stirred at ambient temperature, a mixture of **6** in water–acetone (1/9, v/v) became homogeneous and colorless. After 3 days, the mixture was reprecipitated with water to afford **5a** in 96% yield. The ^{1}H NMR spectrum of the obtained polymer **5a** agreed completely with that of the original *gem*-diol polymer **5a** (Figure 2.9).

Scheme 2.3 Recovery of Polymer **5a**

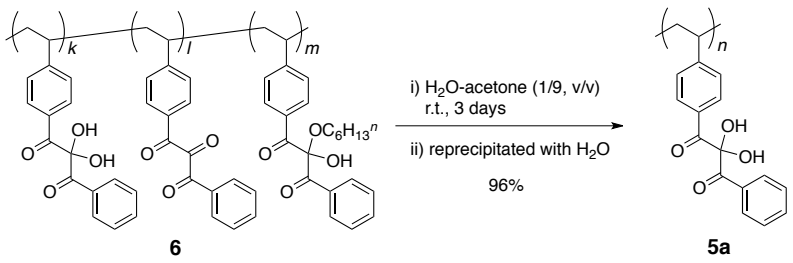

2.3.3 Reversible Crosslinking and Decrosslinking through Water–Alcohol Exchange

The author investigated the reversible crosslinking–decrosslinking of the *gem*-diol polymer **5a** through the water–alcohol exchange reaction by using 1,6-hexanediol as a bifunctional crosslinking reagent (Figure 2.11). The author used acetone for the solvent, because it is a good solvent for **5a** so that the author could achieve a high concentration of **5a**, which is advantageous for the crosslinking reaction. A small amount of 1,6-hexanediol (0.2 eq of OH group relative to the *gem*-diol moiety of **5a**) was added to a concentrated solution of **5a** ($M_n = 1.5 \times 10^4$, PDI = 10.3) in acetone (2.0 M). After 1 day at ambient temperature, the magnetic stirring had been stopped because of significantly increased viscosity of the mixture. The mixture displayed an orange color, which indicated the existence of vicinal tricarbonyl units. The highly viscous mixture was allowed to stand for 4 more days and washed with acetone. The insoluble part was dried *in vacuo* at room temperature to afford the networked polymer **7** in 99% yield as a yellow solid. In the IR spectrum of the obtained networked polymer, a peak due to methylene moiety of 1,6-hexanediol and a weak peak originating from the vicinal tricarbonyl structure were observed at 2,932 cm^{-1} and 1,721 cm^{-1}, respectively (Figure 2.7).[1,13-15] The TGA profile of **7** showed a weight loss of 9 wt% up to *ca*. 250 °C, which agreed well with the combined weight of water and 1,6-hexanediol covalently attached to the polymer side chain (Figure 2.10). Figure 2.11 shows the photographs for the polymer mixture before (a) and after (b) the crosslinking. While the solution of **5a** in acetone exhibited high fluidity as solution, a transparent self-standing gel was formed after the crosslinking with 1,6-hexanediol. The scanning electron microscopy (SEM) images of the fracture surface of the networked polymer are shown in Figure 2.12. The morphology of the networked polymer **7** showed smooth and homogeneous surface, and no phase-separated morphology was observed in the micrometric scale.

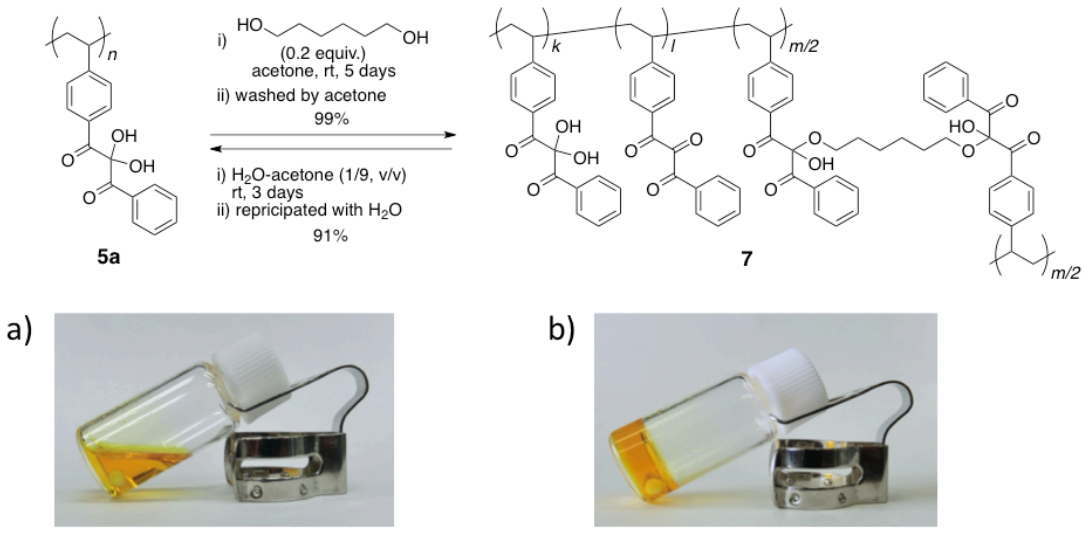

Figure 2.11 Photographs of before (a) and after (b) crosslinking of the polystyrene derivative **5a** through water–alcohol exchange reaction on its vicinal tricarbonyl moieties.

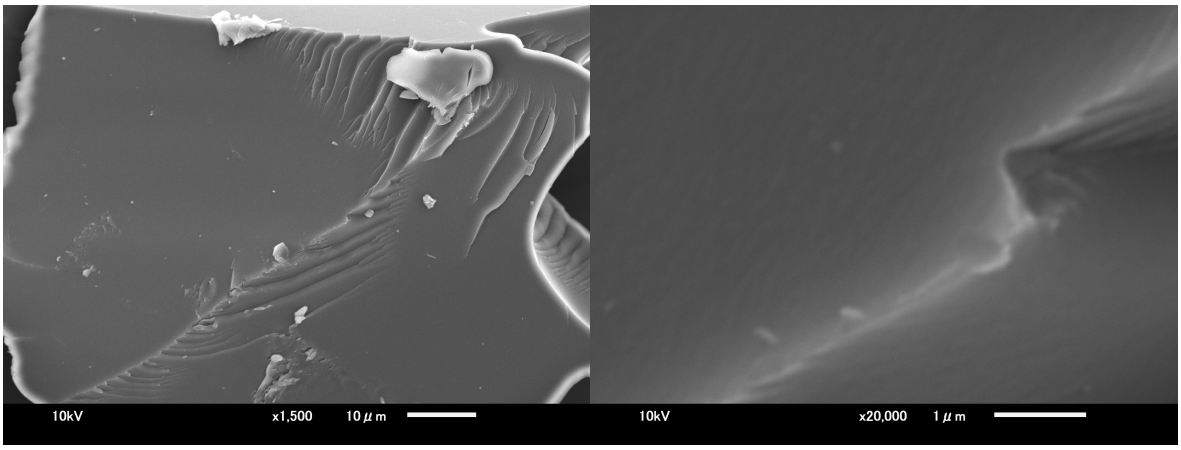

Figure 2.12 SEM images of networked polymer **7**.

The author demonstrated the decrosslinking of the obtained networked polymer **7** through water–alcohol exchange reaction. A pea-sized piece of **7** was immersed in water–acetone (1/9. v/v) and the mixture was gently stirred at ambient temperature. The polymer swelled gradually and then completely dissolved within 2 days. The resultant solution was stirred for one more day and became colorless. After reprecipitation with water, the water-insoluble part was dried *in vacuo* at ambient

temperature to afford the *gem*-diol polymer **5a** in 91% yield, of which the ^{1}H NMR spectrum was completely identical to that of the original polymer **5a** (Figure 2.13).

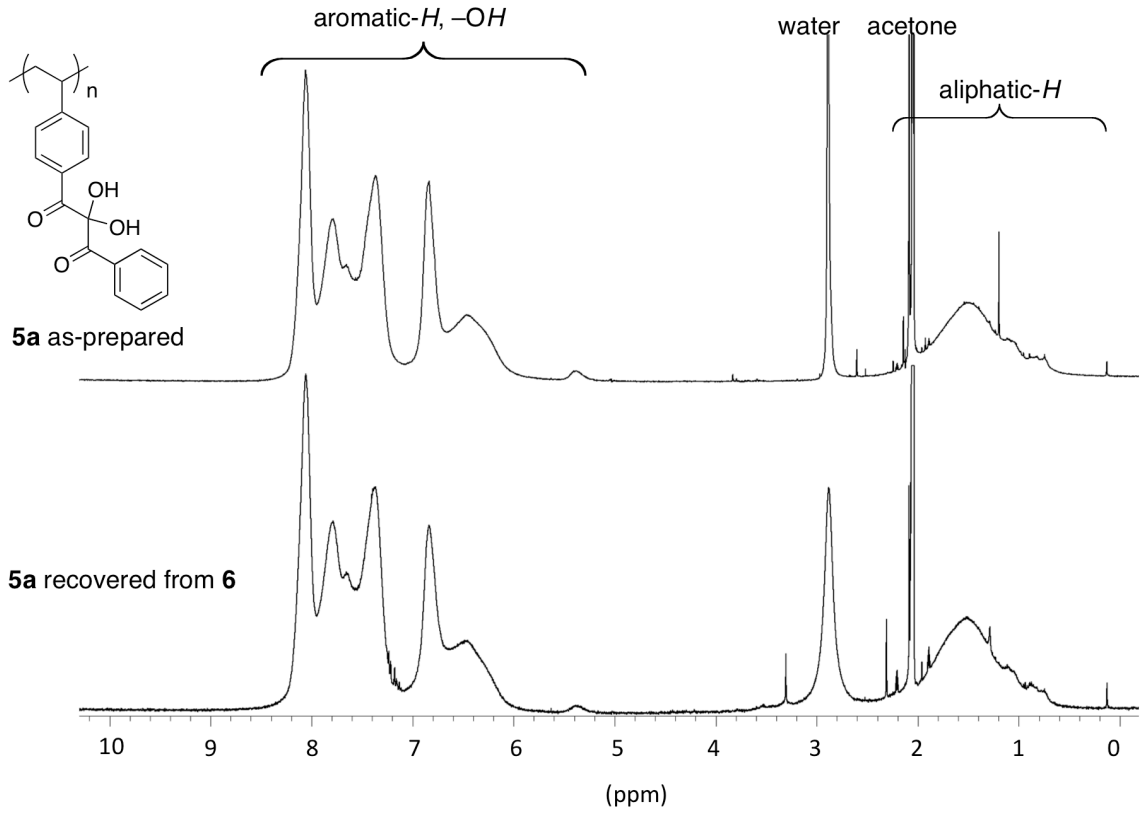

Figure 2.13 ^{1}H NMR spectra of the **5a** as-prepared (top) and the **5a** recovered from the networked polymer **7** (acetone-d_6, 400 MHz, 298K).

Finally, the author attempted SEC analysis of the reaction mixture prior to the gel point, in order to visualize the crosslinking–decrosslinking behavior of **5a**.[21] To this end, the author prepared polymer **5a** with a lower molecular weight (M_n = 3.8 × 10^3, PDI = 2.9) and allowed to react with 1,6-hexanediol in the same manner. The SEC analysis of the reaction mixture showed an increase in molecular weight as well as PDI after 24 h (M_w = 4.5 × 10^3, PDI = 5.0) and after 48 h (M_n = 4.6 × 10^3, PDI = 8.5), indicating the formation of network polymer *via* crosslinking (Figure 2.14a-c). Upon treatment of the resulting partially networked polymer with excess amount of water at

ambient temperature for 3 days, the SEC profile of the polymer (M_n = 3.4 × 10^3, PDI = 2.9) showed good accordance with that of the original polymer **5a** as-prepared (Figure 2.14d), indicating that the decrosslinking was completed.

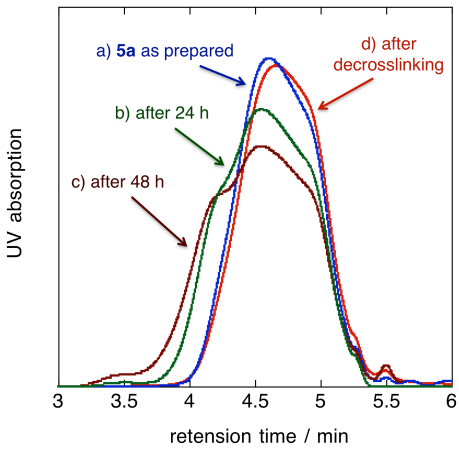

Figure 2.14 SEC profiles of polymer **5a** (a) as-prepared, (b) after crosslinking for 48h, (c) after crosslinking for 96 h, and (d) after decrosslinking.

2.4 Conclusions

The author has thus demonstrated here that the direct water–alcohol exchange reactions on the vicinal tricarbonyl compounds can be carried out reversibly in both directions by changing solvents, exploiting the reversible nature of the addition of alcohols to vicinal tricarbonyl compounds as well as that of the elimination of alcohols from the alcohol adducts. It should be noted here that the water–alcohol exchange reactions proceed without any catalysts and under mild conditions such as ambient temperature. By virtue of the above characteristic features of the water–alcohol exchange reactions on vicinal tricarbonyl compounds, the polystyrene derivative bearing monohydrate structure of vicinal tricarbonyl group can be networked with 1,6-hexanediol at ambient temperature through the water–alcohol exchange reaction to afford the networked polymer

in almost quantitative yield. On the other hand, the treatment of the networked polymer with water affords the original polymer in high yield as a result of decrosslinking through the water–alcohol exchange reaction. Thus, the author believes that the crosslinking and decrosslinking system based on the water–alcohol exchange reactions on vicinal tricarbonyl compounds is promising for development of new chemical recycling and self-healing materials because of its reversible nature as well as the feasibility under mild conditions.

2.5 References

1) (a) M. B. Rubin, R. Gleiter, *Chem. Rev.* **2000**, *100*, 1121–1164. (b) M. B. Rubin, *Chem. Rev.* **1975**, *75*, 177–202.

2) H. H. Wasserman, J. Parr, *J. Acc. Chem. Res.* **2004**, *37*, 687–701.

3) M. Hirama, Y. Fukuzawa, S. Ito, *Tetrahedron Lett.* **1978**, *19*, 1299–1302.

4) R. Moubasher, A. M. Othman, *J. Am. Chem. Soc.* **1950**, *72*, 2667–2669.

5) A. R. Lepley, J. P. Thelman, *Tetrahedron* **1966**, *22*, 101–110.

6) (a) J. C. Netto-Ferreira, M. T. Silva, F. P. Puget, *J. Photochem. Photobiol. A: Chem.* **1998**, *119*, 165–170. (b) M. T. Silva, R. Braz-Filho, J. C. Netto-Ferreira, *J. Braz. Chem. Soc.* **2000**, *11*, 479–485.

7) M. R. Mahran, W. M. Abdou, M. M. Sidky, H. Wamhoff, *Synthesis* **1987**, *5*, 506–508.

8) D. B. Sharp, H. A. Hoffman, *J. Am. Chem. Soc.* **1950**, *72*, 4311–4313.

9) J. D. Roberts, D. R. Smith, C. C. Lee, *J. Am. Chem. Soc.* **1951**, *73*, 618–625.

10) G. B. Gill, M. S. H. Idris, K. S. Kirollos, *J. Chem. Soc., Perkin Trans. 1* **1992**, 2355–2365.

11) A. Schönberg, E. Singer, *Chem. Ber.* **1970**, *103*, 3871–3884.

12) T. Endo, M. Okawara, *Bull. Chem. Soc. Jpn.* **1979**, *52*, 2733–2734.

13) T. Dei, K. Morino, A. Sudo, T. Endo, *J. Polym. Sci., Part A: Polym. Chem.* **2011**, *49*, 2245–2251.

14) T. Dei, K. Morino, A. Sudo, T. Endo, *J. Polym. Sci., Part A: Polym. Chem.* **2012**, *50*, 2619–2625.

15) K. Morino, A. Sudo, T. Endo, *Macromolecules* **2012**, *45*, 4494–4499.

16) For a polymer bearing cyclic tricarbonyl moiety, see: T. Endo, E. Fujiwara, M. Okawara, *J. Polym. Sci. Polym. Chem. Ed.* **1981**, *19*, 1091–1099.

17) For selected reviews on networked polymers, see; (a) H. Uyama, S. Kobayashi, *Curr. Org. Chem.* **2003**, *7*, 1387. (b) M. Funaoka, *Macromol. Symp.* **2003**, *201*, 213. (c) T. Takeichi, T. Kawauchi, T. Agag, *Polym. J.* **2008**, *40*, 1121. (d) Y. Yagci, B. Kiskan, N. N. Ghosh, *J. Polym. Sci., Part A: Polym. Chem.* **2009**, *47*, 5565. (e) K. Suyama, M. Shirai, *Prog. Polym. Sci.* **2009**, *34*, 194. (f) G. Tillet, B. Boutevin, B. Ameduri, *Prog. Polym. Sci.* **2010**, *36*, 191.

18) For selected reviews on polymer recycling, see; (a) F. Sanda, T. Endo, *Polym. Recycl.* **1998**, *3*, 159-163. (b) T. Endo, D. Nagai, *Macromol. Symp.* **2005**, *226*, 79-86. (c) T. Takata, *Polym. J.* **2006**, *38*, 1-20. (d) H. Nishida, *Polym. J.* **2011**, *43*, 435–447.

19) For selected reviews on self-healing polymers, see; (a) M. D. Hager, P. Greil, C. Leyens, S. van der Zwaag, U. S. Schubert, *Adv. Mater.* **2010**, *22*, 5424. (b) C. J. Kloxin, T. F. Scott, B. J. Adzima, C. N. Bowman, *Macromolecules* **2010**, *43*, 2643. (c) N. K. Guimard, K. K. Oehlenschlaeger, J. Zhou, S. Hilf, F. G. Schmidt, C. Barner-Kowollik, *Macromol. Chem. Phys.* **2012**, *213*, 131. (d) M. W. Urban, *Nat. Chem.* **2012**, *4*, 80.

20) Crystal data for **3a**: $C_{22}H_{18}O_4$: FW = 346.36, monoclinic, space group $P2_1/n$ (no. 14), a = 12.031(3) Å , b = 17.789(5) Å , c = 9.608(3) Å, β = 121.262(18), V = 1.757.8(8) Å^3, Z = 4, Dx = 1.309, 4,135 reflections measured, 2,718 unique reflections, 2.542 observations ($I > 2.0\sigma(I)$), R = 0.0324 ($I > 2.0\sigma(I)$), Rw = 0.0893 ($I > 2.0\sigma(I)$). CCDC 885018.

21) A. J. Inglis, L. Nebhani, O. Altintas, F. G. Schmidt, C. Barner-Kowollik, *Macromolecules* **2010**, *43*, 5515-5520.

Chapter 3

Synthesis and X-ray Structural Analysis of an Acyclic Bifunctional Vicinal Triketone, Its Hydrate, and Its Ethanol-Adduct

3.1 Introduction

Vicinal tricarbonyl compounds, such as alloxan, 1,2,3-indanetrione, dehydroascorbic acid, and diphenylpropanetrione (DPPT, **1**), are known to have a highly electrophilic nature due to the three contiguous carbonyl groups, which are activated by the adjacent two carbonyl groups.[1,2] Consequently, they are highly reactive toward various nucleophiles, such as water and alcohols, to afford the corresponding hydrate or alcohol-adduct. These covalently-bonded water or alcohols can be eliminated to give pure free tricarbonyls by heating under vacuum,[3,4] sublimation,[4,5] distillation,[6–8] crystallization,[7] azeotropic removal,[8] and utilization of molecular sieves or P_2O_5.[5,8,9] Of particular interest is that the hydration and alcohol-addition processes are reversible[10] and are accompanied by disappearance and appearance of the distinctive yellow–orange color due to the collapse and recovery of the contiguous three carbonyl groups, respectively, hence being detectable by the naked eye.[1]

Endo *et al.* have started their studies to develop new polymer materials based on the vicinal tricarbonyl structures, motivated by the characteristic features of vicinal tricarbonyl compounds. Recently, Endo *et al.* reported design and synthesis of a polystyrene bearing acyclic vicinal tricarbonyl structures in the side chains and detailed investigation of reversible addition–elimination behavior of water or alcohols to the vicinal tricarbonyl moiety of the polymer.[11–13] Moreover, the

author has successfully constructed the reversible crosslinking and decrosslinking system that can be controllable at ambient conditions, utilizing the direct water–alcohol exchange reaction on the vicinal tricarbonyl groups.[14]

Several bifunctional vicinal polycarbonyl compounds have been reported to date. For example, Wasserman and Baldino synthesized bifunctional α,β-diketoesters tethered by phenylene, naphthylene, and decamethylene linkers and found that these compounds acted as dielectrophiles toward the amino groups of DNA bases, effectively crosslinked the DNA strands.[15] Gleiter and Schang synthesized two bifunctional cyclic vicinal triketones (1,2,3,5,6,7-*s*-hydrindacenehexone, and 1,2,3,6,7,8-pyrenehexone), which formed 1:1 donor-acceptor complexes with pyrene.[16] The same group also reported the synthesis and structure of a cyclic bifunctional vicinal tetraketone, and disclosed the presence of some intra-annular interactions in the solid state by X-ray single crystal structure analysis.[17] Thus, bifunctional vicinal polycarbonyl compounds are of interest from a viewpoint of not only their molecular structures but also their chemical properties that could lead to the application to crosslinking agents. Another important feature of the vicinal tricarbonyl compounds is their relatively large structural changes accompanied by the addition of water and alcohols, which could be applied to polymer systems to create new stimuli-responsive materials or supramolecular systems such as molecular machines or molecular muscles.[18] Investigation on the structural changes of bifunctional vicinal tricarbonyl compounds is an important, preliminary step toward future design and synthesis of such stimuli-responsive supramolecular systems consisting of vicinal tricarbonyl polymers. Herein, the author reports the facile synthesis, structures, and chemical properties of an acyclic bifunctional vicinal tricarbonyl compound (bistriketone, **3**), its hydrate **4**, and its ethanol-adduct **5** together with the drastic structural changes accompanying their reversible interconversion.

3.2 Experimental Section

3.2.1 Materials

Chloroform, chloroform-*d* ($CDCl_3$), dimethyl sulfoxide, dimethyl sulfoxide-d_6 (DMSO-d_6), and ethyl acetate were distilled over molecular sieves 4A (MS 4A). Acetone and acetophenone were distilled over $CaCl_2$. Ethanol was distilled over CaH_2. Tetrahydrofuran (THF) and 1,4-dioxane were distilled over sodium benzophenone ketyl. NaH (60% in oil) (WAKO, Japan) was washed with *n*-hexane before use. Diphenylpropanetrione (DPPT, **1**) was synthesized according to the literature.[11] Other reagents were used as received.

3.2.2 General Measurements

^1H and ^{13}C NMR spectra were measured on a JEOL JNM-ECS 400 spectrometer at a resonance frequency of 400 and 100 MHz, respectively, with tetramethylsilane (TMS) as the internal standard. NMR chemical shifts were reported in delta unit (δ). IR spectra were recorded on a Thermo Scientific Nicolet iS10 spectrometer. UV/vis spectra were measured with a JASCO V-570 spectrophotometer in a 1-cm quartz cell. Melting points were measured on a Stuart Scintific SMP3 apparatus. Elemental analyses were carried out using a LECO CHNS-932. The single crystal X-ray data were collected on a Bruker Smart Apex CCD-based X-ray diffractometer with Mo-K*a* radiation (λ = 0.71073 Å). Cyclic voltammograms were recorded at a scan rate of 100 mV/s on an ALS Electrochemical Analyzer Model 612D using a glassy carbon working, a Pt counter, and an Ag/Ag^+ reference electrodes, and Bu_4NPF_6 (0.1 M) was used as supporting electrolyte for CH_2Cl_2 solutions.

3.2.3 Synthesis of Bistriketone, Its hydrate, and Its Ethanol-adduct

3,3'-(1,4-phenylene)bis(1-phenylpropane-1,3-dione) (2) To a suspension of NaH (4.80 g, 200 mmol) in dry THF (100 mL), dimethyl terephthalate (9.71 g, 50.0 mmol) and acetophenone (11.7 mL, 100 mmol) were added and stirred for 20 min at ambient temperature under Ar atmosphere. Then the mixture was stirred at 50 ºC for 33 h. After cooling the mixture to ambient temperature, the reaction was quenched by the addition of aqueous HCl (2 M, 100 mL) and a large amount of water. The resultant suspension was filtered and the collected solid was washed with water and chloroform, and dried *in vacuo* to yield **2**. The combined filtrate was extracted with chloroform and washed with water, dried over $MgSO_4$, filtered, and concentrated *in vacuo*. The crude material was recrystallized from toluene to yield **2** (14.0 g, 37.8 mmol, 76%) as a light yellow solid; m.p. 175.9–176.7 ºC (lit. 176–177 ºC)[21]. ^{1}H NMR (400 MHz, $CDCl_3$, 298 K): δ 16.84 (s, 2H, enol-O*H*), 8.10 (s, 4H, Ar-*H*), 8.05-7.99 (m, 4H, Ar–*H*), 7.63-7.56 (m, 2H, Ar–*H*), 7.56-7.49 (m, 4H, Ar–H), 6.93 (s, 2H, enol-C*H*) ppm. ^{13}C NMR (100 MHz, $CDCl_3$, 298 K): δ 187.2, 183.6 (4C, *C*=O), 138.8, 135.5, 133.0, 128.9, 127.5, 127.5 (18C, Ar-*C*), 93.9 (2C, –*C*H_2–) ppm. IR (ATR): 3048 (C–H), 1524 (C=O) cm^{-1}.

3,3'-(1,4-phenylene)bis(2,2-dihydroxy-1-phenylpropane-1,3-dione) (4)

3,3'-(1,4-Phenylene)bis(1-phenylpropane-1,3-dione) **2** (926 mg, 2.50 mmol) and NBS (890 mg, 5.00 mmol) were dissolved in DMSO (25 mL). The mixture was stirred at 80 ºC for 24 h. After cooling to ambient temperature, distilled water (5.0 mL) was added to the solution and stirred for 1 h. The reaction was quenched by the addition of a large amount of water and the resultant suspension was filtered. The collected solid was washed with water and chloroform, and dried *in vacuo* to yield **4** (940 mg, 2.16 mmol, 87%) as a white solid; m.p. 98 ºC (decomp.). ^{1}H NMR (400 MHz, DMSO-d_6, 298 K): δ 8.06 (s, 4H, Ar-*H*), 8.02 (d, J = 7.6 Hz, 4H, Ar–*H*), 7.88 (s, 2H, –O*H*), 7.60 (t, J = 7.4 Hz, 2H, Ar–*H*), 7.47 (dd, J_1 = 7.8 Hz, J_2 = 7.6 Hz, 4H, Ar–H) ppm. ^{13}C NMR (100

MHz, DMSO-d_6, 298 K): δ 196.2, 196.1 (4C, *C*=O), 136.9, 133.8, 133.3, 130.2, 129.9, 128.7 (18C, Ar-*C*), 97.2 (2C, *C*$(OH)_2$) ppm. IR (ATR): 3368 (O–H), 1679 (C=O) cm^{-1}. Anal. Calcd for $C_{24}H_{18}O_8$: C, 66.36; H, 4.18; O, 29.47. Found: C, 65.83; H, 4.12; N, 0.17.

3,3'-(1,4-phenylene)bis(1-phenylpropane-1,2,3-trione) (3)

3,3'-(1,4-Phenylene)bis(2,2-dihydroxy-1-phenylpropane-1,3-dione) **4** (1.53 g, 3.52 mmol) was heated at 100 ºC for 4 h under reduced pressure (2 mmHg) to give **3** (1.40 g, 3.52 mmol, quant.) as an orange solid; m.p. 140.0–141.0 ºC. ^{1}H NMR (400 MHz, $CDCl_3$, 298 K): δ 8.25 (s, 4H, Ar-*H*), 8.02 (d, *J* = 6.8 Hz, 4H, Ar–*H*), 7.74 (t, *J* = 7.4 Hz, 2H, Ar–*H*), 7.58 (dd, J_1 = 7.9 Hz, J_2 = 7.6 Hz, 4H, Ar–H) ppm. ^{13}C NMR (100 MHz, $CDCl_3$, 298 K): δ 191.9, 191.8, 187.2 (6C, *C*=O), 136.6, 135.8, 132.0, 130.6, 130.4, 129.3 (18C, Ar-*C*) ppm. IR (ATR): 1723 (central C=O), 1675 (side C=O) cm^{-1}. Anal. Calcd for $C_{24}H_{14}O_6$: C, 72.36; H, 3.54; O, 24.10. Found: C, 71.80; H, 3.38; N, 0.00.

Hydration of 3 To a solution of **3** (267 mg, 0.670 mmol) in acetone (6.3 mL), water (0.70 mL) was added and the solution was stirred at ambient temperature. After 1 h, the solvent of the resulting suspension was removed under reduced pressure to give **4** (291 mg, 0.670 mmol, quant.) as a white solid.

3,3'-(1,4-phenylene)bis(2-ethoxy-2-hydroxy-1-phenylpropane-1,3-dione) (5)

3,3'-(1,4-Phenylene)bis(1-phenylpropane-1,2,3-trione) **3** (851 mg, 2.14 mmol) was suspended in ethanol (4.0 mL) at ambient temperature and then the suspension was heated to 70 ºC. After 20 min, the resulting solution was cooled to ambient temperature and allowed to stand for 1 h. The resulting precipitation was filtered, washed with *n*-hexane, and dried *in vacuo*. The crude product was recrystallized in dry EtOAc to afford **5** (798 mg, 1.63 mmol, 76%) as colorless blocks; m.p. 103 ºC

(decomp.). ^{1}H NMR (400 MHz, $CDCl_3$, 298 K): δ 8.25 (s, 4H, Ar-*H*), 8.18 (d, *J* = 7.4 Hz, 4H, Ar–*H*), 7.61 (t, *J* = 7.4 Hz, 2H, Ar–*H*), 7.46 (dd, J_1 = 7.8 Hz, J_2 = 7.6 Hz, 4H, Ar–H), 5.91 (s, 2H, –O*H*), 3.69-3.48 (m, 4H, –OCH_2–), 1.20 (t, *J* = 6.9 Hz, 6H, –CH_3) ppm. ^{13}C NMR (100 MHz, $CDCl_3$, 298 K): δ 195.7, 195.3 (4C, *C*=O), 136.7, 134.5, 132.5, 130.7, 130.5, 128.7 (18C, Ar-*C*), 99.6 (2C, *C*(OH)(OR)), 59.2 (2C, –O*C*H_2–), 15.5 (2C, –O*C*H_3) ppm. IR (ATR): 3419 (O–H), 2978 (C–H), 1694, 1674 (C=O) cm^{-1}. Anal. Calcd for $C_{28}H_{26}O_8$: C, 68.56; H, 5.34; O, 26.09. Found: C, 67.99; H, 5.12; N, 0.00.

Ethanol-elimination from 5

3,3'-(1,4-Phenylene)bis(2-ethoxy-2-hydroxy-1-phenylpropane-1,3-dione) (**5**) (123 mg, 0.250 mmol) was heated at 120 ºC for 1 h under reduced pressure (2 mmHg) to give **3** (100 mg, 0.250 mmol, quant.) as an orange solid.

3.3 Results and Discussion

3.3.1 Synthesis of a Bifunctional Vicinal Triketone, Its hydrate, and Its Ethanol-Adduct

The bifunctional vicinal tricarbonyl compound **3** (bistriketone), its hydrate **4**, and its ethanol-adduct **5** were synthesized according to Scheme 3.1. Treatment of dimethyl terephthalate and acetophenone with NaH in THF at 50 ºC afforded the bifunctional 1,3-diketone **2**. Oxidation of the two 1,3-diketone moieties of **2** by *N*-bromosuccinimide (NBS) in DMSO at 80 ºC for 1 day resulted in the formation of the corresponding bistriketone **3**, confirmed *in situ* with the orange coloration of the reaction mixture originating from the vicinal tricarbonyl structures. Since the tricarbonyl compound **3** is labile to hydration by moisture in solvents or air during isolation processes, the author isolated its hydrate form **4** instead of **3**; on addition of an excess of water to the reaction mixture, the color of the solution immediately turned light yellow indicating hydration

of **3**. After 1 h, a large amount of water was added to the solution and the resulting suspension was filtered. The residue was washed with water and chloroform to obtain bis(*gem*-diol) **4** as a colorless solid. Heating **4** at 100 ºC *in vacuo* for 4 h resulted in quantitative generation of orange-colored bistriketone **3**. Conversely, hydration of **3** proceeded smoothly upon treatment with water/acetone (1/9, v/v) for 1 h and **4** was quantitatively obtained after evaporation of the volatile components. The ethanol-adduct **5** was obtained by treatment of **3** with hot ethanol; when a suspension of bistriketone **3** in ethanol was heated at 70 ºC, it became homogeneous. The solution was then cooled to r.t., to form a white precipitate, which was collected by suction filtration and washed with *n*-hexane to obtain the ethanol-adduct **5**. The white microcrystalline solid of **5** contained ethanol molecules included in the crystalline lattice, which were hardly removed by simply heating *in vacuo*. The ethanol-containing solid of **5** was subjected to recrystallization from ethyl acetate to give pure **5** as a white microcrystalline solid that did not contain any solvent molecules. Similarly to the hydrate **4**, elimination of the ethanol from **5** proceeded by heating; **3** was regenerated quantitatively by heating **5** at 120 ºC *in vacuo* for 1 h.

Scheme 3.1 Synthesis of the bistriketone **3**, its hydrate **4**, and its ethanol-adduct **5**.

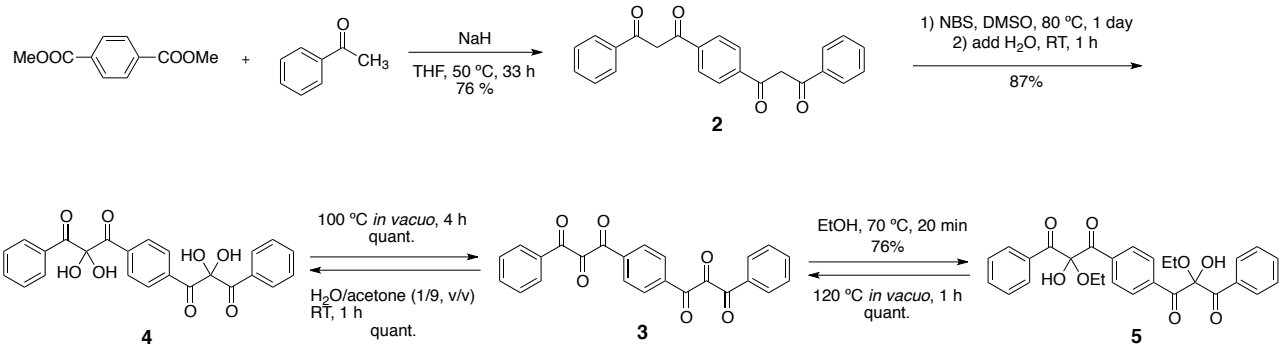

3.3.2 Spectral Properties

The structures of bistriketone **3**, its hydrate **4**, and its ethanol-adduct **5** were confirmed unambiguously by NMR, IR, and UV/vis spectroscopies. Four peaks assignable to the phenyl and *p*-phenylene protons were observed in the ^{1}H NMR spectrum of bistriketone **3** in $CDCl_3$, whereas an additional singlet peak due to the *gem*-diol protons was observed at 7.88 ppm for hydrate **4** in DMSO-d_6 (Figure 3.1). Similarly, the signals assignable to the hemiketal hydroxyl protons along with the ethoxy groups were observed in addition to those due to the aromatic protons in the ^{1}H NMR spectrum of **5** in $CDCl_3$. In the ^{13}C NMR spectrum of bistriketone **3**, the three sequential carbonyl carbons gave three peaks at 191.9, 191.8, and 187.2 ppm (Figure 3.2). On the other hand, only two carbonyl signals along with one signal for the quaternary carbon for the *gem*-diol or hemiketal signal were observed in the ^{13}C NMR spectra of **4** or **5**, respectively.

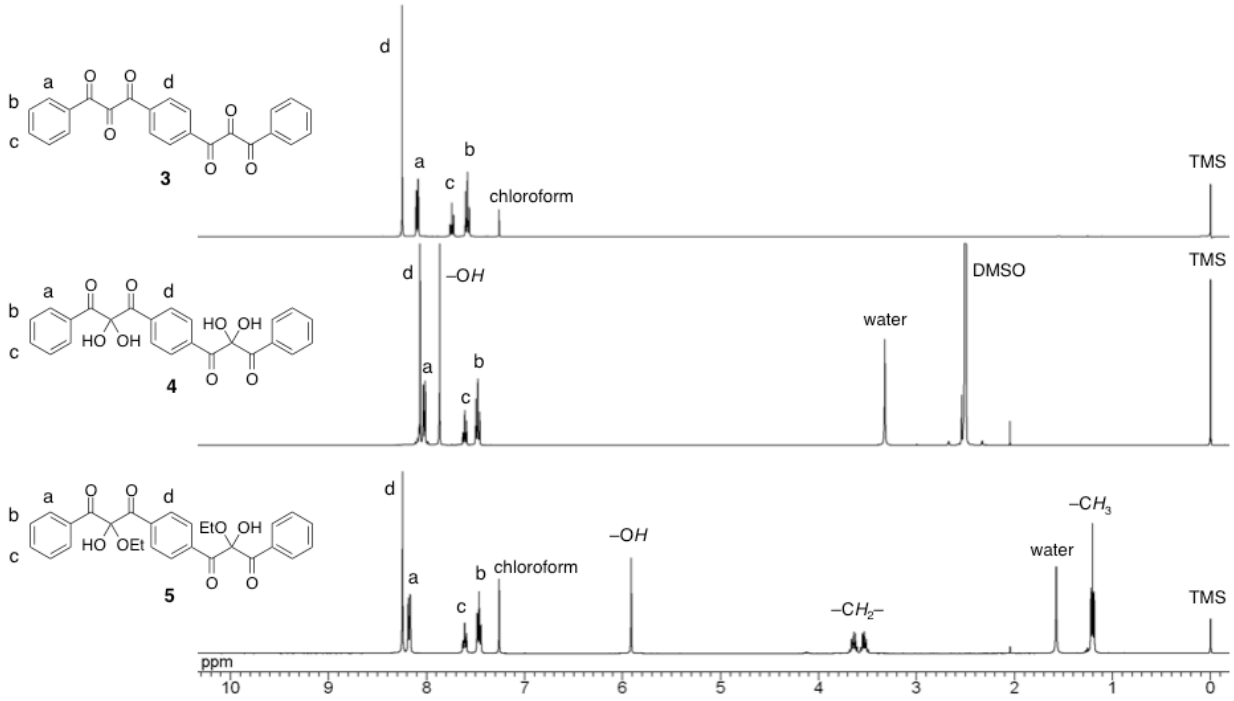

Figure 3.1 ^{1}H NMR spectra of **3**, **4**, and **5** (400 MHz, 298 K, **3**, **5**: $CDCl_3$, **4**: DMSO-d_6).

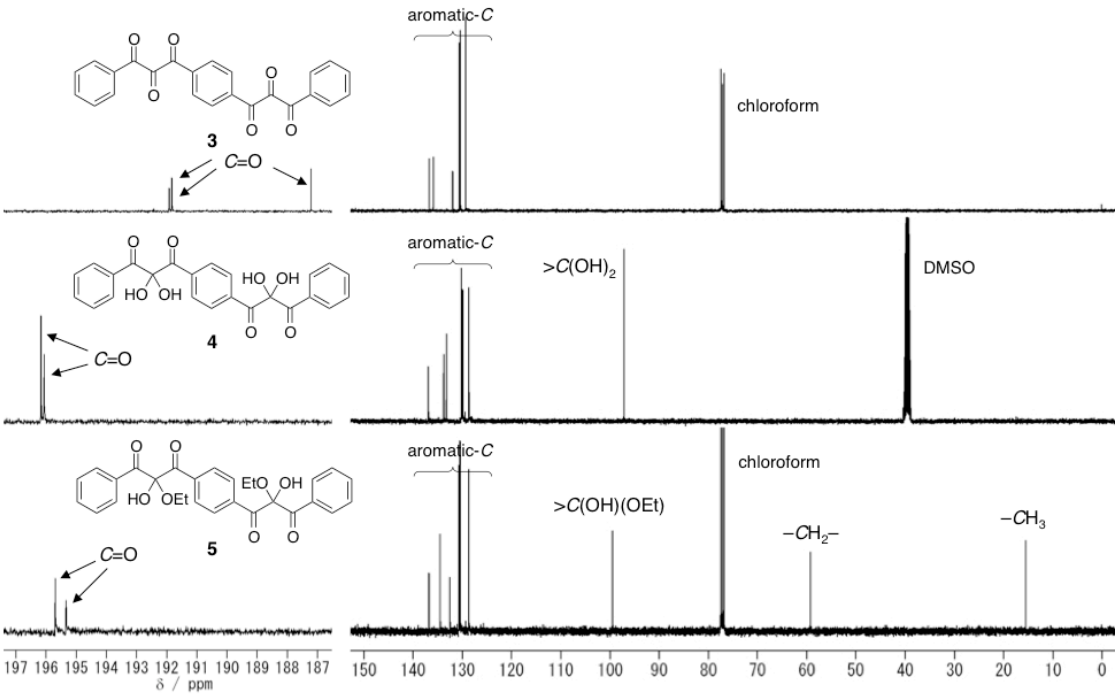

Figure 3.2 ^{13}C NMR spectra of **3**, **4**, and **5** (100 MHz, 298 K, **3**, **5**: $CDCl_3$, **4**: DMSO-d_6).

The IR and UV/vis spectra of **3** showed characteristic absorptions originating from its vicinal tricarbonyl structure. As for IR, the bistriketone **3** exhibited the diagnostic absorption of the stretching vibration of its vicinal tricarbonyl groups at 1723 cm^{-1}, a close value to that of the monofunctional triketone DPPT **1** (1715 cm^{-1}, Figure 3.3). On the other hand, the hydrate **4** and the ethanol-adduct **5** offered absorption peaks at around 3400 cm^{-1} due to the O–H groups of the *gem*-diol or hemiketal structures instead of the tricarbonyl absorption at around 1720 cm^{-1}. UV/vis absorption spectra of **3**, **4**, and **5** together with that of DPPT **1** were shown in Figure 3.4. A solution of the bistriketone **3** in dry 1,4-dioxane exhibited an absorption in the region from 400 to 500 nm with a maximum ε value of 128 $M^{-1}cm^{-1}$ at 456 nm arising from the carbonyl n-π* transitions. The maximal absorption wavelength of **3** approximately coincided with that of DPPT **1** (450 nm),[11] indicating clearly that the conjugated system of the vicinal tricarbonyl structure was not elongated. In contrast to the bistriketone **3**, the hydrate **4** in 1,4-dioxane/water (97/3, v/v) and the ethanol-adduct **5** in 1,4-dioxane/ethanol (97/3, v/v) showed a negligible absorption in the same

region, which is attributable to the collapse of the conjugate systems consisting of the three sequential carbonyl groups as a result of the addition of water or ethanol to the central ones.

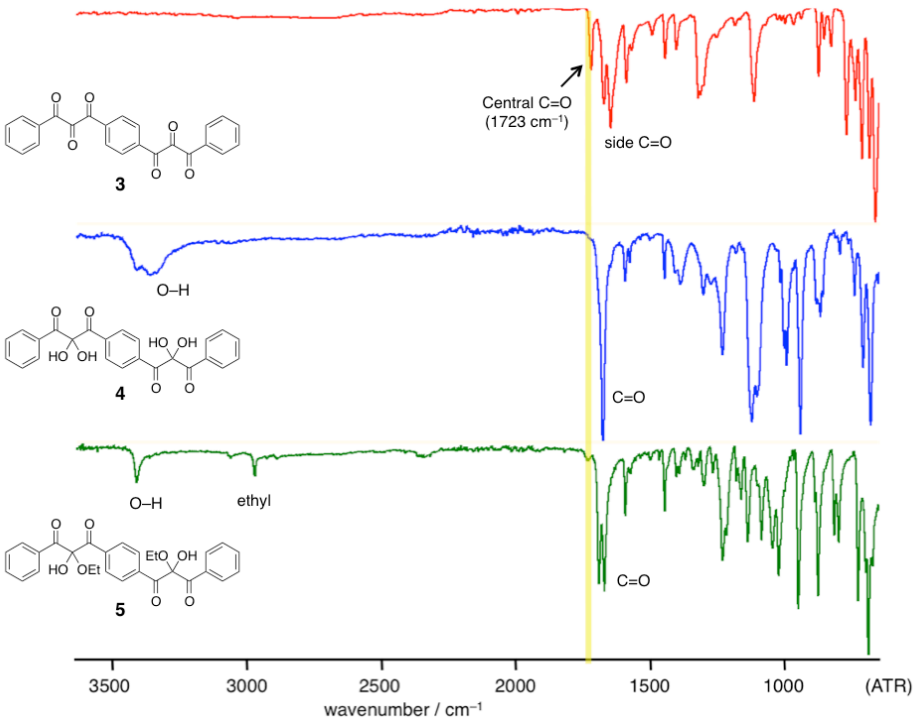

Figure 3.3 FT-IR (ATR) spectra of **3**, **4**, and **5**.

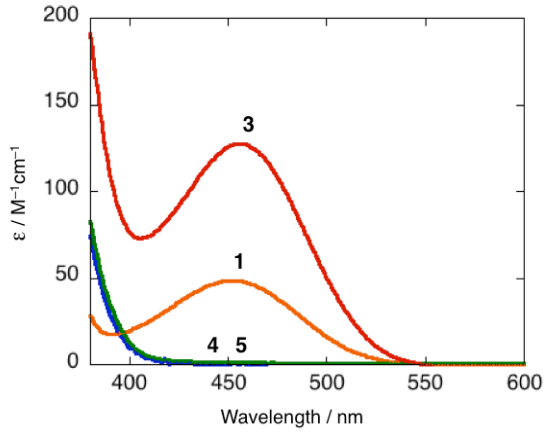

Figure 3.4 UV/vis absorption spectra of **3** in 1,4-dioxane, **4** in 1,4-dioxane/water (97/3, v/v), and **5** in 1,4-dioxane/ethanol (97/3, v/v) along with DPPT **1** in 1,4-dioxane.

3.3.3 X-ray Crystallographic Analysis

Finally, the structures of these three species were determined by X-ray crystallographic analysis.[19] Figure 3.5 shows the ORTEP drawings of **3**, **4**, and **5**; single crystals of **3**, **4**, and **5** suitable for X-ray analysis were grown from chloroform, acetone, and ethyl acetate, respectively. In the crystal structure of the bistriketone **3**, the sequential three carbonyl groups adopt helical conformations with slightly shorter bond lengths (*ca*. 0.01 Å) of the central carbonyl C8=O2 (1.209 Å) than those of the side ones C7=O1 (1.220 Å) and C9=O3 (1.217 Å), as often the case with other vicinal tricarbonyl compounds (Figure 3.5a).[1] As a whole, the bistriketone molecule took a rod-like structure, in which the distance between the two terminal phenyl rings was 15.49 Å. The crystal structure of the hydrate **4** revealed that the two central carbon atoms (C8, C17) adopted sp^3-hybrid orbitals and the four hydroxyl groups formed intramolecular hydrogen bonds with the neighboring carbonyl oxygen atoms (O1···O2, O3···O4, O5···O6, O7···O8) with lengths of 2.61–2.63 Å (Figure 3.5b). Similarly to the hydrate **4**, the central carbonyl carbons (C8) of the ethanol-adduct **5** adopted tetrahedral configurations as a result of the addition of ethanol molecules (Figure 3.5c). Intramolecular hydrogen bonds are also observed between the hemiketal hydroxyl moieties and the neighboring carbonyl oxygen atoms of **5** (O1···O3) with a length of 2.58 Å. The crystallized **5** is its meso isomer. In contrast to the rod-like structure of **3**, the molecules of **4** and **5** adopted zigzag-shaped structures in the solid state, in which the two terminal phenyl groups are located with distances of 10.76 Å and 13.77 Å, respectively. It follows from the changes in distance that the bistriketone molecule shrinks in length by 31% and 11% upon addition of the water and ethanol molecules, respectively.

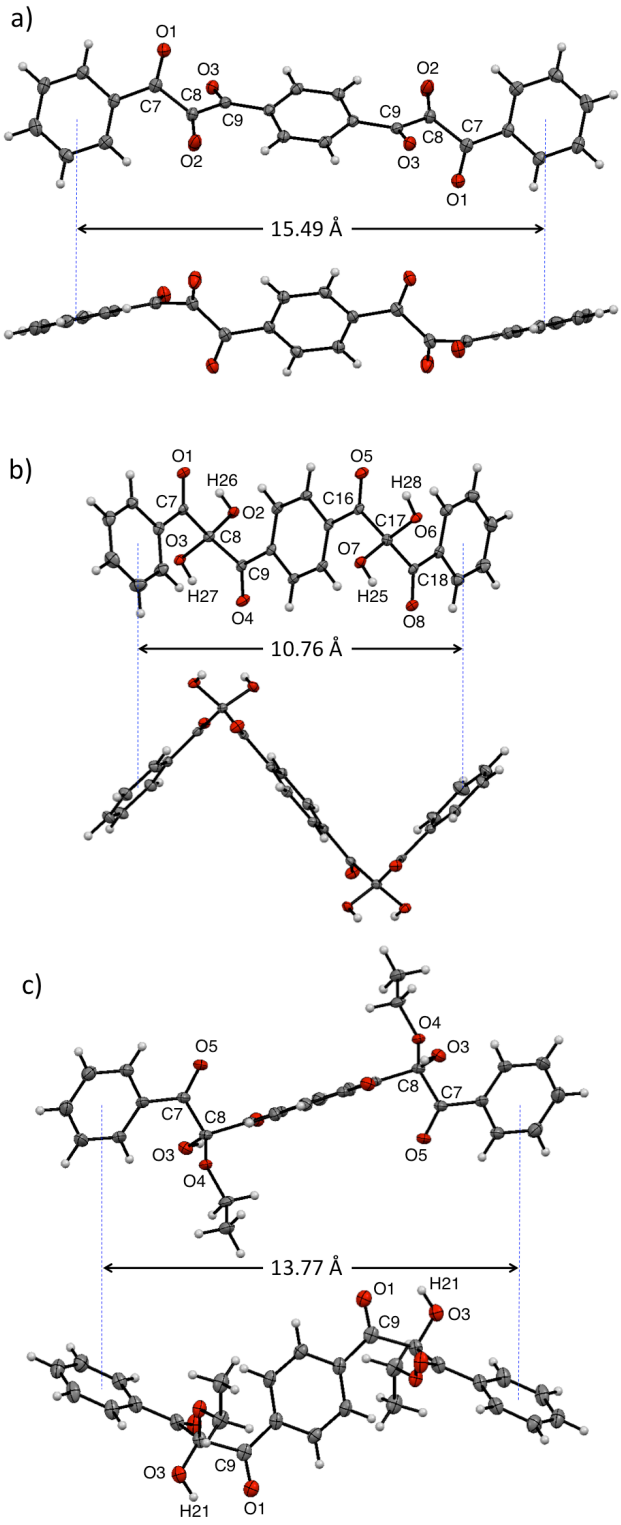

Figure 3.5 Single crystal X-ray structures of (a) **3**, (b) **4**, and (c) **5**, top views (above) and side views (below) along with the distances between the centroids of the terminal phenyl rings. Thermal ellipsoids are drawn at 50 % probability. Acetone molecules in the crystal structure of **4** are omitted for clarity.

3.3.4 CV Measurements

The electrochemical properties of bistriketone **3** and its ethanol-adduct **5** were evaluated by cyclic voltammetry (CV) analysis. The cyclic voltammograms of **3** and **5** in CH_2Cl_2 containing *n*-Bu_4NPF_6 are shown in Figure 3.6 along with that of DPPT **1**. Whereas the DPPT **1** showed almost reversible single-electron-transfer peak, the bistriketone **3** exhibited quasi-reversible, two-step, and two-electron-transfer peaks. The half-wave reduction potentials of **3** were observed at $E^1_{1/2}$ = –0.84 V and $E^2_{1/2}$ = –1.11 V (vs. Ag/Ag^+), which were presumably attributed to the formation of anionic radical and dianion with *p*-quinodimethane structure,[20] respectively. The $E^1_{1/2}$ of **3** was less negative than $E_{1/2}$ of DPPT **1** (–1.06 V vs. Ag/Ag^+) because of the electron-withdrawing tricarbonyl moiety on the other side of **3**. The decrease in the current intensity of the oxidation peak indicated that the anionic species generated from **3** was less stable than that of **1**. In contrast to these triketones, ethanol-adduct **5** exhibited a completely irreversible reduction peak at $E_{1/2}$ = –1.12 V (vs. Ag/Ag^+).

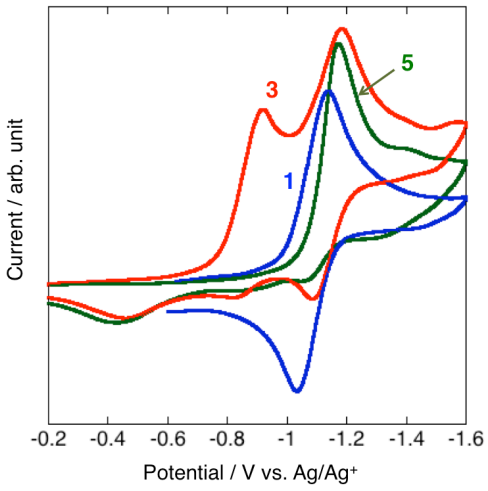

Figure 3.6 Cyclic voltammograms of bistriketone **3** (red line), its ethanol-adduct **5** (green line), and DPPT **1** (blue line) at 1.0 mM in CH_2Cl_2 solutions containing *n*-Bu_4NPF_6 (0.10 M). Sweep rate were 100 $mV \cdot s^{-1}$.

3.4 Conclusions

In summary, the author has synthesized and fully characterized the acyclic bifunctional vicinal tricarbonyl compound **3**, its hydrate **4**, and its ethanol-adduct **5**. The bistriketone **3** was readily and quantitatively hydrated upon treatment with water-containing solvent. Conversely, the hydrate **3** was dehydrated quantitatively by heating *in vacuo*. Similarly, the bistriketone **3** was converted to its ethanol-adduct by treatment with ethanol, from which the bistriketone **3** was quantitatively regenerated by heating under vacuum. As revealed by the X-ray crystallographic analysis, water and ethanol molecules added to the central carbonyl sp^2-carbon atoms of the bistriketone **3** that changed to a tetrahedral configuration, so that the hydrate **4** and the ethanol-adduct **5** adopted a zigzag structure in contrast to the rod-shaped bistriketone **3**. The changes in the crystal structures indicated that the bistriketone **3** expanded and contracted by 10–30% in length as a result of the addition and elimination of water and ethanol molecules. The cyclic voltammogram of bistriketone indicated that the two vicinal tricarbonyl groups acted as two-electron acceptors though the generated dianion species is relatively labile when compared to its monofunctional counterpart **1**. As is evident from the bifunctional nature of the bistriketone **3**, it can be utilized as a reversible crosslinking reagent for multifunctional alcoholic polymers such as poly(vinyl alcohol) (PVA) or poly(2-hydroxyethyl methacrylate) (PHEMA). Moreover, the author envisages that the chemistry of the bistriketone investigated herein, though a little premature, would be a first step toward a future design and synthesis of supramolecular systems that can undergo reversible extension and contraction motion in response to some external stimuli.

3.5 References

1) (a) M. B. Rubin, R. Gleiter, *Chem. Rev.* **2000**, *100*, 1121–1164. (b) M. B. Rubin, *Chem. Rev.* **1975**, *75*, 177–202.

2) H. H. Wasserman, J. Parr, *Acc. Chem. Res.* **2004**, *37*, 687–701.

3) (a) M. Hirama, Y. Fukuzawa, S. Ito, *Tetrahedron Lett.* **1978**, *19*, 1299–1302. (b) R. Moubasher, A. M. Othman, *J. Am. Chem. Soc.* **1950**, *72*, 2667–2669.

4) A. R. Lepley, J. P. Thelman, *Tetrahedron* **1966**, *22*, 101–110.

5) (a) J. C. Netto-Ferreira, M. T. Silva, F. P. Puget, *J. Photochem. Photobiol. A: Chem.* **1998**, *119*, 165–170. (b) M. T. Silva, R. Braz-Filho, J. C. Netto-Ferreira, *J. Braz. Chem. Soc.* **2000**, *11*, 479–485.

6) (a) M. R. Mahran, W. M. Abdou, M. M. Sidky, H. Wamhoff, *Synthesis* **1987**, *5*, 506–508. (b) D. B. Sharp, H. A. Hoffman, *J. Am. Chem. Soc.* **1950**, *72*, 4311–4313.

7) J. D. Roberts, D. R. Smith, C. C. Lee, *J. Am. Chem. Soc.* **1951**, *73*, 618–625.

8) G. B. Gill, M. S. H. Idris, K. S. Kirollos, *J. Chem. Soc., Perkin Trans. 1* **1992**, 2355–2365.

9) A. Schönberg, E. Singer, *Chem. Ber.* **1970**, *103*, 3871–3884.

10) T. Endo, M. Okawara, *Bull. Chem. Soc. Jpn.* **1979**, *52*, 2733–2734.

11) (a) T. Dei, K. Morino, A. Sudo, T. Endo, *J. Polym. Sci., Part A: Polym. Chem.* **2011**, *49*, 2245–2251. (b) T. Dei, K. Morino, A. Sudo, T. Endo, *J. Polym. Sci., Part A: Polym. Chem.* **2012**, *50*, 2619–2625.

12) K. Morino, A. Sudo, T. Endo, *Macromolecules* **2012**, *45*, 4494-4499.

13) For a polymer bearing cyclic tricarbonyl moiety, see: T. Endo, E. Fujiwara, M. Okawara, *J. Polym. Sci.: Polym. Chem. Ed.* **1981**, *19*, 1091–1099.

14) M. Yonekawa, Y. Furusho, T. Endo, *Macromolecules* **2012**, *45*, 6640–6647.

15) H. H. Wasserman, C. M. Baldino, *Bioorg. Med. Chem. Lett.* **1995**, *5*, 3033–3038.

16) R. Gleiter, P. Schang, *Angew. Chem. Int. Ed. Engl.* **1980**, *19*, 715–716.

17) M. Peter, R. Gleiter, F. Rominger, T. Oeser, *Eur. J. Org. Chem.* **2004**, 3212–3220.

18) For examples of organic molecules that undergo muscle-like extension-contraction motion, see: (a) T. W. Bell, H. Jousselin, *Nature* **1994**, *367*, 441–444. (b) M. C. Jiménez, C. Dietrich-Buchecker, J.-P. Sauvage, *Angew. Chem. Int. Ed.* **2000**, *39*, 3284–3287. (c) E. Berni, B. Kauffmann, C. Bao, J. Lefeuvre, D. M. Bassani, I. Huc, *Chem. Eur. J.* **2007**, *13*, 8463–8469. (d) L. Fang, M. Hmadeh, J. Wu, M. A. Olson, J. M. Spruell, A. Trabolsi, Y.-W. Yang, M. Elhabiri, A.-M. Albrecht-Gary, J. F. Stoddart, *J. Am. Chem. Soc.* **2009**, *131*, 7126–7134. (e) K. Miwa, Y. Furusho, E. Yashima, *Nat. Chem.* **2010**, *2*, 444–449.

19) Crystal data for **3**: $C_{24}H_{14}O_6$: FW = 398.35, monoclinic, space group $P2_1/c$, a = 11.301(3) Å, b = 5.8285(15) Å, c = 14.258(4) Å, β = 108.868(3), V = 888.7(4) Å^3, Z = 2, D_{calcd} = 1.489, 3,846 reflections measured, 1,563 unique reflections, 1,302 observations ($I > 2.0\sigma(I)$), R = 0.0330 ($I > 2.0\sigma(I)$), Rw = 0.0888 ($I > 2.0\sigma(I)$). CCDC 917094, Crystal data for **4**: $C_{27}H_{24}O_9$: FW = 492.46, triclinic, space group *P-1*, a = 9.4625(13) Å, b = 11.3827(16) Å, c = 11.5726(17) Å, α = 92.198(2), β = 110.599(2), γ = 98.513(2), V = 1,148.4(3) Å^3, Z = 2, D_{calcd} = 1.424, 5,521 reflections measured, 3,983 unique reflections, 3,230 observations ($I > 2.0\sigma(I)$), R = 0.0381 ($I > 2.0\sigma(I)$), Rw = 0.1037 (I

> 2.0$\sigma(I)$). CCDC 917095, Crystal data for **5**: $C_{28}H_{26}O_8$: FW = 490.49, triclinic, space group *P-1*, *a* = 8.337(3) Å, *b* = 8.518(4) Å, *c* = 8.983(4) Å, α = 71.791(5), β = 77.809(5), γ = 80.783(6), *V* = 589.2(4) Å^3, *Z* = 1, D_{calcd} = 1.382, 2,815 reflections measured, 2,035 unique reflections, 1,731 observations ($I > 2.0\sigma(I)$), *R* = 0.0582 ($I > 2.0\sigma(I)$), *R*w = 0.1553 ($I > 2.0\sigma(I)$). CCDC 917096.

20) J. A. Campbell, R. W. Koch, J. V. Hay, M. A. Ogliaruso, J. F. Wolfe, *J. Org. Chem.* **1974**, *39*, 146–152.

21) D. F. Martin, M. Shamma, W. C. Fernelius, *J. Am. Chem. Soc.* **1958**, *80*, 4891–4895.

Chapter 4

Reversible Crosslinking and Decrosslinking of Polymers Containing Alcohol Moiety Utilizing an Acyclic Bifunctional Vicinal Triketone

4.1 Introduction

Polymer materials that can be reversibly crosslinked and decrosslinked have recently attracted much attention from the standpoint of chemical recycling as well as self-healing materials.[1,2] One of the effective strategies for constructing such systems is to utilize covalent bonds that can be reversibly formed and dissociated. These reversible reactions involve thermoreversible Diels–Alder reaction,[3] disulfide exchange,[4] imine formation,[5] radical exchange reaction,[6] photoinduced [2 + 2] cycloaddition,[7] reversible ring-opening–closing reaction of heterocycles,[8] and so on. Most of these works were demonstrated by utilizing polymers in which the functionalities had been incorporated into their side chains or termini in advance.

Vicinal tricarbonyl compounds, such as alloxan, 1,2,3-indanetrione, dehydroascorbic acid, and diphenylpropanetrione (DPPT, **1**), have by definition the three contiguous carbonyl groups, and are characterized by a highly electrophilic central carbonyl group (Scheme 4.1).[9,10] Consequently, weak nucleophiles, such as water or alcohols, attack to the central carbonyl without any catalysts to form *gem*-diol (**2**) or hemiketal (**3**) structure, respectively, which can dissociate to give the free tricarbonyl by heating or treatment with appropriate solvents or reagents (Scheme 4.1a). Furthermore, these addition–elimination behaviors are detectable by the naked eye, since they are accompanied by collapse and recovery of the three sequential carbonyl groups characterized by

yellow–orange coloration. Intrigued by these characteristic features, the author has designed and synthesized polystyrenes bearing tricarbonyl and its hydrate structures.[11] The author carried out crosslinking of the polystyrenes through hemiketal linkages by using α,ω-diols and the crosslinked polymer could be decrosslinked by treatment with water-containing solvents to give the original polystyrenes in high yields.[12,13] Very recently, the author has also reported the facile synthesis of an acyclic bifunctional vicinal tricarbonyl compound, 1,4-phenylenebis(phenylpropanetione) **4**, and revealed by single X-ray crystallographic analysis that water and ethanol molecules covalently attached to the central carbonyl carbon atoms of **4** to form its hydrate **5a**, and its ethanol-adduct **5c**, respectively.[14] These three species could be reversibly converted to one another in a facile manner (Scheme 4.1b).

Scheme 4.1 Reversible Addition–Elimination of Water and Alcohols to Vicinal Tricarbonyl Compounds

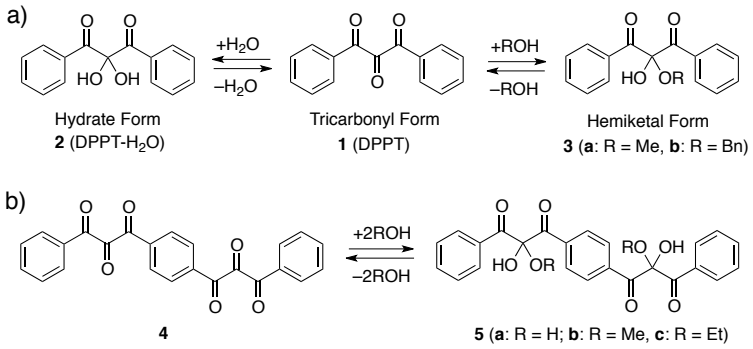

Here the author describes new reversible crosslinking and decrosslinking systems of commercially available, alcoholic polymers, namely, poly(2-hydroxyethyl methacrylate) (PHEMA) and poly(vinyl alcohol) (PVA), utilizing the bifunctional vicinal tricarbonyl compound **4** as a crosslinking reagent. These polymers were crosslinked through hemiketal linkages formed between the hydroxyl groups of the polymer side chains and the central carbonyl groups of the vicinal tricarbonyl moieties of the bistriketone **4**. The resulting networked polymers could be decrosslinked

by treating with water-containing solvent or alcoholic solvent to regenerate the original linear polymers in high yield as well as to recover a certain amount of bistriketone **4**.

4.2 Experimental Section

4.2.1 Materials

DMSO and DMSO-d_6 were distilled over molecular sieves 4A (MS 4A). Acetone was distilled over $CaCl_2$. Methanol and methanol-d_4 were distilled over CaH_2. THF and diethyl ether were distilled over sodium benzophenone ketyl. D_2O (Merck KGaA, Germany) was purchased and used without further purification. PHEMA (M_v 300,000, Aldrich) and PVA (polymerization degree: *ca.* 2,000 (corresponding to M_n 88,000), saponification degree: min. 98.5%, Nacalai tesque, Japan) were purchased and dried *in vacuo* at 80 ºC for 12 h before use. DPPT **1**[11] and Bistriketone **4**[14] were synthesized according to the literature. Copolymer of 2-hydroxyethyl methacrylate (HEMA) and methyl methacrylate (MMA) with a number-average molecular weight of 4.3×10^3 and a PDI of 2.0 was prepared by radical copolymerization of HEMA and equimolar MMA with 20 mol % of 2,2'-azobis(isobutyronitrile) (AIBN) in DMF (1.0 M) at 60 ºC for 22 h.

4.2.2 General Measurements

^{1}H NMR spectra were measured on a JEOL JNM-ECS 400 spectrometer at a resonance frequency of 400 MHz with tetramethylsilane (TMS) as an internal standard. NMR chemical shifts were reported in delta unit (δ). IR spectra were recorded on a Thermo Scientific Nicolet iS10 spectrometer. Number-average and weight-average molecular weights (M_n, M_w) and polydispersity indices (M_w/M_n) of the polymers were estimated by size exclusion chromatography (SEC) using tetrahydrofuran (THF) as the eluent at a flow rate of 0.6 mL/min at 40 ºC, performed on a Tosoh

chromatograph model HLC-8320 system equipped with Tosoh TSKgel SuperHM-H styrogel columns (6.0 mm ϕ × 15 cm, 3 and 5 μm bead sizes), refractive index (RI) detector, and UV–vis detector (254 nm). The molecular weight calibration curve was obtained with polystyrene standards. Thermogravimetric analysis (TGA) was performed on a Seiko Instrument Inc. TG-DTA 6200 with an aluminum pan under a 150 mL/min N_2 flow at a heating rate of 10 ºC/min. Differential scanning calorimetry (DSC) was carried out with a Seiko Instrument DSC-6200 with an aluminum pan under a 20 mL min^{-1} N_2 flow at the heating rate of 10 ºC/min.

4.2.3 Model Reactions

Addition Reaction of DPPT 1 to PHEMA and Subsequent Dissociation Reaction. A typical experimental procedure was as follows. PHEMA (130 mg, 1.00 mmol) was dissolved in 0.50 mL of DMSO-d_6 under argon atmosphere. To the solution was added DPPT **1** (238 mg, 1.00 mmol), the solution was transferred to an NMR tube. After 4 days, to the solution was added 55.0 μL of D_2O. The reaction progress was monitored by ^{1}H NMR.

4.2.4 Crosslinking and Decrosslinking

Crosslinking of PHEMA with Bistriketone 4. A typical experimental procedure was as follows. To a solution of PHEMA (260 mg, 2.00 mmol) in DMSO (1.0 mL) was added bistriketone **4** (79.7 mg, 0.200 mmol), and the reaction mixture was stirred at ambient temperature under argon atmosphere for 4 days. The resultant highly viscous mixture was filtered and washed by THF (10 mL × 3). The insoluble part was dried *in vacuo* to afford the networked polymer **6** (330 mg, 97%) as a yellow solid. IR (ATR): 3388 (O–H), 2945 (C–H), 1720 (C=O) cm^{-1}; glass transition temperature (T_g) 84 ºC; 5% weight loss temperature (T_{d5}) 182 ºC; 10% weight loss temperature (T_{d10}) 245 ºC; 15% weight loss temperature (T_{d15}) 292 ºC.

Decrosslinking of Networked Polymer 6. To the DMSO-containing networked polymer **6** prepared as described above, MeOH (9.0 mL) was added and the mixture was stirred for 4 days. The resulting solution was precipitated with diethyl ether (200 mL) and filtered to obtain PHEMA (244 mg, 94%) as a white solid. ^{1}H NMR (400 MHz, 298 K, DMSO-d_6): see Figure 4.10. To the filtrate, H_2O (100 mL) was added and the mixture was stirred for several hours. The resulting precipitate was collected and heated *in vacuo* (100 ºC, 1 mmHg) to afford bistriketone **4** as an orange solid (43.0 mg, 54%).

Crosslinking of PVA with Bistriketone 4. A typical experimental procedure was as follows. PVA (176 mg, 4.00 mmol) was dissolved in DMSO (2.0 mL) at 50 ºC for 12 h. Then the solution was cooled to ambient temperature. To the solution was added bistriketone **4** (159 mg, 0.400 mmol), and the reaction mixture was stirred under argon atmosphere for 4 days. The resultant highly viscous mixture was filtered and washed by THF (10 mL × 3). The insoluble part was dried *in vacuo* to afford the networked polymer **7** (246 mg, 73%) as an orange solid. IR (ATR): 3290 (O–H), 2907 (C–H), 1725 (central C=O), 1684 (side C=O) cm^{-1}; glass transition temperature (T_g) 76 ºC; 5% weight loss temperature (T_{d5}) 248 ºC; 10% weight loss temperature (T_{d10}) 276 ºC; 15% weight loss temperature (T_{d15}) 295 ºC.

Decrosslinking of Networked Polymer 7. To the DMSO-containing networked polymer **7** prepared as described above, H_2O-DMSO (1/9, v/v, 20 mL) was added and the mixture was stirred for 7 days. The resulting mixture was precipitated with acetone (300 mL) and filtered to obtain PVA (176 mg, quant.) as a light yellow solid. ^{1}H NMR (400 MHz, 298 K, DMSO-d_6): see Figure 4.14. To the filtrate, H_2O (100 mL) was added and the mixture was stirred for several hours. The resulting precipitate was collected and heated *in vacuo* (100 ºC, 1 mmHg) to afford bistriketone **4** as an orange solid (92.0 mg, 58%).

4.3 Results and Discussion

4.3.1 Reversible Addition and Elimination of DPPT with PHEMA

First, the author examined the reactivity of the hydroxyl group of the polymer side chain with vicinal triketone moiety, using the monofunctional triketone, DPPT **1**, as a model. DPPT **1** equimolar to the OH groups of PHEMA was added to a solution of PHEMA in DMSO-d_6 at a concentration of 1.7 M, and the reaction was monitored by ^{1}H NMR spectroscopy at ambient temperature (*ca*. 25 ºC) (Scheme 4.2a). Figure 4.1a–c shows the time dependence of ^{1}H NMR spectra of this reaction mixture. At an early stage of the reaction, three sharp peaks originating from the phenyl protons of the free tricarbonyl **1** were detected in the aromatic region and broad signals of PHEMA were observed in the aliphatic region, separately (Figure 4.1a). After several hours, additional broad peaks attributable to the phenyl protons and the hemiketal OH signals of DPPT bonding to the PHEMA side chains appeared in the aromatic region, simultaneously with a decrease in the OH signal intensity of PHEMA at around 4.8 ppm (Figure 4.1b). The mixture reached equilibrium within 3 days (Figure 4.1c). The contents of the hemiketal formed on the polymer side chain were estimated based on the integral ratios of the hydroxyl signal of PHEMA compared with the residual signal of the DMSO-d_6 solvent. The content ratios of the hemiketal unit to the free tricarbonyl unit were plotted against the reaction time, along with those of the reaction between benzyl alcohol (BnOH) with DPPT **1** (1.7 M)[12] (Figure 4.2). The content ratio of the hemiketal unit at the equilibrium state was estimated to be 60%. Both the reaction rate and the final content ratio of the hemiketal unit were slightly lower than those of DPPT **1** with BnOH, probably because of the steric hindrance due to the PHEMA main chain. In addition, the concentration also affected the addition reaction: at lower concentration of 1.0 M, the reaction rate became slower and the hemiketal contents decreased to 44% at equilibrium.

Scheme 4.2 Addition reaction of DPPT **1** to PHEMA, and its dissociation by alcohol–water exchange or alcohol–alcohol exchange reaction

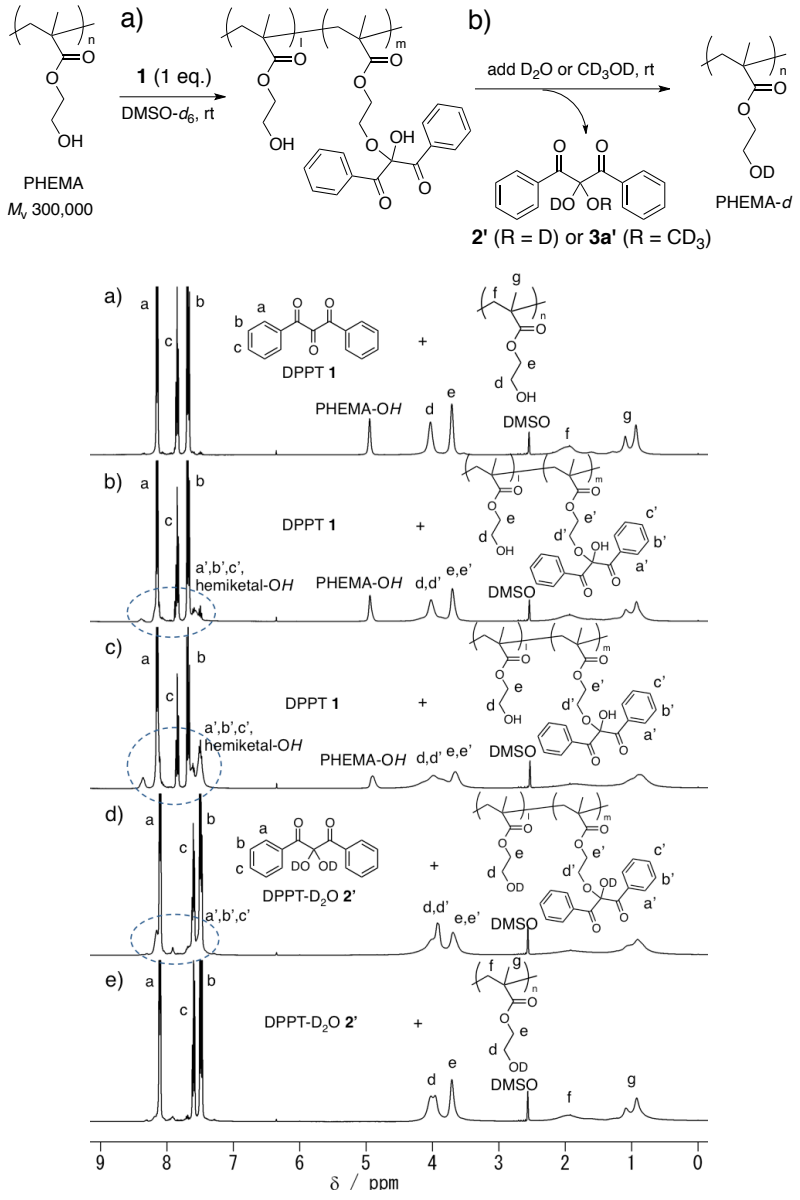

Figure 4.1 ^{1}H NMR (400 MHz, 298 K) spectra of a reaction mixture of PHEMA and DPPT **1** in DMSO-d_6 (1.7 M) after (a) 10 min, (b) 6 h, (c) 72 h, and (d) 1 day and (e) 7 days after adding D_2O.

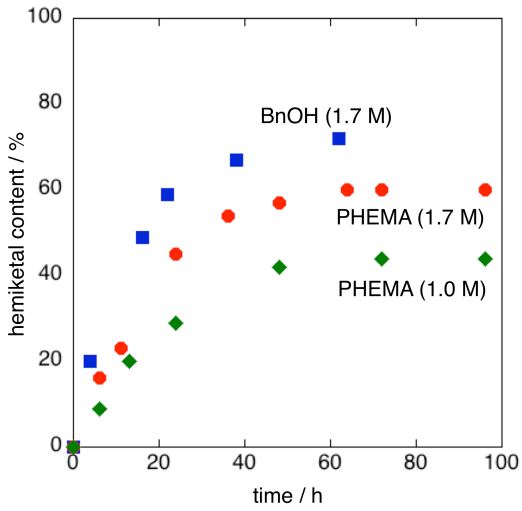

Figure 4.2 Changes in the content ratios of the hemiketal DPPT-ROH (ROH = BnOH or PHEMA) in DMSO-d_6.

The author investigated the dissociation reaction of the DPPT moiety from the PHEMA side chain through alcohol–water exchange or alcohol–alcohol exchange reaction by adding D_2O or CD_3OD directly into the equilibrium mixtures, respectively (Scheme 4.2b). An excess of D_2O was added to the equilibrium mixture, and the progress of the dissociation reaction was monitored by ^1H NMR (D_2O/DMSO-d_6 = 1/9, v/v). The signals of the hydroxyl protons of the PHEMA side chain and the hemiketal disappeared immediately because of proton–deuteron exchange with D_2O. The unreacted free DPPT **1** was also smoothly converted into its D_2O-adduct, DPPT-D_2O **2'**, whereas the attached DPPT moiety was slowly dissociated through alcohol–water exchange (Figure 4.1d). Eventually, the exchange reaction had almost completed within several days after adding D_2O (Figure 4.1e). By utilizing CD_3OD instead of D_2O, an almost quantitative dissociation was also achieved within several days; DPPT moiety was detached from the polymer chain and converted into its methanol-adduct, DPPT-CD_3OD **3a'**, by alcohol–alcohol exchange reaction (Figure 4.3).

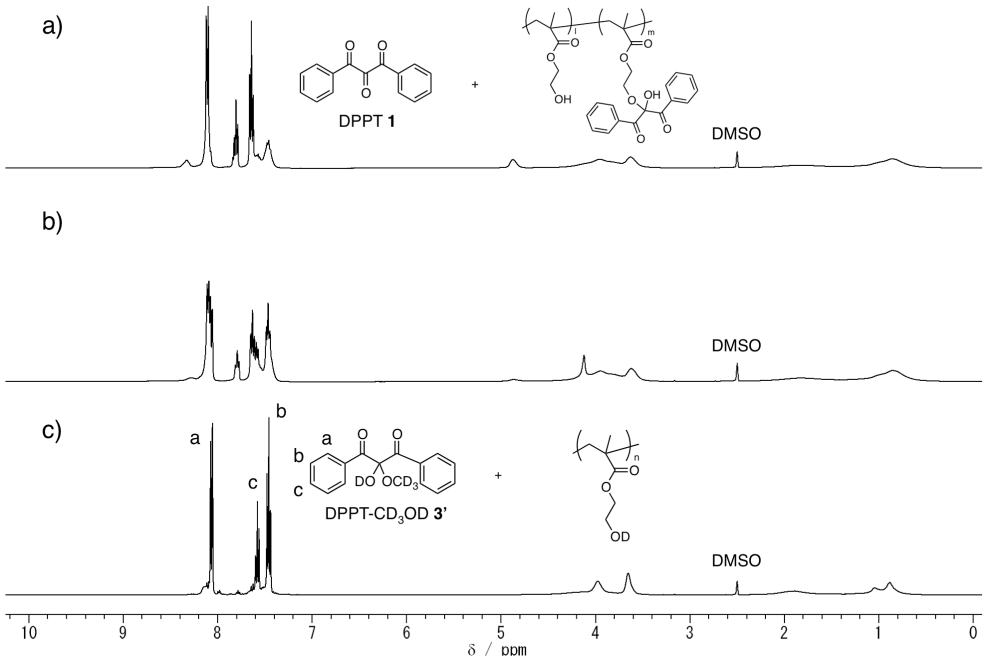

Figure 4.3 ^{1}H NMR spectra (400 MHz, 298 K) of a reaction mixture of PHEMA (1.0 M) and DPPT **1** (1.0 M) in DMSO-d_6 (a) 72 h after mixing, (b) 2 h and (c) 8 days after addition of CD_3OD.

4.3.2 Reversible Crosslinking and Decrosslinking of PHEMA

On the basis of the model reactions, the author demonstrated reversible crosslinking–decrosslinking of PHEMA utilizing bifunctional vicinal triketone **4** (Scheme 4.3). A small amount of bistriketone **4** (0.2 equiv. of the tricarbonyl moiety relative to the OH group of PHEMA) was added to a concentrated solution (1.7 M) of PHEMA in DMSO, and the resulting mixture exhibited the characteristic orange coloration due to the free tricarbonyl functionalities (Figure 4.4a). Viscosity of the solution gradually increased and a yellow-colored gel was formed after several hours. The highly viscous mixture was allowed to stand for 4 more days (Figure 4.4b). The resulting networked polymer gel was washed with THF and the insoluble part was dried *in vacuo* to afford the crosslinked PHEMA **6** in 97% yield. The IR absorption peak of the carbonyl groups of **6** at 1720 cm^{-1} was broadened when compared to that of the original PHEMA (1714 cm^{-1}), indicating the presence of the unreacted vicinal tricarbonyl structure (*ca*. 1723 cm^{-1} and *ca*. 1675 cm^{-1}) as well

as the hemiketal structure (*ca*. 1674 cm^{-1}) (Figure 4.5).[14] The glass transition temperature (T_g) of the crosslinked PHEMA **6** was 84 ºC (Figure 4.6), which was much the same as that of the linear PHEMA (T_g 85 ºC)[15]. Thermogravimetric analysis (TGA) showed that the T_{d15} of the networked polymer **6** (292 ºC) was higher than that of the original PHEMA (282 ºC), whereas the T_{d5} and T_{d10} of **6** (182 ºC and 218 ºC, respectively) were lower than those of the PHEMA (218 ºC and 247 ºC, respectively) (Figure 4.7). These results could be explained in terms of a balance between decomposition of the bistriketone component and stabilization by the network formation. In order to further investigate the crosslinking behavior, the author performed an additional ^{1}H NMR experiment. A solution of PHEMA (1.0 M) and **4** (0.10 M) in DMSO-d_6 was subjected to ^{1}H NMR measurement to monitor the network formation reaction (Figure 4.8). In its initial stage, four sharp signals for the aromatic protons of **4** were observed over the range of δ 8.5–7.5 ppm. As is the case with DPPT **1**, broad peaks appeared in the aromatic region after several hours. The mixture reached equilibrium within 48 h, where the conversion of the triketone into the hemiketal structure was estimated to be *ca.* 70% on the basis of the relative integral intensity of the signal of the OH group of the PHEMA at 4.8 ppm. The network formation was also confirmed by SEC analysis (Figure 4.9).[3d,13] To facilitate to detect the changes in the molecular weight, a THF-soluble random copolymer of HEMA and methyl methacrylate (MMA) with a lower molecular weight (poly(HEMA$_{54}$-*co*-MMA$_{46}$), M_n = 4.3 × 10^3, PDI = 2.0) was prepared by free radical copolymerization and allowed to react with bistriketone **4** (0.2 equiv. of the tricarbonyl moiety relative to the OH group of the copolymer) in DMSO (1.0 M). The progress of the network formation was monitored by SEC measurements, which showed that both the molecular weight and the PDI of the copolymer increased monotonously; the M_n (PDI) evaluated by refractive index (RI) after 4 h and 24 h were 5.9 × 10^3 (2.4) and 6.9 × 10^3 (3.0), respectively (Figure 4.9a). The SEC profiles obtained with a UV detector (254 nm) clearly represented the attachment process of the

aromatic bistriketone crosslinker to the aliphatic polymer (Figure 4.9b). The UV absorption intensity of the polymer component increased with time whereas that of the sharp signal at 5.5 min originating from the bistriketone decreased.

Scheme 4.3 Crosslinking and decrosslinking of PHEMA exploiting bistriketone **4**

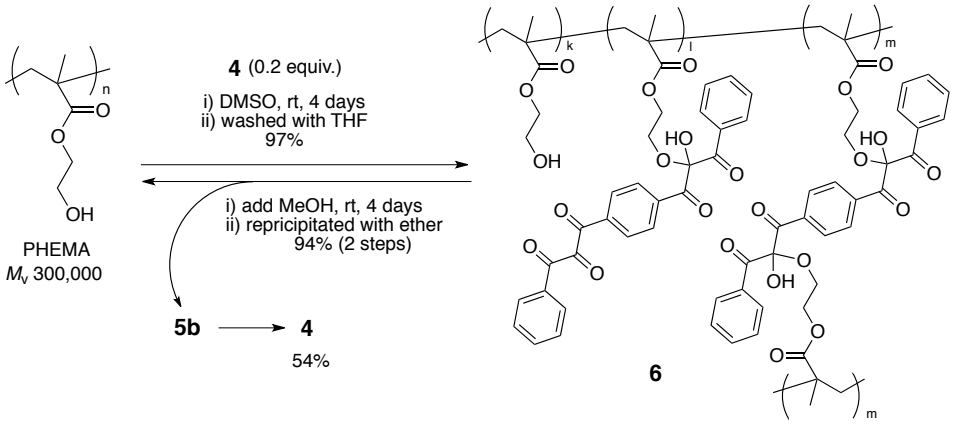

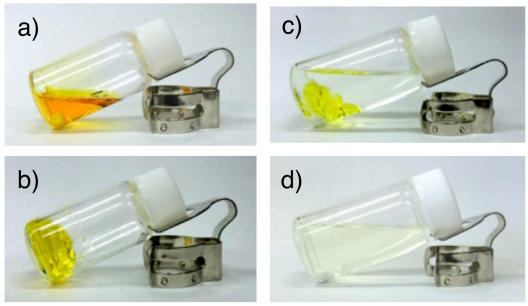

Figure 4.4 Photographs showing the crosslinking and decrosslinking behavior of PHEMA exploiting bistriketone **4**: (a) just after and (b) 4 days after adding bistriketone **4**, (c) just after and (d) 4 days after adding MeOH to the networked PHEMA **6**.

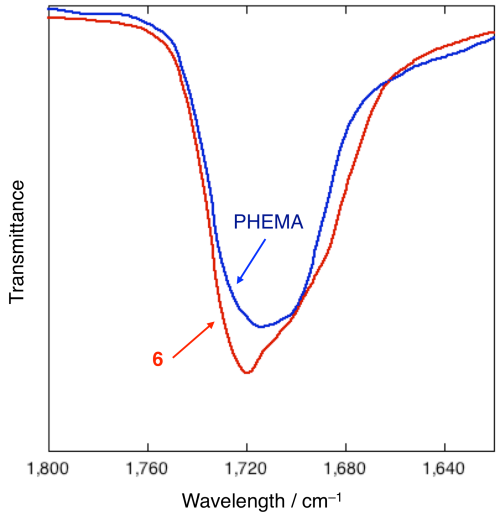

Figure 4.5 Partial IR spectra (ATR) of the as-prepared PHEMA and the crosslinked PHEMA **6**.

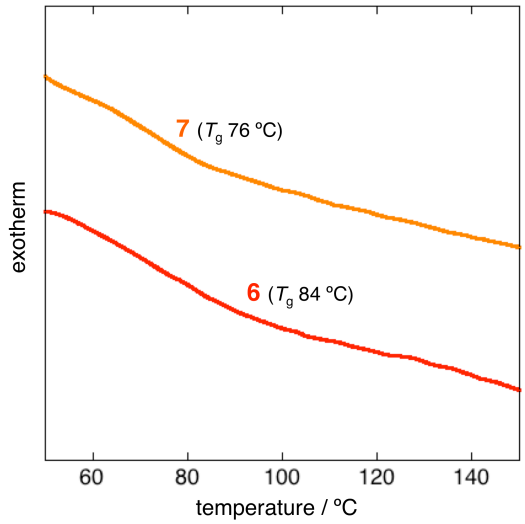

Figure 4.6 DSC profiles of **6** and **7** at a scan rate of 10 °C/min with a N_2 flow of 20 mL/min.

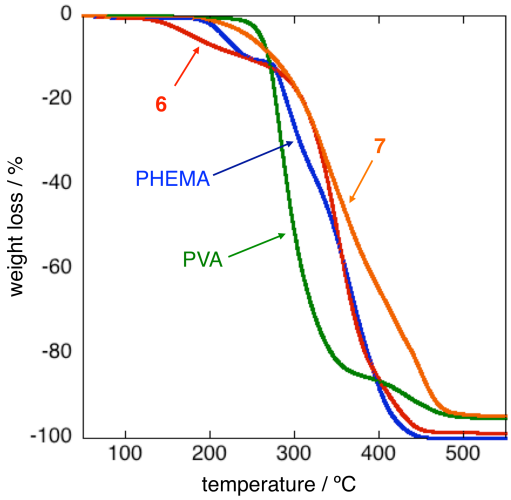

Figure 4.7 TG profiles of **6**, **7**, the original PHEMA, and the original PVA at a scan rate of 10 °C/min with a N_2 flow of 150 mL/min.

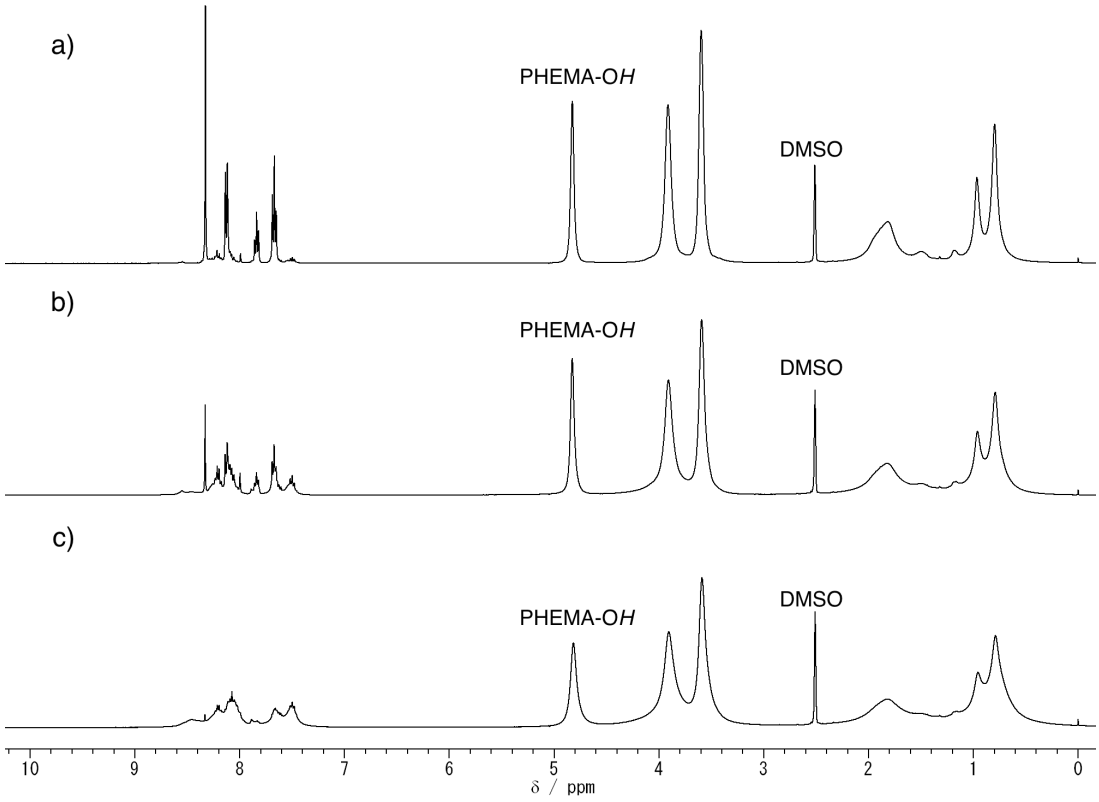

Figure 4.8 ^{1}H NMR spectra (400 MHz, 298 K, DMSO-d_6) of a reaction mixture of PHEMA (1.0 M) and bistriketone **4** (0.10 M) (a) after 20 min, (b) 4 h, and (c) 48 h.

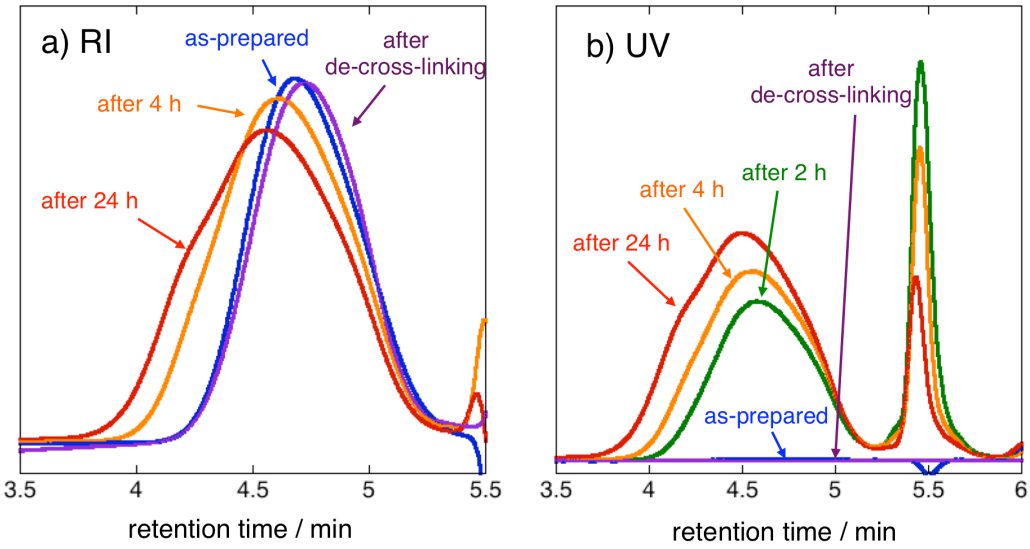

Figure 4.9 SEC profiles of the crosslinking reaction mixture of poly(HEMA-*co*-MMA) with bistriketone **4** along with those of the original, as-prepared poly(HEMA-*co*-MMA) and the poly(HEMA-*co*-MMA) recovered after decrosslinking: (a) refractive index (RI), and (b) UV absorption (254 nm).

The author then conducted the decrosslinking of the resulting networked polymer **6** by adding an excess of methanol to the gel prepared in DMSO at ambient temperature (Figure 4.4c). After being gently stirred for several hours, the mixture became a faintly yellow-colored homogeneous solution, which was stirred for 4 days in total (Figure 4.4d). The original, linear PHEMA was isolated in high yield by simple reprecipitation with diethyl ether: the insoluble part was collected and dried *in vacuo* to obtain PHEMA as a white solid in 94% yield, of which the ^{1}H NMR spectrum was identical with that of the original PHEMA (Figure 4.10). No peaks were detected in the aromatic region unambiguously indicating a complete dissociation of the bistriketone moiety from the polymer chain. Moreover, the bistriketone **4** was also recovered from the filtrate by evaporating volatile components followed by precipitation from water and subsequent heating at 100 ºC *in vacuo*[14] in 54% yield. The complete decrosslinking was also supported by SEC analysis. The

above-mentioned reaction mixture of the partially crosslinked copolymer was treated with an excess of MeOH for 3 days. The SEC profiles of the resulting mixture in both RI and UV detection modes (M_n = 4.5 × 10^3, PDI = 1.8) agreed well with those of the original, as-prepared polymer (Figure 4.9).

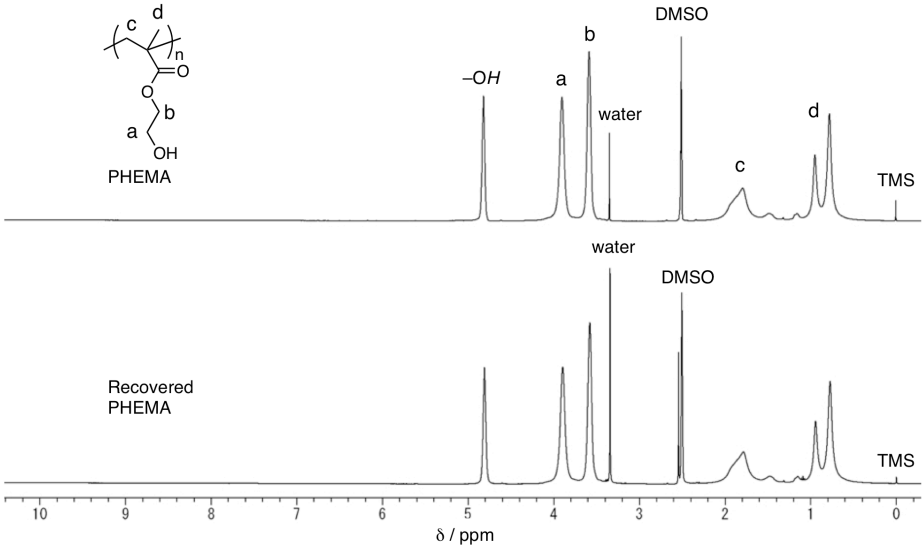

Figure 4.10 ^{1}H NMR spectra (400 MHz, 298 K, DMSO-d_6) of the original and the recovered PHEMA.

4.3.3 Reversible Crosslinking and Decrosslinking of PVA

Finally, the author demonstrated reversible crosslinking–decrosslinking of PVA using bistriketone **4** (Scheme 4.4). In the same manner as PHEMA, bistriketone **4** (0.2 equiv. of the tricarbonyl moiety relative to the OH group of PVA) was added to a concentrated solution of a fully hydrolyzed (≥ 98.5%) PVA in DMSO (1.7 M, Figure 4.11a). A deeply red-colored gel was formed after 1 day, and the mixture was allowed to stand for 3 more days (Figure 4.11b). The resulting gel was washed with THF and the insoluble part was dried *in vacuo* to afford the crosslinked PVA **7** as a deep-red solid in 76% yield. The deeper coloring and the lower yield of the networked polymer compared to those of the networked PHEMA **6** indicated that the PVA gel **7** contained a larger amount of the unreacted tricarbonyl moiety. Steric hindrance around the secondary OH groups

directly attached to the PVA main chain accounts for this considerably low reactivity in comparison with PHEMA having the primary OH groups relatively distant from its main chain. This observation was consistent with the results that the bulkiness of alcohol has a great influence on the reaction rate with DPPT, as discussed in the previous report.[12] In fact, the THF-soluble part consisted mainly of the unreacted bistriketone **4**. The IR absorption spectrum of **7** exhibited two additional peaks at 1725 cm^{-1} and 1684 cm^{-1} along with those of the original PVA, originating from the central and side carbonyl groups of the tricarbonyl moiety, respectively (Figure 4.12). The observed T_g of **7** was 76 ºC (Figure 4.6), which is lower than that of the original PVA (T_g 85 ºC)[16]. A possible explanation for the decrease of the T_g of PVA is likely that the bistriketone moiety attached to the PVA disrupted the hydrogen-bonding interaction among the nearby OH groups. The networked polymer **7** exhibited a high thermal stability above 270 ºC in comparison with the original PVA, although its thermal decomposition started at a lower temperature than that of the original PVA (Figure 4.7). In the same manner as that for PHEMA, the author examined the network formation reaction in DMSO-d_6 and monitored the changes in the ^{1}H NMR spectra with time (Figure 4.13). Some spectral change was observed in the aromatic region within a few days, suggesting that a certain amount of the hemiketal structure was formed. Although the content of the hemiketal linkage was too low to be estimated by NMR or IR, the insoluble polymer gel was thus obtained with a small amount of crosslinking points.

Scheme 4.4 Reversible crosslinking and decrosslinking of PVA exploiting bistriketone **4**

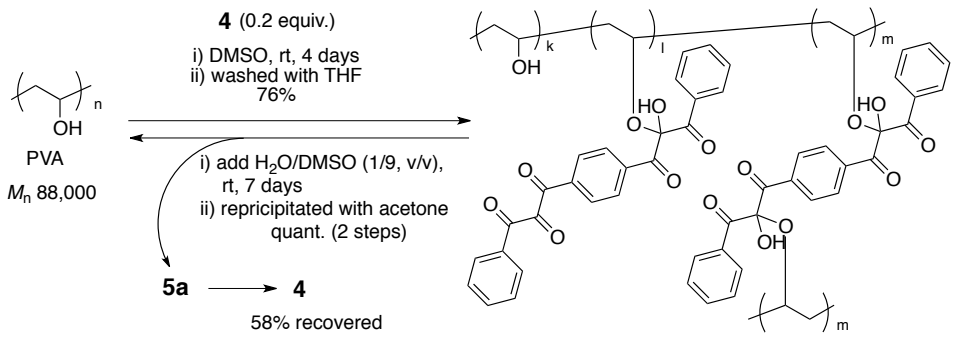

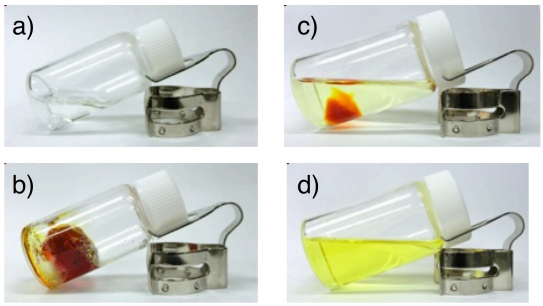

Figure 4.11 Photographs showing the crosslinking and decrosslinking behavior of PVA exploiting bistriketone **4**: (a) before and (b) 4 days after adding bistriketone **4** to a PVA solution, (c) just after and (d) 7 days after adding H_2O-DMSO (1/9, v/v) to the networked PVA.

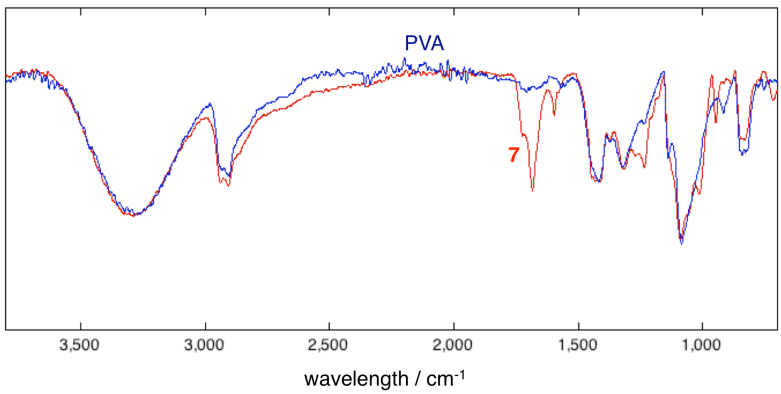

Figure 4.12 IR spectra (ATR) of the original and crosslinked PVA **7**.

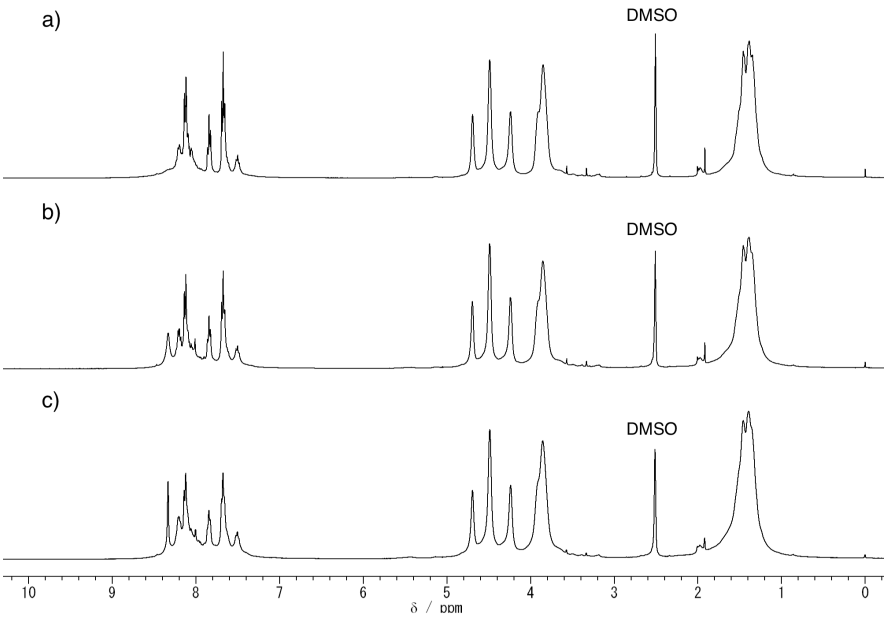

Figure 4.13 ^{1}H NMR spectra (400 MHz, 298 K, DMSO-d_6) of a reaction mixture of PVA (1.0 M) and bistriketone **4** (0.10 M) (a) after 20 min, (b) 2 h, and (c) 48 h.

Decrosslinking of the networked polymer **7** was carried out by adding a large amount of water-DMSO (1/9, v/v) (Figure 4.11c). The mixture was slowly turned into a yellow, homogeneous solution within 1 day, and allowed to stand at ambient temperature for an additional 6 days (Figure 4.11d). Reprecipitation of the solution with acetone yielded a light yellow solid, of which the ^{1}H NMR spectrum showed small signals in the aromatic region indicating an incomplete dissociation of the bistriketone crosslinker (Figure 4.14). This incomplete decrosslinking behavior might be due to the low reaction rate of the vicinal tricarbonyl group with the secondary hydroxyl group of PVA. Addition of water to the filtrate after evaporation of volatile components precipitated the bistriketone hydrate **5a**, which was heated at 100 ºC *in vacuo* to gave **4** in 58% yield.[14] The bistriketone thus recovered was sufficiently pure, in contrast to the recovered PVA.

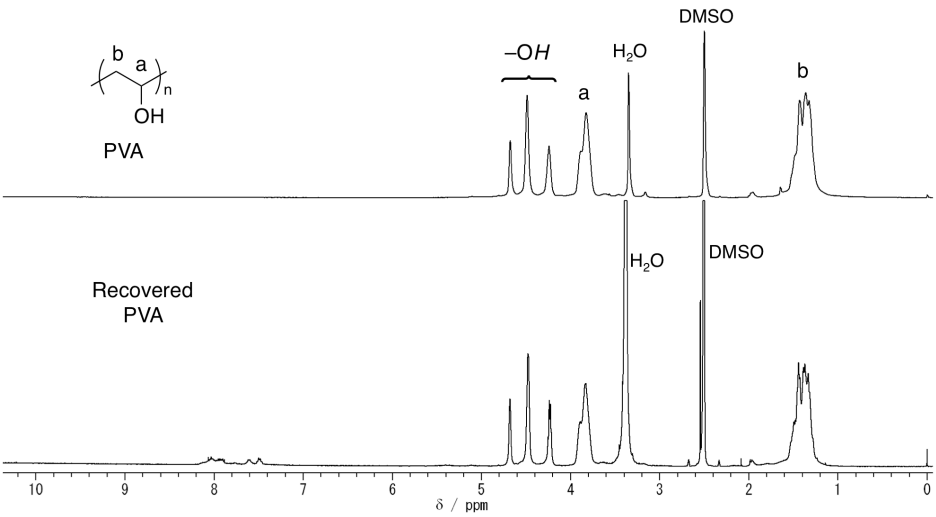

Figure 4.14 ^{1}H NMR spectra (400 MHz, 298 K, DMSO-d_6) of the original and the recovered PVA.

4.4 Conclusions

In conclusion, the author has constructed the reversible crosslinking and decrosslinking systems of commercially available alcoholic polymers, utilizing the acyclic bifunctional vicinal triketone. The network formation proceeded simply by adding bistriketone **4** to the polymer solution without catalyst or external stimuli. Conversely, treatment of the crosslinked polymers with water-containing solvent or alcoholic solvent resulted in dissociation of the network to recover the original, linear alcoholic polymers along with the bistriketone crosslinker. Through this study, the author has demonstrated that vicinal tricarbonyl structure is an efficient functionality for reversible crosslinking and decrosslinking systems, thereby being considered to be promising structural motif for constructing recycling polymers or sophisticated macromolecular architectures.

4.5 References

1) For selected reviews on polymer recycling, see; (a) F. Sanda, T. Endo, *Polym. Recycl.* **1998**, *3*, 159–163. (b) T. Endo, D. Nagai, *Macromol. Symp*. **2005**, *226*, 79–86. (c) T. Takata, *Polym. J*. **2006**, *38*, 1-20. (d) H. Nishida, *Polym. J.* **2011**, *43*, 435–447.

2) For selected reviews on self-healing materials, see; (a) M. D. Hager, P. Greil, C. Leyens, S. van der Zwaag, U. S. Schubert, *Adv*. *Mater*. **2010**, *22*, 5424–5430. (b) C. J. Kloxin, T. F. Scott, B. J. Adzima, C. N. Bowman, *Macromolecules* **2010**, *43*, 2643–2653. (c) N. K. Guimard, K. K. Oehlenschlaeger, J. Zhou, S. Hilf, F. G. Schmidt, C. Barner-Kowollik, *Macromol*. *Chem*. *Phys*. **2012**, *213*, 131–143. (d) M. W. Urban, *Nat*. *Chem*. **2012**, *4*, 80–82.

3) (a) X. Chen, M. A. Dam, K. Ono, A. Mal, H. Shen, S. R. Nutt, K. Sheran, F. Wudl, *Science* **2002**, *295*, 1698–1702. (b) X. Chen, F. Wudl, A. K. Mal, H. Shen, S. R. Nutt, *Macromolecules* **2003**, *36*, 1802–1807. (c) P. Reutenauer, E. Buhler, P. J. Boul, S. J. Candau, J.-M. Lehn, *Chem. Eur. J.* **2009**, *15*, 1893–1900. (d) A. J. Inglis, L. Nebhani, O. Altintas, F. G. Schmidt, C. Barner-Kowollik, *Macromolecules* **2010**, *43*, 5515–5520. (e) K. Ishida, V. Weibel, N. Yoshie,. *Polymer* **2011**, *52*, 2877–2882. (f) N. Yoshie, S. Saito, N. Oya, *Polymer* **2011**, *52*, 6074–6079. (g) P. M. Imbesi, C. Fidge, J. E. Raymond, S. I. Cauët, K. L. Wooley, *ACS Macro. Lett.* **2012**, *1*, 473–477.

4) (a) T. Oku, Y. Furusho, T. Takata, *Angew. Chem. Int. Ed.* **2004**, *43*, 966–969. (b) T. Bilig, T. Oku, Y. Furusho, Y. Koyama, S. Asai, T. Takata, *Macromolecules* **2008**, *41*, 8496–8503. (c) J. A. Yoon, J. Kamada, K. Koynov, J. Mohin, R. Nicolaÿ, Y. Zhang, A. C. Balazs, T. Kowalewski, K. Matyjaszewski, *Macromolecules* **2012**, *45*, 142–149.

5) (a) W. G. Skene, J.-M. Lehn, *Proc. Natl. Acad. Sci. USA* **2004**, *101*, 8270–8275. (b) J. F. Folmer-Andersen, J.-M. Lehn, *J. Am. Chem. Soc.* **2011**, *133*, 10966–10973. (c) H. Kanazawa, M. Higuchi, K. Yamamoto, *Macromolecules* **2006**, *39*, 138–144. (d) G. Deng, C. Tang, F. Li, H. Jiang, Y. Chen, *Macromolecules* **2010**, *43*, 1191–1194.

6) (a) Y. Higaki, H. Otsuka, A. Takahara, *Macromolecules* **2006**, *39*, 2121–2125. (b) Y. Amamoto, Y. Higaki, Y. Matsuda, H. Otsuka, A. Takahara, *J. Am. Chem. Soc.* **2007**, *129*, 13298–13304. (c) K. Imato, M. Nishihara, T. Kanehara, Y. Amamoto, A. Takahara, H. Otsuka, *Angew. Chem. Int. Ed.* **2012**, *51*, 1138–1142. (d) T. Iwamura, M. Sakaguchi, *Macromolecules* **2008**, *41*, 8995–8999.

7) (a) P. O. Jackson, M. O'Neill, *Chem. Mater.* **2001**, *13*, 694–703. (b) C.-M. Chung, Y.-S. Roh, S.-Y. Cho, J.-G. Kim, *Chem. Mater.* **2004**, *16*, 3982–3984. (c) M. Nagata, Y. Yamamoto, *J. Polym. Sci., Part A: Polym. Chem.* **2009**, *47*, 2422–2433. (d) N. Oya, P. Sukarsaatmadja, K. Ishida, K. Yoshie, *Polym. J.* **2012**, *44*, 724–729.

8) (a) K. B. Wagener, L. P. Engle, *Macromolecules* **1991**, *24*, 6809–6815. (b) T. Endo, T. Suzuki, F. Sanda, T. Takata, *Macromolecules* **1996**, *29*, 3315–3316. (c) T. Endo, T. Suzuki, F. Sanda, T. Takata, *Macromolecules* **1996**, *29*, 4819. (d) T. Nakamura, B. Ochiai, T. Endo, *Macromolecules* **2005**, *38*, 4065–4066. (e) T. Miyagawa, M. Shimizu, F. Sanda, T. Endo, *Macromolecules* **2005**, *38*, 7944–7949. (f) A. W. Kawaguchi, A. Sudo, T. Endo, *ACS Macro Lett.* **2013**, *2*, 1–4.

9) (a) M. B. Rubin, R. Gleiter, *Chem. Rev.* **2000**, *100*, 1121–1164. (b) M. B. Rubin, *Chem. Rev.* **1975**, *75*, 177–202.

10) H. H. Wasserman, J. Parr, *Acc. Chem. Res.* **2004**, *37*, 687–701.

11) (a) T. Dei, K. Morino, A. Sudo, T. Endo, *J. Polym. Sci., Part A: Polym. Chem.* **2011**, *49*, 2245–2251. (b) T. Dei, K. Morino, A. Sudo, T. Endo, *J. Polym. Sci., Part A: Polym. Chem.* **2012**, *50*, 2619–2625.

12) K. Morino, A. Sudo, T. Endo, *Macromolecules* **2012**, *45*, 4494–4499.

13) M. Yonekawa, Y. Furusho, T. Endo, *Macromolecules* **2012**, *45*, 6640–6647.

14) M. Yonekawa, Y. Furusho, Y. Sei, T. Takata, T. Endo, *Tetrahedron* **2013**, *69*, 4076–4080.

15) D. Zaldivar, C. Peniche, A. Bulay, J. San Rowán, *J. Polym. Sci., Part A: Polym. Chem.* **1993**, *31*, 625–631.

16) R. M. Hodge, T. J. Bastow, G. H. Edward, G. P. Simon, A. J. Hill, *Macromolecules* **1996**, *29*, 8137–8143.

Chapter 5

Conclusions

In this thesis, the author have described the results of constructing reversible crosslinking and decrosslinking systems based on reversible addition–elimination reactions between vicinal tricarbonyl compounds and alcohols, with the aim of fabrication of polymer materials which potentially possess chemically recyclable or self-healable properties based on the reactivity of vicinal tricarbonyl compounds. This chapter summarizes the results from each chapter, and describes the perspectives of creation of functional polymer materials utilizing vicinal tricarbonyl functionalities.

Chapter 1 summarized the development of reversible covalent bonds from the early thermodynamic polymer synthesis to recent sophisticated supramolecular construction. Leading investigations of cross-linking and decrosslinking systems utilizing the reversible covalent linkages were described and these materials were capable of chemical recycling and self-healing. The author emphasized that reversible addition–elimination of vicinal tricarbonyl moieties with alcohols were promising reaction for construction of networked polymer systems that can be reversibly crosslinked and decrosslinked under mild conditions.

Chapter 2 focused on the direct water–alcohol exchange reactions on vicinal tricarbonyl moieties, which facilitates crosslinking and decrosslinking procedure of polystyrene bearing vicinal tricarbonyl structure in comparison with the addition–elimination method (Scheme 5.1). By employing DPPT as a unit model compound for the polymer, the author demonstrated that the water–alcohol exchange reactions could be carried out reversibly in both directions by changing

solvents. Similarly to the model reactions, the polystyrene bearing monohydrate structure of vicinal tricarbonyl group was crosslinked with 1,6-hexanediol in acetone at ambient temperature for 5 days to afford the networked polymer in almost quantitative yield. On the other hand, the networked polymer was treated with an excess of water at ambient temperature for 3 days to afford the original linear polymer in high yield as a result of decrosslinking through the water–alcohol exchange reaction.

Scheme 5.1

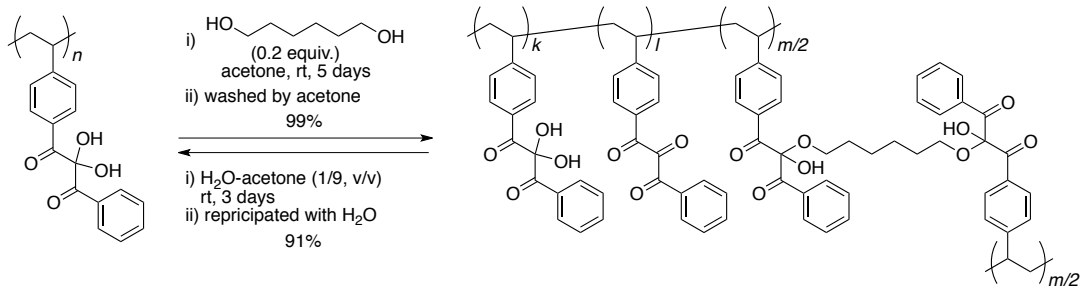

Chapter 3 reported the synthesis and characterization of an acyclic bifunctional vicinal tricarbonyl compound (bistriketone), its hydrate, and its ethanol-adduct (Scheme 5.2). The bistriketone was synthesized by oxidation of the corresponding bis(1,3-diketone) with NBS in DMSO. The bistriketone was readily converted into its hydrate or its ethanol-adduct upon treatment with water-containing solvent or ethanol, respectively. Conversely, heating the hydrate or the ethanol-adduct *in vacuo* quantitatively regenerated the bistriketone. The X-ray crystallographic analysis disclosed that the water and ethanol molecules added to the central carbonyl carbon atoms of the bistriketone. The cyclic voltammogram of the bistriketone indicated that the two vicinal tricarbonyl moieties acted as two-electron acceptor, though the generated dianion species was relatively labile.

Scheme 5.2

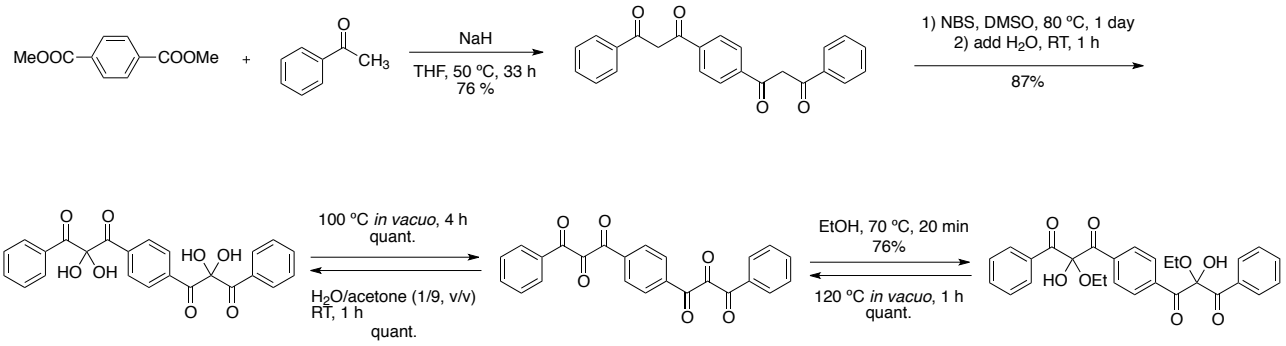

In Chapter 4, the bistriketone was employed as a reversible crosslinking–decrosslinking reagent for polymers containing hydroxyl groups. The network formation proceeded simply by adding a small amount of bistriketone to a solution of PHEMA in DMSO (Scheme 5.3). Conversely, treatment of the crosslinked polymers with MeOH resulted in dissociation of the network to recover the original linear PHEMA in 94% yield along with the bistriketone in 54% yield. The network formation and dissociation behaviors were investigated in detail by ^{1}H NMR and SEC experiments. Similarly to PHEMA, reversible crosslinking and decrosslinking of PVA were achieved by addition of the bistriketone and by treatment of the resulting gel with H_2O/DMSO (1/9, v/v), respectively (Scheme 5.4).

Scheme 5.3

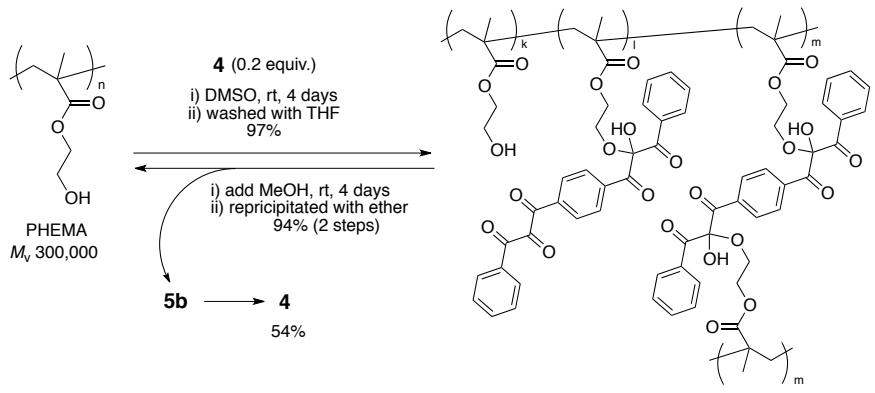

Scheme 5.4

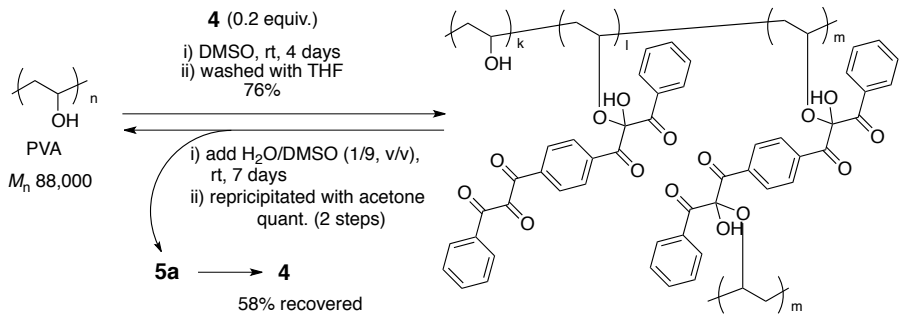

As stated above, this thesis has demonstrated that addition–elimination equilibria between alcohols and vicinal tricarbonyl compounds could be shifted in both directions under mild conditions, and therefore, vicinal tricarbonyl–alcohol linkages are highly useful for construction of reversible crosslinking and decrosslinking systems.

This thesis has demonstrated the polystyrene bearing the hydrate structure of vicinal tricarbonyl was crosslinked with an α,ω-diol and the resulting networked polymer was decrosslinked utilizing water–alcohol exchange reactions. Although the reactions proceeded under mild conditions and in facile manners, it requires several days for the crosslinking or decrosslinking processes. It is expected that a diamine crosslinker accelerates network formation than α,ω-diol crosslinker due to its nucleophilicity higher than that of hydroxyl group. Moreover, vicinal tricarbonyl–amine bond formation probably occurs in preference to hydration of tricarbonyl. In other words, the amination of vicinal tricarbonyl group will proceed even in the presence of an excess of water, so that hydrogels fabrication will be possible by employing diamine linkers.

This thesis has also reported crosslinking and decrosslinking of PHEMA and PVA utilizing the newly synthesized bifunctional vicinal tricarbonyl compound. After the decrosslinking, the original linear polymers were retrieved in high yields along with the bistriketone crosslinker. The author foresees that utilizing a tricarbonyl polymer in this system instead of the bistriketone will

allow hybridization of (immiscible) polymers and separation to the original linear polymers, thereby giving access to smart polymeric materials responding to external stimuli.

Vicinal tricarbonyl–alcohol linkage that can be reversibly formed and dissociated under mild condition is of great interest from the viewpoint of supramolecular synthesis, chemical recycling, and self-healable polymeric materials. The author is convinced that this thesis offers fundamental knowledge to achieve such tasks.

X-ray Crystallographic Data

X-ray diffraction data were collected on a Bruker Smart APEX-II CCD-based X-ray diffractometer with Mo-Kα radiation (l = 0.71073 Å) at 90 K.

Single crystals of DPPT-BnOH [$C_{22}H_{18}O_4$, MW = 346.36] suitable for X-ray analysis were grown from a solution in benzyl alcohol, and a single colorless crystal with dimensions 0.2 × 0.2 × 0.14 mm^3 was selected for intensity measurements. The unit cell was monoclinic with the space group *Cc*. Lattice constants with Z = 4, ρ_{calcd} = 1.309 g cm^{-3}, $\mu(Mo_{Ka})$ = 0.090 mm^{-1}, $F(000)$ = 728, $2\theta_{max}$ = 50.04° were a = 12.031(3) Å, b = 17.789(5), c = 9.608(3) Å, β = 121.262(3)°, and V = 17,578(8) Å^3. A total of 4,135 reflections were collected, of which 2,718 reflections were independent (R_{int} = 0.0110). The structure was refined to final R_1 = 0.0324 for 2,542 data [$I>2\sigma(I)$] with 235 parameters and wR_2 = 0.0921 for all data, *GOF* = 1.046, and residual electron density max/min = 0.191/–0.183 e Å^{-3}. The ORTEP drawing is shown in Figure S1, and crystal data and structure refinement are listed in Table S1.

Single crystals of bistriketone [$C_{24}H_{14}O_6$, MW = 398.35] suitable for X-ray analysis were grown from a solution in chloroform, and a single orange crystal with dimensions 0.20 × 0.20 × 0.20 mm^3 was selected for intensity measurements. The unit cell was monoclinic with the space group $P2_1/c$. Lattice constants with Z = 2, ρ_{calcd} = 1.489 g cm^{-3}, $\mu(Mo_{Ka})$ = 0.108 mm^{-1}, $F(000)$ = 412, $2\theta_{max}$ = 56.38° were a = 11.301(3) Å, b = 5.8285(15), c = 14.258(4) Å, β = 108.868(3)°, and V = 888.7(4) Å^3. A total of 3,846 reflections were collected, of which 1,563 reflections were independent (R_{int} = 0.0388). The structure was refined to final R_1 = 0.0330 for 1.302 data [$I>2\sigma(I)$] with 137 parameters and wR_2 = 0.0930 for all data, *GOF* = 1.084, and residual electron density max/min = 0.192/–0.183 e Å^{-3}. The ORTEP drawing is shown in Figure S2, and crystal data and

structure refinement are listed in Table S2.

Single crystals of bistriketone-2H_2O [$C_{27}H_{24}O_9$, MW = 492.46] suitable for X-ray analysis were grown from a solution in acetone, and a single colorless crystal with dimensions 0.20 × 0.20 × 0.02 mm^3 was selected for intensity measurements. The unit cell was triclinic with the space group *P-1*. Lattice constants with $Z = 2$, $\rho_{calcd} = 1.424$ g cm^{-3}, $\mu(Mo_{Ka}) = 0.108$ mm^{-1}, $F(000) = 516$, $2\theta_{max} = 56.96°$ were $a = 9.4625(13)$ Å, $b = 11.3827(16)$, $c = 11.5726(17)$ Å, $\alpha = 92.198(2)°$, $\beta = 110.599(2)°$, $\gamma = 98.513(2)°$, and $V = 1{,}148.4(3)$ $Å^3$. A total of 5,521 reflections were collected, of which 3,983 reflections were independent ($R_{int} = 0.0141$). The structure was refined to final $R_1 = 0.0381$ for 3.230 data [$I>2\sigma(I)$] with 343 parameters and $wR_2 = 0.1189$ for all data, $GOF = 0.909$, and residual electron density max/min = 0.279/–0.217 e $Å^{-3}$. The ORTEP drawing is shown in Figure S3, and crystal data and structure refinement are listed in Table S3.

Single crystals of bistriketone-2EtOH [$C_{28}H_{26}O_8$, MW = 490.49] suitable for X-ray analysis were grown from a solution in ethyl acetate, and a single colorless crystal with dimensions 0.20 × 0.20 × 0.10 mm^3 was selected for intensity measurements. The unit cell was triclinic with the space group *P-1*. Lattice constants with $Z = 1$, $\rho_{calcd} = 1.382$ g cm^{-3}, $\mu(Mo_{Ka}) = 0.102$ mm^{-1}, $F(000) = 258$, $2\theta_{max} = 57.14°$ were $a = 8.337(3)$ Å, $b = 8.518(4)$, $c = 8.983(4)$ Å, $\alpha = 71.791(5)°$, $\beta = 77.809(5)°$, $\gamma = 80.783(6)°$, and $V = 589.2(4)$ $Å^3$. A total of 2,816 reflections were collected, of which 2,035 reflections were independent ($R_{int} = 0.0390$). The structure was refined to final $R_1 = 0.0582$ for 1,731 data [$I>2\sigma(I)$] with 168 parameters and $wR_2 = 0.1650$ for all data, $GOF = 1.071$, and residual electron density max/min = 0.316/–0.485 e $Å^{-3}$. The ORTEP drawing is shown in Figure S4, and crystal data and structure refinement are listed in Table S4.

Data collection, indexing, and initial cell refinements were carried out using the program

SMART[1]. Frame integration and final cell refinements were performed using SAINT software[2]. A multiple absorption correction for each data set was applied using the program SADABS[3]. The structures were solved by direct methods and Fourier techniques using the program SHELXS-97[4] and refined by full-matrix least squares methods on F^2 using SHELXL-97[5] incorporated in SHELXTL-PC[6]. All non-hydrogen atoms were refined anisotropically. All hydrogen atoms were calculated geometrically and refined using the riding models.

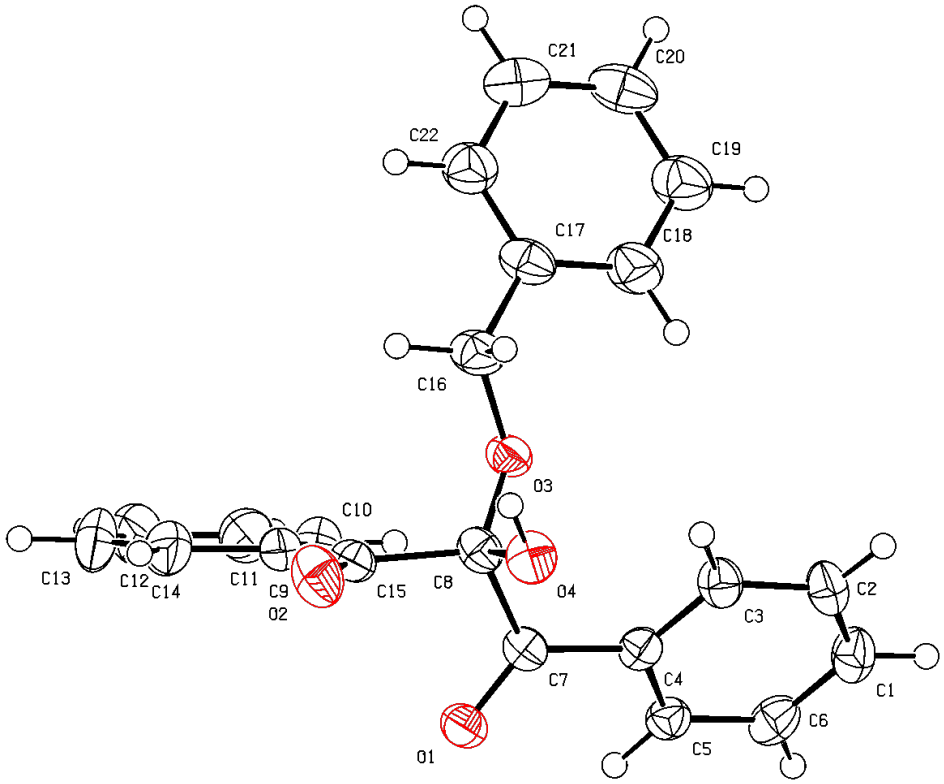

Figure S1. ORTEP drawing of the crystal structure of DPPT-BnOH with thermal ellipsoids at 50% probability.

Table S1. Crystal data and structure refinement for DPPT-BnOH

Empirical formula	$C_{22}H_{18}O_4$
Formula weight	346.36
Temperature	90 K
Wavelength	0.71073 Å
Crystal system	Monoclinic
Space group	*Cc*
Unit cell dimensions	a = 12.031(3) Å α = 90°.
	b = 17.789(5) Å β = 121.262(3)°.
	c = 9.608(3) Å γ = 90°.
Volume	1,757.8(8) $Å^3$
Z	4
Density (calculated)	1.309 g cm^{-3}
Absorption coefficient	0.090 mm^{-1}
F(000)	728
Crystal size	0.20 × 0.20 × 0.14 mm^3
Theta range for data collection	2.29 to 25.02°
Index ranges	$-14 \le h \le 14$, $-12 \le k \le 21$, $-11 \le l \le 10$
Reflections collected	4,135
Independent reflections	2,718 [R_{int} = 0.0110]
Completeness to theta	99.9%
Absorption correction	Semi-empirical from equivalents
Max. and min. transmission	0.9876 and 0.9823
Refinement method	Full-matrix least-squares on F^2
Data / restraints / parameters	2,542 / 2 / 235
Goodness-of-fit on F^2	1.046
Final R indices [$I>2\sigma(I)$]	R_1 = 0.0324, wR_2 = 0.0893
R indices (all data)	R_1 = 0.0361, wR_2 = 0.0921
Largest diff. peak and hole	0.191 and –0.183 e $Å^{-3}$
CCDC reference number	CCDC-885018

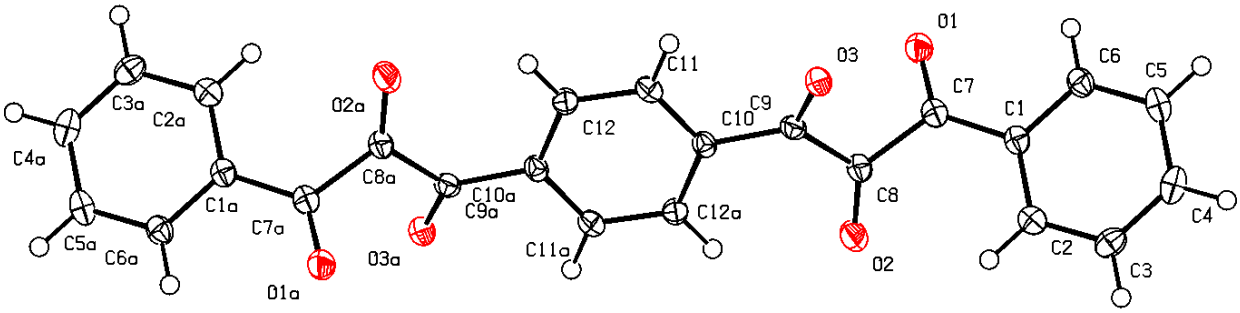

Figure S2. ORTEP drawing of the crystal structure of bistriketone with thermal ellipsoids at 50% probability.

Table S2. Crystal data and structure refinement for bistriketone

Empirical formula	$C_{24}H_{14}O_6$
Formula weight	398.35
Temperature	90 K
Wavelength	0.71073 Å
Crystal system	Monoclinic
Space group	$P2_1/c$
Unit cell dimensions	a = 11.301(3) Å α = 90°.
	b = 5.8285(15) Å β = 108.868(3)°.
	c = 14.258(4) Å γ = 90°.
Volume	888.7(4) Å^3
Z	2
Density (calculated)	1.489 g cm^{-3}
Absorption coefficient	0.108 mm^{-1}
F(000)	412
Crystal size	0.20 × 0.20 × 0.20 mm^3
Theta range for data collection	1.90 to 25.02°
Index ranges	$-8 \le h \le 13$, $-5 \le k \le 6$, $-16 \le l \le 15$
Reflections collected	3,846
Independent reflections	1,563 [R_{int} = 0.0388]
Completeness to theta	99.7%
Absorption correction	Semi-empirical from equivalents
Max. and min. transmission	0.9787 and 0.9787
Refinement method	Full-matrix least-squares on F^2
Data / restraints / parameters	1,563 / 0 / 137
Goodness-of-fit on F^2	1.084
Final R indices [$I>2\sigma(I)$]	R_1 = 0.0330, wR_2 = 0.0888
R indices (all data)	R_1 = 0.0413, wR_2 = 0.0930
Largest diff. peak and hole	0.192 and –0.183 e Å^{-3}
CCDC reference number	CCDC-917094

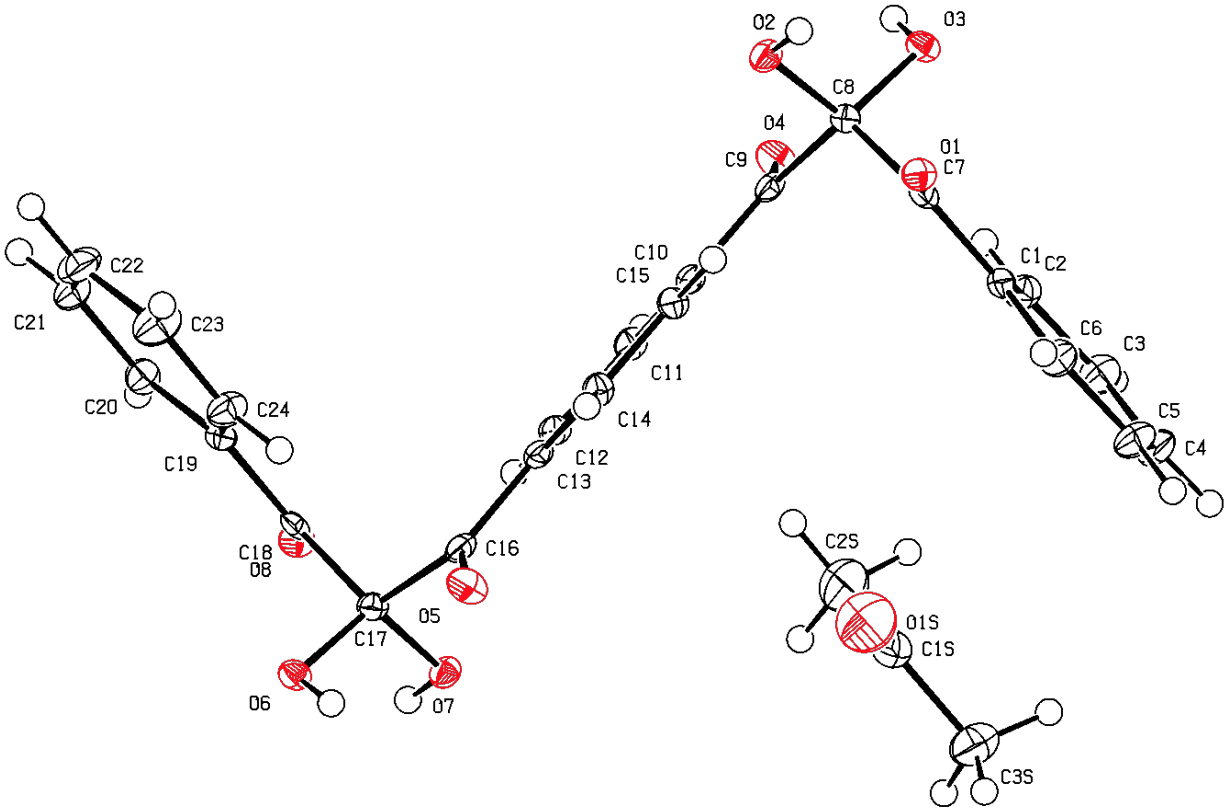

Figure S3. ORTEP drawing of the crystal structure of bistriketone-2H_2O with thermal ellipsoids at 50% probability.

Table S3. Crystal data and structure refinement for bistriketone-2H_2O

Empirical formula	$C_{27}H_{24}O_9$
Formula weight	492.46
Temperature	90 K
Wavelength	0.71073 Å
Crystal system	Triclinic
Space group	*P-1*
Unit cell dimensions	a = 9.4625(13) Å α = 92.198(2)°.
	b = 11.3827(16) Å β = 110.599(2)°.
	c = 11.5726(17) Å γ = 98.513(2)°.
Volume	1,148.4(3) $Å^3$
Z	2
Density (calculated)	1.424 g cm^{-3}
Absorption coefficient	0.108 mm^{-1}
F(000)	516
Crystal size	0.20 × 0.20 × 0.02 mm^3
Theta range for data collection	2.41 to 28.48°
Index ranges	$-7 \le h \le 11$, $-12 \le k \le 13$, $-13 \le l \le 13$
Reflections collected	5,521
Independent reflections	3,983 [R_{int} = 0.0141]
Completeness to theta	98.2%
Absorption correction	Semi-empirical from equivalents
Max. and min. transmission	0.9788 and 0.9979
Refinement method	Full-matrix least-squares on F^2
Data / restraints / parameters	3,983 / 0 / 343
Goodness-of-fit on F^2	0.909
Final R indices [$I>2\sigma(I)$]	R_1 = 0.0381, wR_2 = 0.1037
R indices (all data)	R_1 = 0.0498, wR_2 = 0.1189
Largest diff. peak and hole	0.279 and –0.217 e $Å^{-3}$
CCDC reference number	CCDC-917095

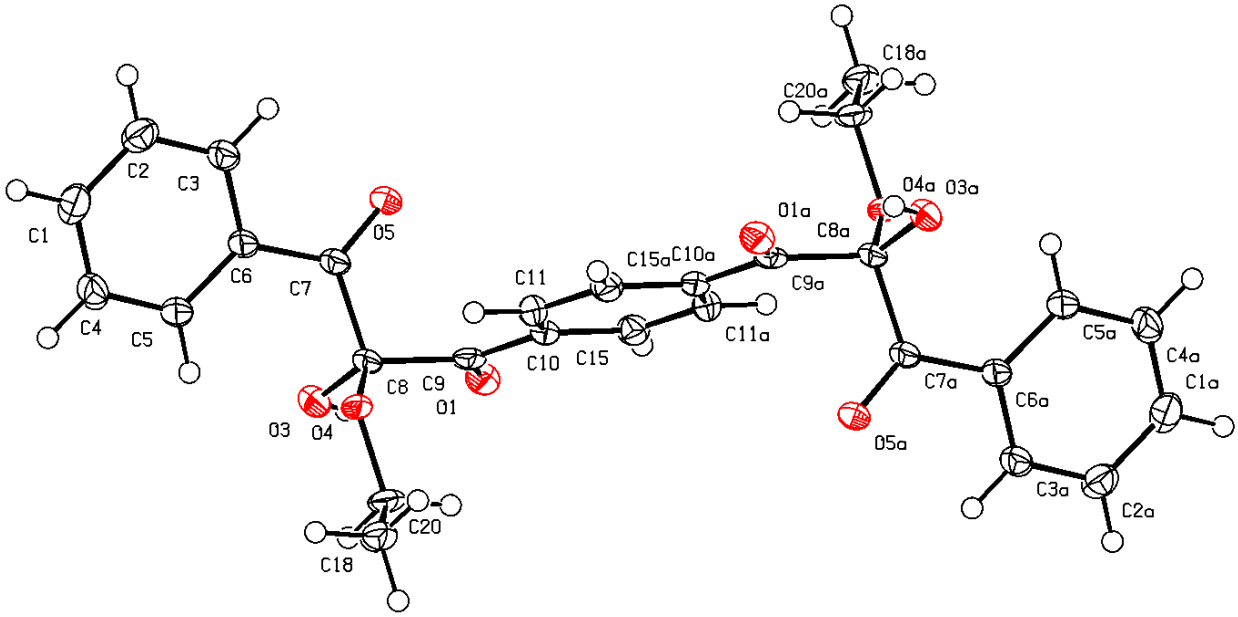

Figure S4. ORTEP drawing of the crystal structure of bistriketone-2EtOH with thermal ellipsoids at 50% probability.

Table S4. Crystal data and structure refinement for bistriketone-2EtOH

Empirical formula	$C_{28}H_{26}O_8$	
Formula weight	490.49	
Temperature	90 K	
Wavelength	0.71073 Å	
Crystal system	Triclinic	
Space group	*P-1*	
Unit cell dimensions	a = 8.337(3) Å	α = 71.791(5)°.
	b = 8.518(4) Å	β = 77.809(5)°.
	c = 8.983(4) Å	γ = 80.783(6)°.
Volume	589.2(4) $Å^3$	
Z	1	
Density (calculated)	1.382 g cm^{-3}	
Absorption coefficient	0.102 mm^{-1}	
F(000)	258	
Crystal size	0.20 × 0.20 × 0.10 mm^3	
Theta range for data collection	2.42 to 25.03°	
Index ranges	$-9 \le h \le 9$, $-10 \le k \le 9$, $-10 \le l \le 8$	
Reflections collected	2.815	
Independent reflections	2,035 [R_{int} = 0.0390]	
Completeness to theta	97.7%	
Absorption correction	Semi-empirical from equivalents	
Max. and min. transmission	0.9800 and 0.9899	
Refinement method	Full-matrix least-squares on F^2	
Data / restraints / parameters	2,035 / 0 / 168	
Goodness-of-fit on F^2	1.071	
Final R indices [$I>2\sigma(I)$]	R_1 = 0.0582, wR_2 = 0.1553	
R indices (all data)	R_1 = 0.0670, wR_2 = 0.1650	
Largest diff. peak and hole	0.316 and –0.485 e $Å^{-3}$	
CCDC reference number	CCDC-917096	

References

1. Bruker, SMART Version 5.624: Program for collecting frames of data, indexing reflection, and determination of lattice parameters; Bruker AXS, Inc., Madison, Wisconsin, USA (2000).
2. Bruker, SAINT Version 6.02: Program for integration of the intensity of reflections and scaling; Bruker AXS, Inc., Madison, Wisconsin, USA (2000).
3. Sheldrick, G. M. SADABS Version 2.03: Program for Performing Absorption Corrections to Single-Crystal X-ray Diffraction Patterns; University of Göttingen, Göttingen, Germany (2001).
4. Sheldrick, G. M. SHELXS-97: Program for the Solution of Crystal Structures; University of Göttingen, Göttingen, Germany (1997).
5. Sheldrick, G. M. SHELXL-97: Program for the Refinement of Crystal Structures; University of Göttingen, Göttingen, Germany (1997).
6. Bruker, SHELXTL Version 5.10: Suite of Programs for Crystal Structure Analysis, Incorporating Structure Solution (XS), Least-Squares Refinement (XL), and Graphics (XP); Bruker AXS, Inc., Madison, Wisconsin, USA (2000).

Achievements

List of Publications

Papers

1) “Reversible Cross-Linking and De-Cross-Linking System of Polystyrene Bearing Monohydrate Structure of Vicinal Tricarbonyl Group through Water–Alcohol Exchange Reactions at Ambient Conditions”
M. Yonekawa, Y. Furusho, T. Endo, *Macromolecules* **2012**, *45*, 6640–6647.

2) “Synthesis and X-ray structural analysis of an acyclic bifunctional vicinal triketone, its hydrate, and its ethanol-adduct”
M. Yonekawa, Y. Furusho, Y. Sei, T. Takata, T. Endo, *Tetrahedron* **2013**, *69*, 4076–4080.

3) “Reversible Cross-Linking and De-cross-Linking of Polymers Containing Alcohol Moiety Utilizing an Acyclic Bifunctional Vicinal Triketone”
M. Yonekawa, Y. Furusho, T. Takata, T. Endo, *J. Polym. Sci. Part A: Polym. Chem.* **2013**, *in press.*

Other Related Papers

1) “New Click Chemistry: Polymerization via 1,3-Dipolar Addition of Homo-ditopic Aromatic Nitrile Oxides Formed In Situ”
Y. Koyama, M. Yonekawa, T. Takata, *Chem. Lett.* **2008**, *37*, 918–919.

2) “New Click Chemistry: Polymerization Based on 1,3-Dipolar Cycloaddition of a Homo Ditopic Nitrile *N*-Oxide and Transformation of the Resulting Polymers into Reactive Polymers”
Y.-G. Lee, Y. Koyama, M. Yonekawa, T. Takata, *Macromolecules* **2009**, *42*, 7709–7717.

3) “Synthesis of Main-Chain-Type Polyrotaxanes by New Click Polymerization Using Homoditopic Nitrile *N*-Oxides via Rotaxanation-Polymerization Protocol”
Y.-G. Lee, Y. Koyama, M. Yonekawa, T. Takata, *Macromolecules* **2010**, *43*, 4070–4080.

4) “Synthesis of a Kinetically Homoditopic Nitrile *N*-Oxide Directed toward Catalyst-free Click Polymerization”
Y.-G. Lee, M. Yonekawa, Y. Koyama, T. Takata, *Chem. Lett.* **2010**, *39*, 420–421.

5) “Intramolecular 1,3-Dipolar Cycloaddition of Nitrile *N*-Oxide Accompanied by Dearomatization”
M. Yonekawa, Y. Koyama, S. Kuwata, T. Takata, *Org. Lett.* **2012**, *14*, 1164–1167.

6) “Polymer Nitrile *N*-Oxide Directed toward Catalyst- and Solvent-Free Click Grafting”
C.-G. Wang, Y. Koyama, M. Yonekawa, S. Uchida, T. Takata, *Chem. Commun.* **2013**, *in press.*

7) “Almightly Cross-linker Consisting of Sufficiently Stabilized Homoditopic Nitrile *N*-Oxide: Highly Reliable Cure Reaction of Ubiquitous Polymers with Unsaturated Bonds”
M. Yonekawa, Y.-G. Lee, A, Seo, Y. Koyama, T. Takata, *submitted*.

8) “Fluorescent Poly(boron enaminoketone): Synthesis via Direct Modification od Polyisoxazole Obtained by Click Polymerization of Homoditopic Nitrile *N*-Oxide and Diyne”
Y. Koyama, T. Matsumura, S. Uchida, M. Yonekawa, M. Yui, T. Takata *submitted.*

Acknowledgement

The author wishes to his grateful acknowledgement to Professor Toshikazu Takata whose encouragement and helpful suggestions have been indispensable to the completion of the present thesis. The author would also like to express his deepest gratitude to Professor Takeshi Endo in Kinki University, who has provided him with valuable guidance, helpful discussion, kind encouragement as well as financial support throughout his research. The author would also like to acknowledge Associate Prof. Yoshio Furusho for their constant guidance, encouragement, pertinent and tolerant advice, and helpful discussion.

The author appreciates Professor Yasuyuki Tezuka, Associate Prof. Teruaki Hayakawa, Associate Prof. Takashi Ishizone, and Associate Prof. Gen-ichi Konishi for reviewing his thesis, and their invaluable comments and useful suggestions.

The author appreciates Assistant Prof. Yoshihisa Sei in Chemical Resources Laboratory in Tokyo Tech for single crystal X-ray measurements.

The author would like to express his thanks to Assistant Prof. Yasuhito Koyama, Assistant Prof. Kazuko Nakazono, Assistant Prof. Satoshi Uchida, and all other members in Takata research group for their kind suggestion, and also, his thanks to Dr. Kazuhide Morino and all other members in Molecular Engineering Institute of Kinki University. The author appreciates the financial support by JSR Corporation.

July, 2013

Morio YONEKAWA